Systems metabolic engineering of *Corynebacterium glutamicum* for production of L-lysine and ectoine

Dissertation

zur Erlangung des Grades

des Doktors der Ingenieurwissenschaften

der Naturwissenschaftlich-Technischen Fakultät

der Universität des Saarlandes

von

Gideon Gießelmann

Saarbrücken

2019

Tag des Kolloquiums: 16.7.2019

Dekan: Prof. Guido Kickelbick

Berichterstatter 1: Prof. Christoph Wittmann

Berichterstatter 2: Prof. Gert-Wieland Kohring

Vorsitz: Prof. Bruce Morgan

Akad. Mitarbeiter: Dr. Björn Becker

Publications

Partial results of this work have been published previously. This was authorized by the Institute of Systems Biotechnology, represented by Prof. Dr. Christoph Wittmann.

Peer-reviewed articles:

Gießelmann G, D. Dietrich, L. Jungmann, M. Kohlstedt, E. Jung Jeon, S. Sun Yim, F. Sommer, D. Zimmer, T. Mühlhaus, M. Schroda, K. Jun Jeong, J. Becker, and C. Wittmann, 2019. Metabolic engineering of *Corynebacterium glutamicum* for high-level ectoine production – design, combinatorial assembly and implementation of a transcriptionally balanced heterologous ectoine pathway. *Biotechnology Journal*, under revision

Becker J, **G. Gießelmann**, SL. Hoffmann, C. Wittmann, 2016: *Corynebacterium glutamicum* for sustainable bioproduction: from metabolic physiology to systems metabolic engineering. In: Zhao H., Zeng AP. (eds) Synthetic Biology – Metabolic Engineering. Advances in Biochemical Engineering/Biotechnology, vol 162. Springer, Cham

The following peer-reviewed articles were published during this work, but are not part of the dissertation:

Rohles CM, L. Gläser, M. Kohlstedt, **G. Gießelmann**, S. Pearson, A. del Campo, J. Becker, C. Wittmann, 2018. A bio-based route to the carbon-5 chemical glutaric acid and to bionylon-6,5 using metabolically engineered *Corynebacterium glutamicum*, *Green Chemistry* 20**:**4662-4674.

Vassilev I, **G. Gießelmann**, SK. Schwechheimer, C. Wittmann, B Virdis, JO. Krömer: 2018, Anodic Electro-Fermentation: Anaerobic production of L-lysine by recombinant *Corynebacterium glutamicum*. *Biotechnol Bioeng*, 115:1499–1508.

Rohles CM, **G. Gießelmann**, M. Kohlstedt, C. Wittmann, J. Becker, 2016: Systems metabolic engineering of *Corynebacterium glutamicum* for the production of the carbon-5 platform chemicals 5-aminovalerate and glutarate. *Microb Cell Fact*, 15**:**154.

Conference contributions

Gießelmann G, R. Schäfer, A. Banz, SL. Hoffmann, S. Schiefelbein, J. Becker, and C. Wittmann 2018: Systems and synthetic biology of lysine producing *Corynebacterium glutamicum* at high temperature, PhD day Faculty NT, Saarland University, Saarbrücken, Germany.

Gießelmann G, R. Schäfer, A. Banz, SL. Hoffmann, S. Schiefelbein, J. Becker, and C. Wittmann, 2018: Systems and synthetic biology of L-lysine producing *Corynebacterium glutamicum* at high temperature, GASB German Association for Synthetic Biology Annual Conference, Berlin, Germany.

Gießelmann G, S. Heiermann, C. Mattes, J. Becker and C. Wittmann, 2016: Metabolic engineering of *Corynebacterium glutamicum* for biosynthesis of health-care products from renewables, PhD day Faculty NT, Saarland University, Saarbrücken, Germany.

Gießelmann G, R. Schäfer, N. Buschke, SL. Hoffmann, J. Becker and C. Wittmann, 2016: Systems metabolic engineering of *Corynebacterium glutamicum* for bioproduction from xylose, Association for General and Applied Microbiology, VAAM Annual Conference, Jena, Germany.

Danksagung

Table of content

Summary

The soil bacterium *Corynebacterium glutamicum* has gained tremendous industrial interest, for the biotechnological production of L-lysine and L-lysine derived products. This work assessed the cellular function of the L-lysine producer *C. glutamicum* LYS-12 at high temperature. The interpretation of transcriptome and proteome- data together with previously generated fluxome data, provided a detailed picture of the regulatory adaption of the cells to 38°C and suggested potential targets for metabolic engineering. In line, the duplication of the *lysGE* gene cluster increased the L-lysine yield by 7% to 460 mmol mol^{-1}. Additionally, the synthesis of the valuable compatible solute ectoine was optimized in *C. glutamicum* via transcriptional balancing of the heterologous ectoine cluster. The shuffling of synthetic promoter and spacer elements yielded a library of the terminal ectoine pathway. Strongly increased production was enabled by regulatory elements of medium strength, where the increased expression of the gene *ectB*, as compared to *ectA* and *ectC*, appeared crucial. The most advanced ectoine producer *C. glutamicum ectABC*^{opt} achieved 65 g L^{-1} ectoine in a fed-batch process. In addition, transcriptome profiling of ectoine producing *C. glutamicum* revealed a yet unknown export mechanism for ectoine, an interesting target for further metabolic engineering.

Zusammenfassung

Das Gram-positive Bodenbakterium *Corynebacterium glutamicum* ist von großem industriellem Interesse und insbesondere für die biotechnologische Herstellung von L-Lysin und L-Lysin– verwandten Produkten von Bedeutung. Diese Arbeit befasst sich mit der Untersuchung des L-Lysin Produzenten *C. glutamicum* LYS-12, kultiviert bei erhöhten Temperaturen. Die Integration von Transkriptom-, Proteom- und bereits im Vorfeld generierten Fluxom-Daten, ergab neue Einsichten in die Adaptierung der Zellen an 38°C und brachte neue Strategien für die Stammoptimierung hervor. Die Verdopplung des Gen-Clusters *lysGE* führte zu einer Steigerung der L-Lysin Ausbeute um 7% auf 460 mmol mol^{-1}. Des Weiteren wurde der terminale heterologe Ectoin-Synthese-Weg in *C. glutamicum* auf der Ebene des Transkriptoms optimiert. Durch das zufällige Abwechseln von Promotoren und regulatorischen Elementen konnte eine Ectoin-Plasmid Bibliothek erstellt werden. Eine hohe Produktion wurde durch regulatorische Elemente mittlerer Stärke erreicht, wobei die erhöhte Expression des Gens *ectB*, verglichen mit *ectA* und *ectC*, von besonderer Bedeutung zu sein schien. Der beste Produzent *C. glutamicum ectABC*^{opt} erreichte einen Ectoin-Titer von 65 g L^{-1} in einem Fed-Batch Prozess. Anschließende Untersuchungen des Transkriptoms eines Ectoin produzierenden *C. glutamicum* Stammes, führten zu der Identifikation eines bislang unbekannten Export-Mechanismus für Ectoin, was ein interessantes Ziel für zukünftige Stammoptimierungen darstellt.

1. Introduction

1.1 General introduction

The microbe *Corynebacterium glutamicum* was originally discovered during the search for a natural L-glutamate overproducing organism (Kinoshita et al. 1957). Throughout the years, the microbe was found capable to produce a large variety of substances (Becker et al. 2018b). The industrial production of the amino acid L-lysine with *C. glutamicum* became one of the great success stories in biotechnology (Wittmann and Becker 2007). L-Lysine is a crucial food additive in farming industries (Lemme et al. 2002; Walz 1985) and has other relevant applications, e.g. for medical use (Lai et al. 2014). With an annual market growth of about 7%, the market volume is expected to exceed 2.5 mio tons in 2019 (Cheng et al. 2018). While first producing strains were obtained via random mutagenesis (Hirao et al. 1989), most mutants suffered from low genetic stability and undesired auxotrophies (Sassi et al. 1996). The availability of the complete genome sequence enabled the development of genetic engineering tools, thus driving the directed engineering of the microbe (Kalinowski et al. 2003). Rational engineering approaches were further promoted by the application of analytical methods for strain characterization (Krömer et al. 2004). As a result, the majority of L-lysine is produced biotechnologically today (Eggeling and Bott 2015).

Techniques like high pressure liquid chromatography, gas-chromatography mass spectrometry, electrospray ionization mass spectrometry and sequencing techniques revealed fascinating insights into metabolome (Ma et al. 2019), transcriptome (Sun et al. 2017), proteome (Chen et al. 2019), and genome (Albersmeier et al. 2017). In combination with a versatile genetic toolbox, the generation of systematically designed producer strains with a minimal amount of targeted modifications has been achieved (Becker et al. 2011). Besides the realization of the advanced L-lysine producing mutant *C. glutamicum* LYS-12 (Becker et al. 2011), which is able to surpass the performance of classically engineered production strains, the microbe was shown to serve as production host for numerous natural and non-natural substances (Becker et al. 2018b). The production of L-lysine derived substances such as the biopolymer precursors glutarate (Rohles et al. 2018) and 1,5-diaminopentane (Kind and Wittmann

2011), were produced at economically feasible yields. Systems metabolic engineering furthermore extended the natural substrate spectrum of *C. glutamicum* to a broad range of raw materials (Buschke et al. 2011). An important aspect for the industrial application of *C. glutamicum* is its natural robustness against environmental changes like temperature (Ehira et al. 2009), osmotic stress (Börngen et al. 2010) and various toxic compounds (Becker et al. 2018a). For the production of L-lysine, consequent optimization of strains and process parameters is crucial in order to face the highly competitive market (Eggeling and Bott 2015).

In addition, *C. glutamicum* can be used to synthesize high-value molecules from sustainable substrates. The compatible solute ectoine is naturally produced by halophilic organisms and has a large field of applications in the biotechnological (Zhang et al. 2006), the cosmetic (Buenger and Driller 2004) or the medical industry (Kanapathipillai et al. 2005). The substance is able to cluster water around proteins, mediating improved resistance against various stresses, e.g. osmotic or temperature stress, by preserving their functionality (Graf et al. 2008). Currently, ectoine is produced in an elaborate and costly process. During this process, halophilic organisms like *Halomonas elongata* are cultivated in high salt medium. Ectoine and its derivative hydroxyectoine are synthesized simultaneously and both products accumulate intracellularly (Kunte et al. 2014). Subsequent product release is triggered by an osmotic downshock (Sauer and Galinski 1998). The expression of the genes *ectA*, *ectB*, *ectC* and *ectD* in *C. glutamicum* enabled the secretion independent from osmotic pressure, directly into the cultivation medium (Becker et al. 2013). Biotechnological production of ectoine under mild conditions would simplify the downstream process and reduce overall production costs. However, previous approaches of heterologous ectoine production were not able to cope with classical industrial processes, due to low titers and productivity, or accumulation of side products (Ning et al. 2016; Pérez-García et al. 2017). Moreover, the underlying principle of ectoine export in *C. glutamicum* is not fully understood, since the substance may not only be released through the natural mechanosensitive compatible solute release system of the host (Morbach and Krämer 2005). In order to provide broad access to the costly small molecule, the optimization of the production process and heterologous synthesis via microbial cell factories like *C. glutamicum* represents an important challenge for synthetic biology.

1.2 Main objectives

The first aim of the present work was the investigation of regulatory changes in the L-lysine producing strain *C. glutamicum* LYS-12 cultivated at 38°C, to identify novel genetic targets for optimized production. In order to complement previous flux analysis data, proteome and transcriptome of *C. glutamicum* LYS-12 should be analyzed. For analysis of the transcriptome, methods for the extraction, quality control and preparation of total RNA should be established first. Data from transcriptome, proteome, and fluxome should then be integrated to gain an insight into the temperature adaption of *C. glutamicum*. These findings should be further exploited to improve L-lysine synthesis at high temperature via targeted strain engineering.

The second aim of this work was the enhancement of the heterologous synthesis of ectoine, using *C. glutamicum.* While earlier approaches mainly focused on the optimization of precursor supply, terminal pathway engineering apparently exhibited a possible bottleneck for expression. For this purpose, the three genes, *ectA*, *ectB* and *ectC* should be transcriptionally balanced with a library of different transcription and translation modulating elements. The different expression levels of these genes should then be investigated in order to identify superior producing strains for ectoine. Furthermore, the not yet fully understood ectoine export mechanism in *C. glutamicum* should be elucidated. To this extent, a basic ectoine producer and its non-producing parent strain should be compared via comparative transcriptional analysis for upregulation of potential transport proteins. Genetic engineering of an ectoine export mechanism should finally lead to optimized production of the target substance.

2. Theoretical Background

2.1 *Corynebacterium glutamicum* as industrial cell factory

Since its discovery approximately 60 years ago (Kinoshita et al. 1957), the Gram-positive soil bacterium *Corynebacterium glutamicum* has evolved into a workhorse for the biotechnological industry (Becker et al. 2018b). The microbe is generally regarded as safe (GRAS). The possibility to conduct genetic modifications via a quickly expanding engineering and editing toolbox, make it an ideal and safe expression host (Becker and Wittmann 2012). The availability of its genome sequence furthermore enabled the development of postgenomic techniques and laid the foundation for systems level analysis of the microbe (Kalinowski et al. 2003).

Engineered strains of *C. glutamicum* efficiently produce various natural and non-natural products, such as amino acids (Becker and Wittmann 2015; Becker et al. 2011; Vogt et al. 2015), organic acids (Rohles et al. 2018; Zhou et al. 2015), diamines (Kind et al. 2010; Kind et al. 2011; Kind et al. 2014) and biofuels (Siebert and Wendisch 2015), as well as cosmetic products (Becker et al. 2013; Tsuge et al. 2018) from different substrates (Becker et al. 2018a; Buschke et al. 2013; Hoffmann et al. 2018; Pérez-García et al. 2017; Tsuge et al. 2015). Several approaches demonstrate anaerobic production of L-lysine (Vassilev et al. 2018; Xafenias et al. 2017), succinate (Chung et al. 2017; Tsuge et al. 2013) and lactate (Tsuge et al. 2013) (Figure 1). Altogether, these achievements highlight the importance of *C. glutamicum* as the preferred host for the present and future industrial biotechnology (Becker et al. 2016; Becker et al. 2018b).

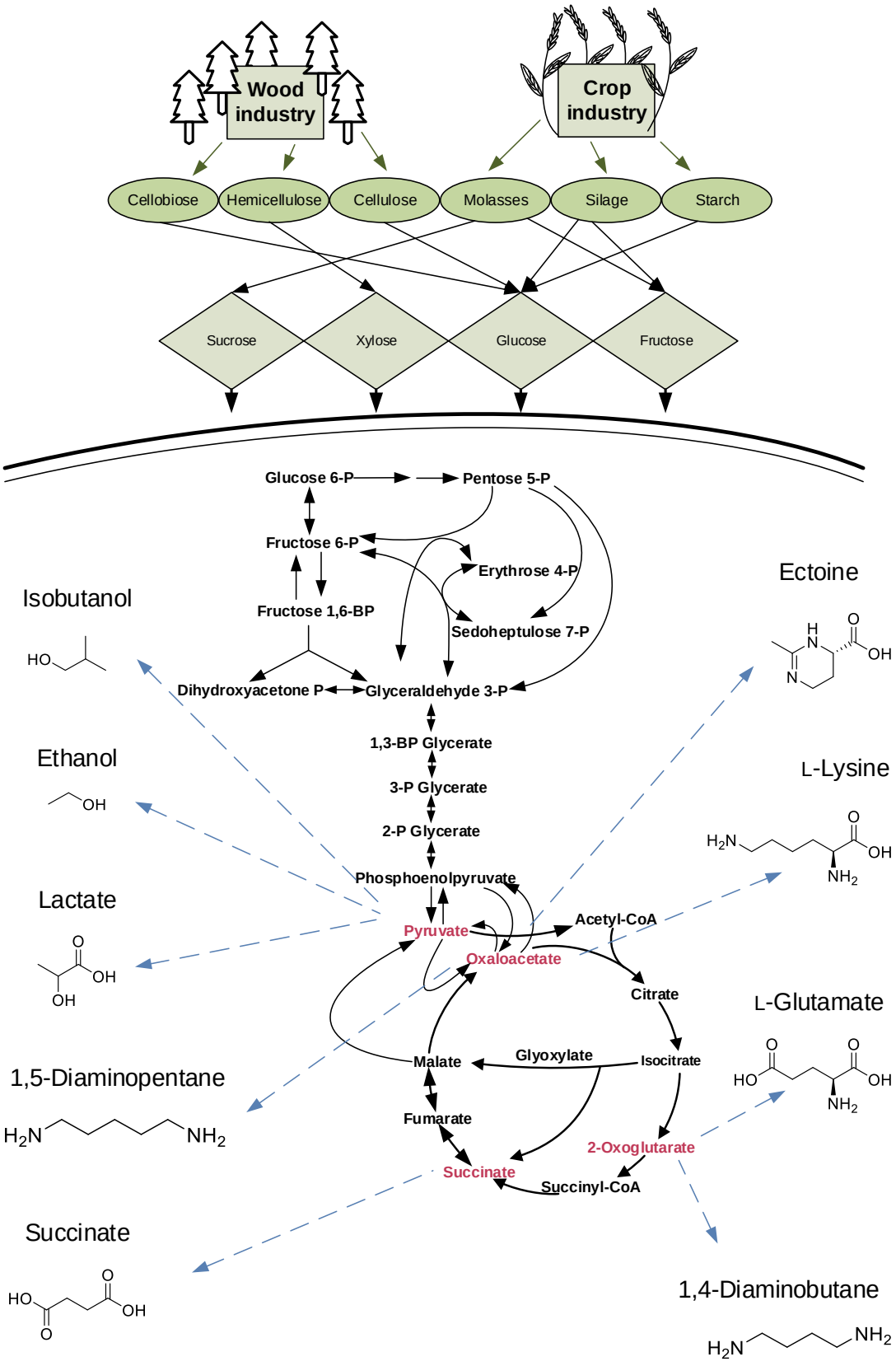

Figure 1. Industrial application of *C. glutamicum* for the conversion of waste streams and renewable materials into valuable products. Adapted and modified from previous work (Becker et al. 2018b; Becker and Wittmann 2015).

2.2 Systems and synthetic biology of *C. glutamicum*

Systems biology involves the application of omics techniques and modeling approaches in order to characterize metabolic and regulatory networks on a systems level (Ng et al. 2015; Wendisch et al. 2006b; Wu et al. 2016). Today, powerful analytical methods provide access to the different functional layers of the cell, i.e. metabolome (Ma et al. 2019), proteome (Chen et al. 2019), transcriptome (Sun et al. 2017), and genome (Albersmeier et al. 2017).

Metabolite profiling provides access to the energy and redox level and a multitude of pathway intermediates. Metabolite analysis is a time critical discipline due to high metabolite turnover rates (Zhang et al. 2018). The technique requires fast quenching in order to achieve an unaltered impression of the metabolite status (Zhang et al. 2018). In addition, high resolution techniques such as gas-chromatography mass spectrometry or liquid-tandem mass spectrometry are required for molecular structure identification (Wellerdiek et al. 2009; Zhang et al. 2018). For detailed investigation of the proteome, a combination of different techniques is applied. Cellular proteins are separated via two dimensional sodium dodecyl sulfate polyacrylamide gels (2D-SDS-PAGE) and further analyzed, using matrix assisted laser desorption ionization-time of flight mass spectrometry (MALDI-TOF) and electrospray ionization mass spectrometry (ESI-MS) (Rosen and Ron 2002; Schluesener et al. 2005; Silberbach et al. 2005).

Transcriptome profiling requires the reverse transcription of extracted mRNA into more stable cDNA for qualitative and quantitative analysis. The quantitative amount of selected transcripts can be determined via reverse transcriptase real time polymerase chain reaction (RT-PCR) (Glanemann et al. 2003). Insights into the total pool of mRNA transcripts are possible via whole transcriptome sequencing, facilitated by RNA sequencing (RNAseq) (Pfeifer-Sancar et al. 2013). The underlying principle of mRNA sequencing is visualized in Figure 2. The sequencing of the entire DNA of a given organism (genomics) can also be performed via next generation sequencing techniques and provides insights into mutations and the arrangement of the genes (Unthan et al. 2015). Most approaches additionally rely on the application of bioinformatical methods and databases for data interpretation.

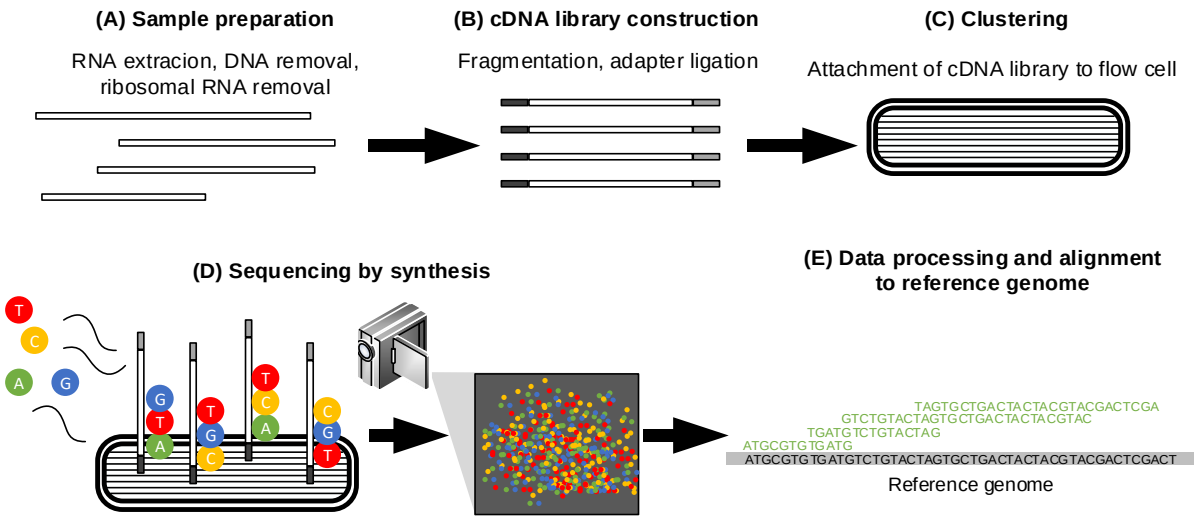

Figure 2. Workflow of RNA sequencing, starting from extracted total RNA. Sample preparation involves the extraction of RNA from the bacterial cells and removal of DNA and ribosomal RNA (A). cDNA libraries are generated by fragmentation of the mRNA and reverse transcription into cDNA. Adapters and linkers are attached for binding and amplification on the flow cell (B, C). Flow cell attached fragments are amplified and bridge polymerized for the creation of clusters. Fluorescently tagged nucleotides compete for the amplification of the strand. A light source excites nucleotides at each incorporation. The emitted light signal is detected by a camera (D). Millions of reads are separated due to the unique index primer sequences. Final reads are aligned to the reference genome and bioinformatically processed (E) (adapted from Illumina, San Diego, CA, USA).

Beyond single omics approaches, multi omics approaches allow even deeper insight into the cellular system (Fondi and Liò 2015; Krömer et al. 2004). Such studies have revealed that proteome and transcriptome do not necessarily match, but can exhibit high differences, due to posttranslational regulation mechanisms (Glanemann et al. 2003; Nie et al. 2007). The thorough interpretation of the different omics data therefore helps to discover regulatory mechanisms (Kohlstedt et al. 2010; Kohlstedt et al. 2014). Towards the design of superior *C. glutamicum* cell factories, systems biology developments are supported by straightforward genome editing tools. The *sacB* selection system has enabled marker-free genome modification of *C. glutamicum* for almost 30 years and is still widely used (Jäger et al. 1992; Schäfer et al. 1994). In addition, new methods recently emerged via application of CRISPR-Cas9 (Cho et al. 2017) or CRISPR-Cpf1 (Jiang et al. 2017), promising one-step editing of multiple genetic targets.

The different genome-editing methods are applied to diminish genes, include novel ones and modulate their expression in *C. glutamicum*. For expression control, a set of chromosomal high efficiency promoters has been identified (Buschke et al. 2013; Kind et al. 2014; Okibe et al. 2010). In addition, expression control enables a more fine-tuned balancing of individual genes within a pathway to optimize the overall pathway

flux. This approach is based on synthetic promoters and ribosomal binding sites (Oh et al. 2015; Rytter et al. 2014; Wei et al. 2018; Zhang et al. 2015). A powerful strategy is provided by synthetic promoter libraries, obtained from random mutagenesis and benchmarking via relative fluorescence measurement of reporter proteins (Rytter et al. 2014; Yim et al. 2013). Recently, their application has led to a significant increase of hemicellulosic biomass (xylan) utilization in *C. glutamicum* (Yim et al. 2016). Here, the responsible genes were equipped with promoters of different strength in order to supply the necessary balance of each module, including xylose utilization, xylose transport and xylan degradation (Yim et al. 2016).

Besides influencing protein expression on the level of transcription, it can also be modulated on the level of translation. Polycistrionic expression cassettes allow the co-expression of closely located genes by one homologous promoter. Simultaneous expression is enabled by the promoter, upstream of the first gene and ribosomal binding sites in front of each additional gene of the operon-like structure (Becker et al. 2013; Pérez-García et al. 2017).

In contrast, the bicistronic design allows an independent control of gene expression (Liu et al. 2017; Mutalik et al. 2013). The combination of a promoter and a bicistronic part, in this case, consists of a 5'-untranslated region with a Shine Dalgarno sequence, a sequence for a short peptide, e.g. from the source gene, and a Shine Dalgarno sequence including a stop codon, overlapping the start codon of the target gene. Both designs are graphically displayed in Figure 3 (Zhao et al. 2016).

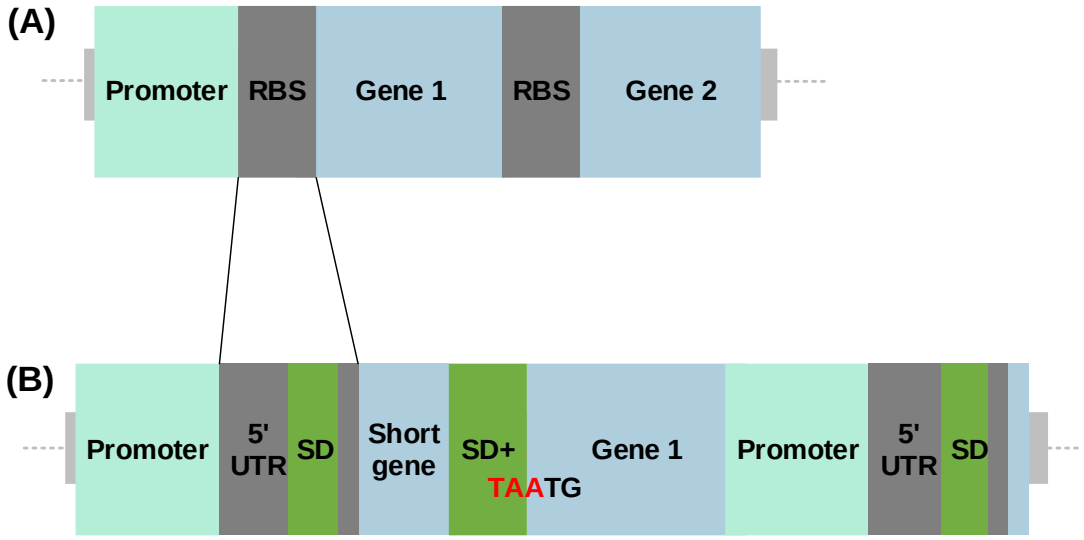

Figure 3. Comparison of polycistronic (A) and bicistronic (B) designs for modulated gene expression in *C. glutamicum*. The polycsitronic design (A) for the simultaneous expression of more than one gene in comparison to the bicistronic design (B), allowing an independent gene expression facilitated by the short gene and the second Shine Dalgarno (SD) sequence with stop codon (TAA) overlapping the start codon (ATG), (Liu et al. 2017).

The established systems biological tools enabled the analysis of the metabolism of *C. glutamicum* in different environments, and under various stress conditions. These conditions are important for the natural life style of the microbe in its natural soil and water habitats (Kinoshita et al. 1957), but are also relevant for industrial fermentation processes. Not only temperature stress (Ehira et al. 2009), but also osmotic (Wolf et al. 2003), and oxidative stress (Park et al. 2012) are typically imposed on *C. glutamicum*, when applied in industrial fermentations.

In this regard, previous work has shown that *C. glutamicum* LYS-12 adapts well to temperatures up to 40°C and exhibits a maximum L-lysine yield at 38°C in minimal glucose medium with a decreased growth rate (Schäfer 2016). Metabolic flux analysis of the strain revealed a redistribution of intracellular fluxes (Schäfer 2016). The promoted pentose phosphate (PP) pathway flux at the high temperature is enabled by massive carbon recycling (Figure 4). At 30°C, *C. glutamicum* LYS-12 channels only 86% of carbon into the PP pathway (Becker et al. 2011; Schäfer 2016). Due to the rerouting of metabolic fluxes, the microbe generates high amounts of NADPH, which are required for the terminal L-lysine producing pathway (Takeno et al. 2010).

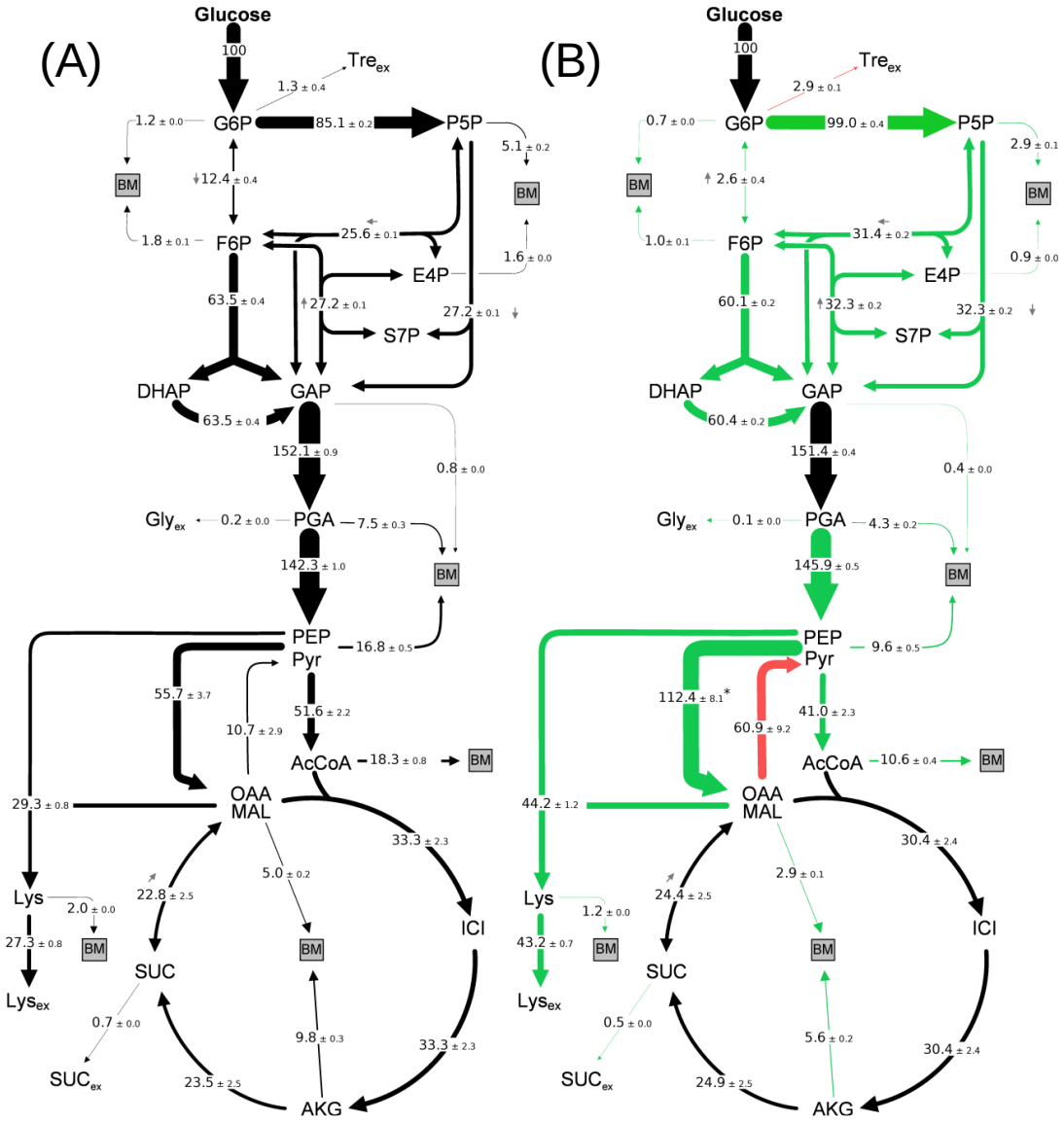

Figure 4. Activity of the central metabolic pathways of *C. glutamicum* LYS-12 at 30°C (A) and 38°C (B). Green arrows indicate *in vivo* fluxes closer to the theoretical optimal flux towards L-lysine synthesis in comparison to 30°C (Buschke et al. 2013; Melzer et al. 2009; Schäfer 2016). Anaplerotic fluxes generated by phosphoenolpyruvate carboxylase and pyruvate carboxylase are labelled green due to their enhanced net-flux from the Pyr/PEP pool to the MAL/OAA pool, calculated by the subtraction of malic enzyme flux from the anaplerotic flux (red). The fluxes are given as relative values normalized to the specific glucose uptake rate (4.1 mmol g^{-1} h^{-1} (30 °C), 3.9 mmol g^{-1} h^{-1} (38 °C)). AcCoA = acetyl Coenzyme A, AKG = α-ketoglutarate, BM = biomass, DAP = diaminopimelate, DHAP = dihydroxyacetone phosphate, E4P = erythrose 4-phosphate, F6P = fructose 6-phosphate, GAP = glyceraldehyde 3-phosphate, Gly_{ex} = extracellular glycine, G6P = glucose 6-phosphate, ICI = isocitrate, Lys = L-lysine, Lys_{ex} = extracellular L-lysine, MAL = malate, OAA = oxaloacetate, PEP = phosphoenolpyruvate, PGA = 3-phosphoglycerate, Pyr = pyruvate, P5P = pentose 5-phosphate, SUC = succinate, SUC_{ex} = extracellular succinate, S7P = sedoheptulose 7-phosphate, Tre_{ex} = extracellular trehalose (Figure kindly provided by Judith Becker and Rudolf Schäfer) (Becker et al. 2011; Schäfer 2016).

An enhanced carbon flux into the PP pathway has been shown to improve the production of L-lysine in *C. glutamicum* LYS-12 (Becker et al. 2007; Becker et al. 2005; Ohnishi et al. 2005). However, strains without a functional EMP (Embden-Meyerhof-Parnas) pathway, which are forced to channel carbon into the PP pathway, show strong imbalances and reduced growth (Marx et al. 2003; Melzer et al. 2009). A high flux through the PP pathway is beneficial for an optimal flux distribution in order to reach the theoretical maximum yield of 75% for L-lysine (Kjeldsen and Nielsen 2009; Melzer et al. 2009). High activity of the PP pathway, together with a downregulated tricarboxylic acid (TCA) cycle, represents the ideal flux distribution for an increased molar yield of L-lysine (Kiss and Stephanopoulos 1992). The decreased growth at high temperature can also be explained by the metabolic flux through the TCA-cycle. *C. glutamicum* LYS-12 already exhibits a reduced TCA flux at 30°C due to the attenuation of the isocitrate dehydrogenase expression (Becker et al. 2011). TCA cycle flux was even further decreased at 38°C, which may have resulted in energy shortage. The limited availability of energy for growth and cellular maintenance, highly demanded at elevated temperature, may also lead to the observed phenotype (Hagerty et al. 2014; Mainzer and Hempfling 1976; Schäfer 2016).

2.3 Metabolic engineering of *C. glutamicum*

Metabolic engineering describes the directed optimization of strains towards new or improved properties (Jones and Koffas 2016). In recent years, *C. glutamicum* has been engineered into an efficient producer of a spectrum of more than 70 natural and non-natural products (Figure 1) (Becker et al. 2018b).

The capability of versatile product export displays one of the important features that explains the suitability of *C. glutamicum* as an ideal host for a large group of products, such as the proteinogenic amino acids L-lysine (Wu et al. 2019), L-glutamate (Wang et al. 2018), L-leucine (Feng et al. 2018), the non-proteinogenic amino acids 5-aminovalerate (Rohles et al. 2016), L-pipecolic acid (Pérez-García et al. 2016) and ectoine (Pérez-García et al. 2017), the organic acids succinate (Chung et al. 2017), *cis,cis*-muconic acid (Becker et al. 2018a) and itaconic acid (Otten et al. 2015), alcohols as ethanol (Jojima et al. 2015), isobutanol (Lange et al. 2018) and 2,3-butanediol (Radoš et al. 2015) and the diamines 1,5-diaminopentane (Kim et al. 2018), 1,4-diaminobutane (Nguyen et al. 2015), the terpenoids lycopene (Matano et al. 2014), astaxanthin (Henke et al. 2016) and β-carotene (Taniguchi et al. 2017), aromatic compounds as violacein (Sun et al. 2016), resveratrol (Braga et al. 2018) and protocatechuic acid (Kallscheuer and Marienhagen 2018), antioxidants like biliverdin (Seok et al. 2019) and many others such as hyaluronic acid (Cheng et al. 2017), oelic acid (Takeno et al. 2018) and palmitic acid (Takeno et al. 2013).

Furthermore, metabolic engineering has been applied to modulate endogenous pathways by exploiting the microbes' own regulatory mechanisms. Homologous regulatory circuits of *C. glutamicum* are able to downregulate certain pathways via feedback regulation (Lu and Liao 1997). These feedback mechanisms can be coupled to an optical signal in order to sense a higher concentration of the desired product in high-throughput screening. As example, the protein LysG is a positive regulator of L-lysine, L-arginine and L-histidine export, promoting the expression of the exporter gene *lysE*. The natural function of metabolite sensing systems is to maintain homeostasis for the organism by adapting the concentration of intracellular substances. In order to prevent an excess of L-lysine or L-arginine, *C. glutamicum* is able to promote their export (Bellmann et al. 2001; Eggeling and Sahm 2003).

A biosensor for amino acids has been designed by fusing LysG to eYFP (enhanced yellow fluorescing protein), which enabled rapid identification of overproducing strains,

directly on agar plates (Binder et al. 2012; Jones et al. 2015). If no biosensor for the product of interest is available, as it is the case in most efforts, or the signal is lacking precision, miniaturized cultivation systems allow simultaneous characterization of numerous mutants via subsequent measurement for product concentration in their culture supernatant (Jones et al. 2015).

Moreover, previous efforts have identified transport mechanisms as one important step towards improved producing strains of *C. glutamicum*. The heterologous expression of the *E. coli* L-threonine exporter *rhtC* in a threonine overproducing *C. glutamicum* led to a 12-fold decrease in intracellular L-threonine concentration (Diesveld et al. 2009). High producing strains with extended product spectra or non-natural product concentrations benefit from the ability of expressing numerous export proteins which belong to the superfamily of major facilitator permeases and enable *C. glutamicum* to export known and unknown substances. As an example, the export mechanism for the heterologous platform chemical 1,5-diaminopentane was identified via transcription profiling. Subsequent overexpression of one of the identified permeases led to a significant increase in product formation (Kind et al. 2011). However, many putative translocator proteins still have unknown functions and likely promote the efflux of additional substances, different from their original ones (Eggeling and Sahm 2003; Saier Jr 2000; Vrljic et al. 1999). In addition to active transport, products like L-glutamate can be exported through mechanosensitive channels (Wang et al. 2018). Figure 5 gives an overview on numerous export mechanisms of *C. glutamicum* for the transport of metabolites through its cell envelope.

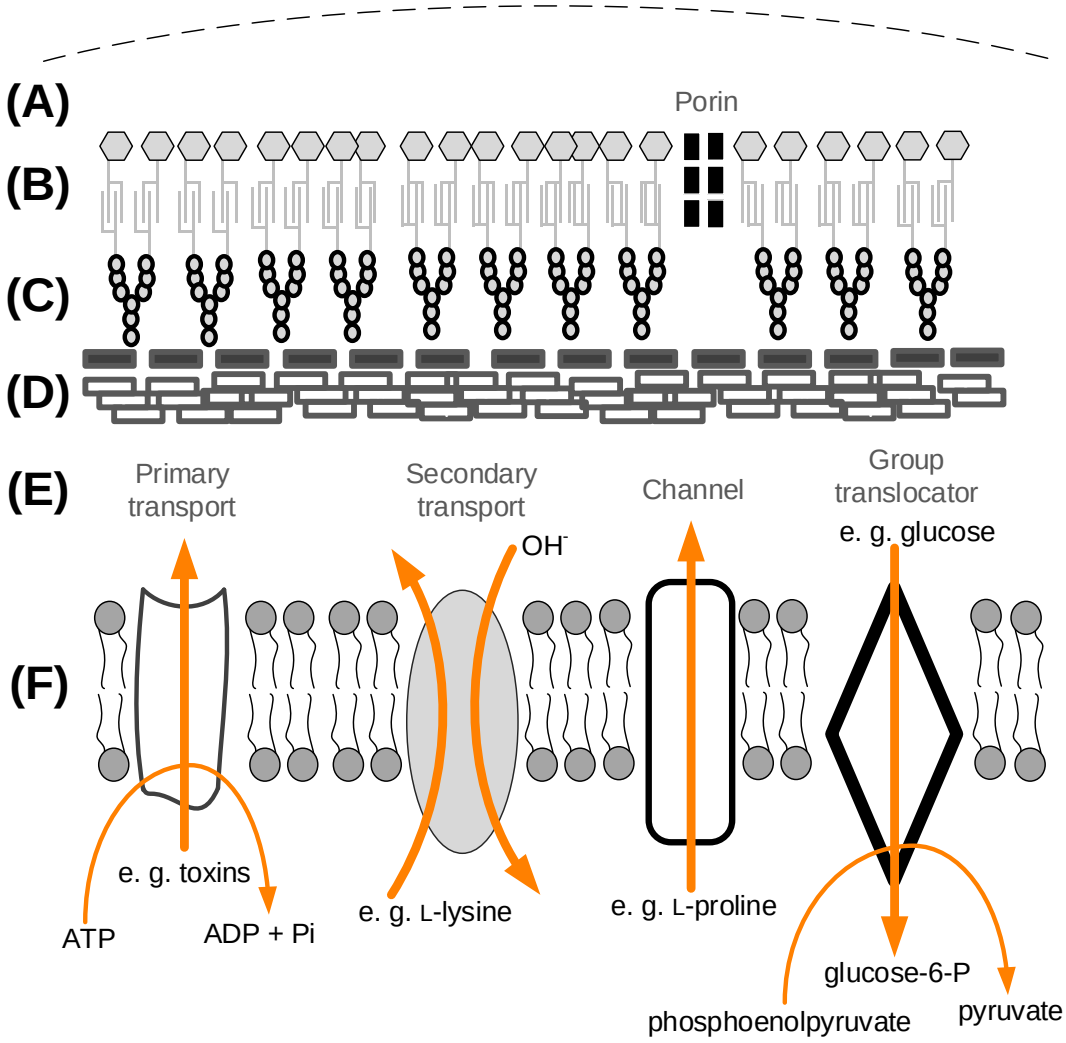

Figure 5. Schematic setup of *C. glutamicum* cell envelope with different types of transporters. A: Polysaccharide matrix. B: Mycomembrane, mucolic acids with non-covalently linked lipids. D: Cell wall core, consisting of peptidoglycan, linked to heteropolysaccharide arabinogalactan (C). E: Periplasm, separates the plasma membrane from the cell wall. F: plasma membrane, bilayer of proteins and phospholipids. Porins in the mycomembrane enable diffusive flux (Lanéelle et al. 2013). Other transporters are located in the plasma membrane. Drug-like toxins are exported via primary transport systems of multi drug exporters at the expense of ATP (Nikaido 1994). Secondary transporters like LysE symport positively charged L-lysine with OH^- (Vrljic et al. 1996). Channels function as valve for solutes (Börngen et al. 2010). Translocators like the phosphotransferase system (PTS) are used for the import and phosphorylation of glucose or sucrose (Moon et al. 2007). The figure has been adapted and modified from Lanéelle et al. (Lanéelle et al. 2013).

2.4 L-Lysine – world leading feed amino acid

2.4.1 Industrial manufacturing and application

The essential amino acid L-lysine has emerged as an important bio-based product. It is the leading food additive in the world and is used to promote growth of mammals (Walz 1985), birds (Lemme et al. 2002), and fishes (Davies et al. 1997). In addition it has important applications in medical (Lai et al. 2014) and chemical industry (Kar et al. 2011).

Turkeys and pigs, supplemented with L-lysine, exhibit a significant increase in muscles mass and a decrease in fat (Lemme et al. 2002; Walz 1985). L-Lysine is crucial for the synthesis of cellular proteins and furthermore acts as an energy source and a promoter for collagen growth (Lai et al. 2014). In addition, L-lysine prevents osteoporosis by improving the absorption of calcium, leading to a recommended daily dose of approximately 1 gram for adults (Flodin 1997; Sallam and Steinbüchel 2010). During infections with the herpes simplex virus, increased doses of L-lysine significantly reduce healing time by limiting virus replication (Flodin 1997). This therapeutic effect is mediated by a shift in the L-lysine to L-arginine ratio, with the latter being overrepresented in viral proteins (Corbin-Lickfett et al. 2010; Flodin 1997). L-Lysine also plays an important role as industrial precursor for the synthesis of pharmacologically active substances such as the drug precursor L-pipecolic acid (Weigelt et al. 2012). L-Pipecolic acid can be formed from L-lysine via two enzymatic steps and is used in the production of anti-cancer drugs, antibiotics, anesthetics or immunosuppressive medicaments (Gatto et al. 2006; He 2006; Pacella et al. 2010; Weigelt et al. 2012).

In the field of polymer synthesis from renewables, L-lysine is an important precursor to derive glutarate (Rohles et al. 2018; Wang et al. 2019), 5-aminovalerate (Rohles et al. 2016) and 1,5-diaminopentane (Li et al. 2014). These substances can be chemically polymerized to form bio-nylon. δ-Valerolactam is directly accessible from 5-aminovalerate and can form bio-nylon by self-polymerization (Park et al. 2014; Rohles et al. 2016). The increasing demand for L-lysine throughout the last years has resulted in a steep market increase. Due to high competition between suppliers (Kats et al. 1994) and continuous improvements in fermentation, strain design, and downstream processing, the price has recently stabilized (Figure 6) (Cheng et al.

2018). The fermentative L-lysine production with *C. glutamicum* is performed in large-scales of approximately 500 m^3 bioreactors in order to meet the market demand (Wittmann and Becker 2007). The industrial fermentation and downstream process for L-lysine is displayed in Figure 7. The biggest industrial L-lysine plants are located in China (1.1 mio tons per year), Indonesia (350k tons per year), Russia (100k tons per year), Brazil (100k tons per year) and the USA (720k tons per year) (Eggeling and Bott 2015).

Depending on the location, different raw materials are used as the basis to provide substrate sugars. Waste streams from starch hydrolysis of maize and wheat plus molasses from sugar refineries contain high amounts of glucose, fructose and sucrose, which can be directly utilized by *C. glutamicum* for L-lysine production (Ikeda 2012; Zhang et al. 2017). Under consideration of the location of the plethora of L-lysine plants in southern countries, process-cooling has one of the biggest shares of the final product price (Ohnishi et al. 2003).

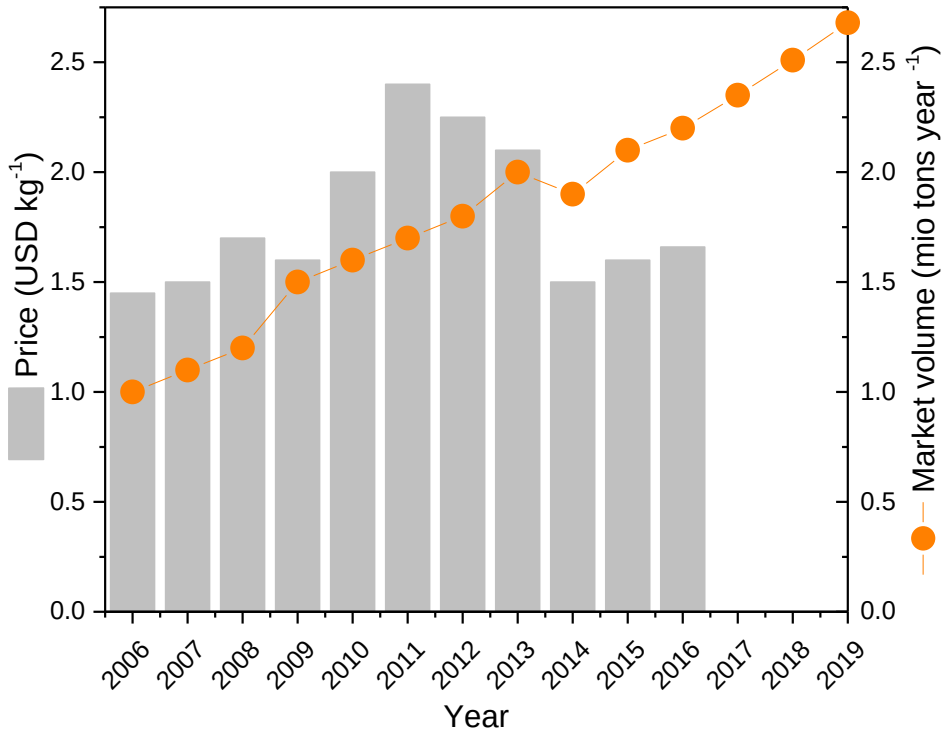

Figure 6. Development of the global L-lysine market volume (orange dots) and price per kg (grey bars). Predicted yields for 2017-2019, expecting a 7% annual growth (Ajinomoto Co., Inc., Tokyo (2018) annual financial report (Cheng et al. 2018; Eggeling and Bott 2015)).

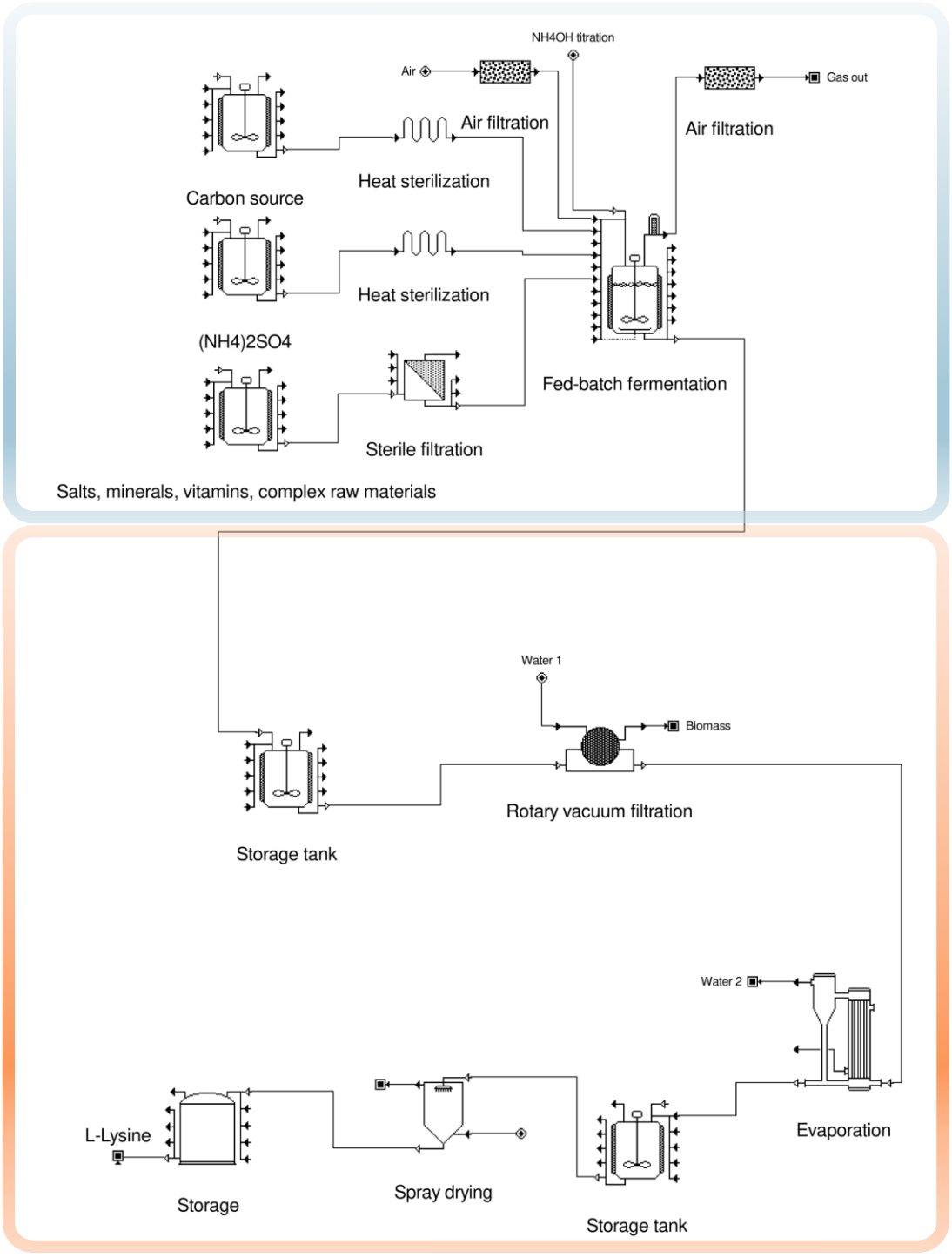

Figure 7. Industrial manufacturing of L-lysine. Upstream process, fermentation (blue) and downstream processing (orange) of an industrial L-lysine fermentation. Nutrients, carbon source and complex elements are sterilized and transferred to the reactor in a fed-batch process. After fermentation, the broth is separated from biomass via filtration or centrifugation. Water is evaporated, the residue is granulated via spray drying. The figure is adapted from previous work (Brunef et al. 2011; Kelle et al. 2005; Knoll and Buechs 2006; Pistikopoulos et al. 2011).

In order to limit production costs, the performance of L-lysine producing *C. glutamicum* at elevated temperatures has been studied (Ohnishi et al. 2003). As an example, *C. glutamicum* LYS-12 (Becker et al. 2011) exhibited a significant increase in L-lysine yield at temperatures up to 38°C (Figure 8) (Schäfer 2016). Higher temperature positively influenced the L-lysine yield at the expense of growth, i.e. biomass yield and specific growth rate. However, the cellular details that mediate these changes have remained largely unclear.

In addition, elevated cultivation temperatures lead to a possible decrease of contamination risks in large scale fermentation processes (Junker et al. 2006). These findings highlight cultivation temperature as an important parameter, not only in terms of economy but also as topic for research.

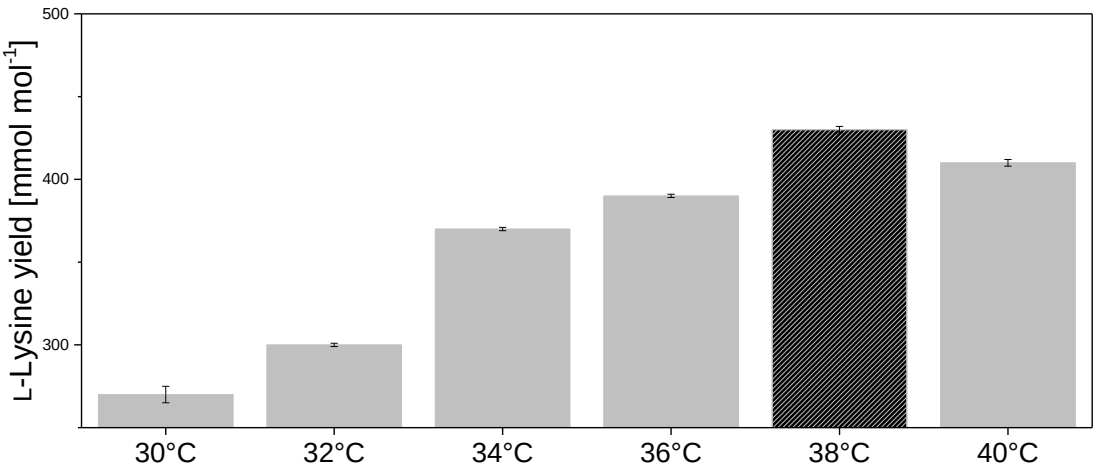

Figure 8. Temperature dependent L-lysine yield of *C. glutamicum* LYS-12. The temperature dependent L-lysine yield of *C. glutamicum* LYS-12, obtained from shake flask cultivations on glucose minimal medium. The data are obtained from previous work (Schäfer 2016)**.**

2.4.2 Strain engineering for L-lysine production

The first L-lysine producing strains of *C. glutamicum* were generated by releasing the enzyme aspartokinase from feedback-inhibition via point mutation (Sano and Shiio 1970). Further optimization of L-lysine synthesis involved the overexpression of key enzymes (Jetten et al. 1995) to enhance the availability of cofactors (Becker et al. 2005) and building blocks (Peters-Wendisch et al. 2001), L-lysine synthesis (Kelle et al. 2005), and L-lysine export (Bellmann et al. 2001). However, these rather local approaches were not able to cope with industrial producing strains, derived from random mutagenesis (Eggeling and Sahm 1999) (Table 1).

More recently, strain optimization was upgraded to systems level metabolic engineering. A systems wide optimization strategy integrated metabolic fluxes and model-based flux prediction into the design of a synthetic L-lysine producing cell factory. This approach led to the development of a highly advanced L-lysine producer, *C. glutamicum* LYS-12 (Becker et al. 2011). The wild-type based strain harbors only twelve genomic modifications and accumulates approximately 120 g L^{-1} L-lysine at a yield of 55% which is in the range of industrial producers (Figure 9) (Becker et al. 2011). *C. glutamicum* LYS-12 exhibits the following complementary modifications: The point mutation T311I results in the replacement of the amino acid L-threonine by L-isoleucine in the enzyme aspartokinase, yielding a feedback insensitive variant (Becker et al. 2005; Kim et al. 2006). Further optimizations improved the supply of reducing power (overexpression of the *tkt*-operon and *fbp*), the supply of the precursor oxaloacetate (overexpression of a point mutated variant of *pyc*, deletion of *pck*), increased flux through the L-lysine biosynthetic pathway (overexpression of *dapB*, *lysA*, *lysC* and *ddh*), and reduced flux through competing pathways (downregulation of *icd* and *hom*) (Figure 9) (Becker et al. 2011).

Likewise, L-lysine producing strains of the last decade were either derived via rational metabolic engineering (Becker et al. 2011; Binder et al. 2012; Ikeda et al. 2011; Ikeda and Takeno 2013; Xu et al. 2014) or more recently, by a combination of classical and rational strain engineering (Xu et al. 2018a; Xu et al. 2018b) (Table 1). These combinatorial approaches provided strains (Xu et al. 2018a) which even exceeded the titers of classical industrial producers (Eggeling and Sahm 1999). So far, *C. glutamicum* LYS-12 exhibits the highest yield and productivity of all strains documented to date (Becker et al. 2011). Besides, *C. glutamicum* related strains like

Brevibacterium flavus (Sano and Shiio 1970)*, Brevibacterium lactofermentum* (Araki et al. 1999) and *Bacillus methanolicus* (Lee et al. 1996) have also been considered for L-lysine production.

Due to the high performance of L-lysine producing strains of *C. glutamicum*, the production of L-lysine related products has gained increasing attraction. The L-lysine production power of *C. glutamicum* LYS-12 was recently used for further approaches. Synthesis of 1,5-diaminopentane (DAP) was enabled by overexpression of the *E. coli* derived gene *ldcC*, achieving DAP titers of more than 80 g L^{-1} (Kind et al. 2010). Equipped with the genes *davA* and *davB* from *Pseudomonas putida*, *C. glutamicum* AVA-3 produced 28 g L^{-1} of 5-aminovalerate (Rohles et al. 2016). Further engineering has provided *C. glutamicum* GTA-4, which was capable of producing more than 90 g L^{-1} of glutarate (Rohles et al. 2018). Another prominent example is the synthesis of L-pipecolic acid. The production of L-pipecolic acid is enabled by overexpression of the *Silicibacter pomeroyi* gene *lysDH* and the endogenous gene *proC* (Pérez-García et al. 2016). In addition, the ability of *C. glutamicum* to channel carbon from numerous substrates efficiently into the L-lysine branch can be further exploited to synthesize the valuable chemical chaperone ectoine (Becker et al. 2013; Pérez-García et al. 2017).

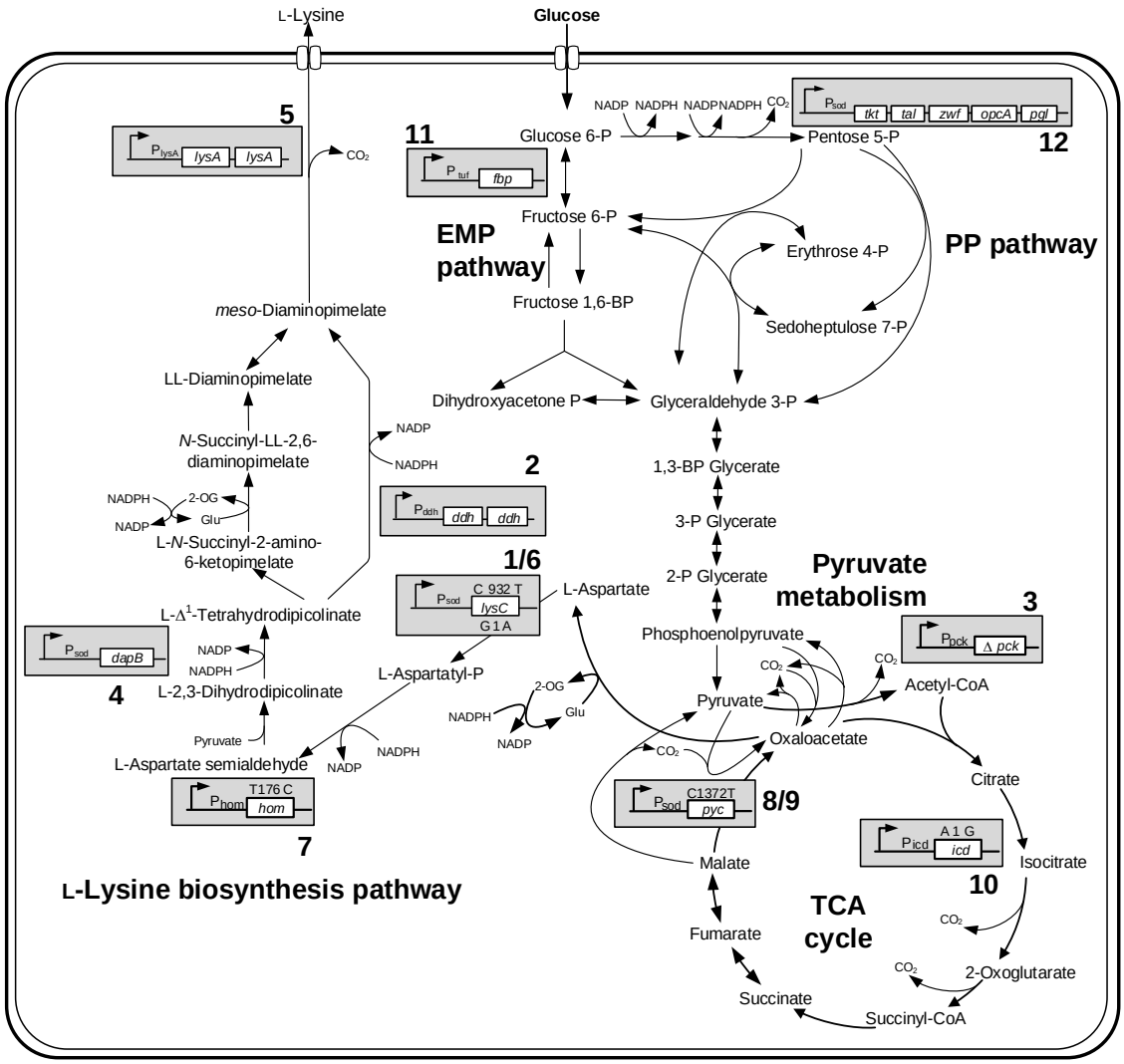

Figure 9. Engineered metabolic pathway of the L-lysine hyper-producer *C. glutamicum* LYS-12. The boxes represent the twelve genetic modifications introduced into the wild type strain *C. glutamicum* ATCC13032 (Becker et al. 2011). 1: nucleotide exchange in *lysC* gene, 2: additional copy of *ddh*, 3: deletion of *pck*, 4: overexpression of *dapB,* 5: additional copy of *lysA*, 6: overexpression of *lysC*, 7: nucleotide exchange in *hom*, 8: nucleotide exchange in *pyc* gene, 9: overexpression of *pyc*, 10: start codon exchange of *icd*, 11: overexpression of *fbp*, 12: overexpression of *tkt*-operon. Figure adapted from Becker et al. 2011 (Becker et al. 2011). PP pathway: pentose phosphate pathway, EMP pathway: Embden-Meyerhof-Parnas pathway, TCA cycle: tricarboxylic acid cycle.

Table 1. Comparison of L-lysine producing strains of *C. glutamicum* regarding yield, titer and productivity.

Strain	Characteristics	Titer [g L^{-1}]	Yield [g g^{-1}]	Productivity [g L^{-1} h^{-1}]	Source
C. glutamicum B6	Derived through mutation with N-nitro-N'-nitro-N-nitrosoguanidine.	100	-	2.1	(Hirao et al. 1989)
C. glutamicum MH20-22B	Derived through mutation.	44	0.44	1.6	(Schrumpf et al. 1992)
C. glutamicum h-8241	Derived through mutation.	48	0.48	-	(Nakano et al. 1994)
C. glutamicum	Derived through mutation, L-leucine and L-homoserine auxotrophy.	60	0.33	-	(Sassi et al. 1996)
C glutamicum MH20-22B/pJC23	MH20-22B, overexpression of *dapA.*	50	0.50	-	(Eggeling et al. 1998)
C. glutamicum	Industrial producer.	170		3.8	(Eggeling and Sahm 1999)
C. glutamicum AHPΔptsH320delA	Mutations: *hom* (V59A), *lysC* (T311I), and *pyc* (P458S), activation of *iolT1*-specified glucose uptake system.	9.3	0.24	-	(Ikeda et al. 2011)
C. glutamicum LYS-12	Mutation: *lysC* (T311I)*, pyc* (P458S), *hom* (V59A), *icd* (A1G); overexpression: *lysC*, *pyc*, *ddh*, *lysA*, *dapB*, *fbp*, *tkt*; deletion: *pck.*	120	0.55	4	(Becker et al. 2011)
C. glutamicum DM1933 *murE*-G81E	Mutation: *murE* (G81E)*, pyc* (P458S), *hom* (V59A), 2x *lysC* (T311I), 2x *asd*, 2x *dapA*, 2x *dapB*, 2x *ddh*, 2x of *lysA*, 2x *lysE*; deletion: *pck.*	7.56	0.36		(Binder et al. 2012)
C glutamicum AGL-6	Mutations: *hom* (V59A), *lysC* (T311I), *pyc* (P458S), *mqo224* (W224opal) *leuC456*	100	0.40	3.3	(Ikeda and Takeno 2013)
C. glutamicum Lys5-8	Mutations:2x *lysC* (C932T), *pyc* (G1A, C1372T), *hom* (T176C), 2x *asd*, 2x *dapA*, 2x *dapB*, 2x *ddh*, 2x *lysA*, *murE* (G242A); deletions: *aceE*, *alaT*, *avtA*, *ldhA*, *mdh*, $ilvN_{C\text{-}T}$, *pck*; integration of *gapC* (*C. acetobutylicum*).	130	0.47	2.73	(Xu et al. 2014)
C. glutamicum $RE2A^{io}$ *lysC gapN*	Combined use of NAD dependent *gapA* and NADPH dependent *gapN.* Mutations: *hom* (T176C), *lysC* (T311I), *pyc* (P458S).	9.55	0.19		(Takeno et al. 2016)
C. glutamicum JL-6ΔdapB::Ec-dapB^{C115G,G116C}	Mutational strain JL-6 as basis. Replacement of the natural *dapB* gene with mutated *E. coli dapB*^{C115G,G116C}.	117.3	0.44	2.93	(Xu et al. 2018b)
*C. glutamicum JL-69*$P_{tac\text{-}M}$ *gdh*	Mutational strain JL-6 as basis. Deletions: *pck, odx*; overexpression: *pyc, ppc, gltA, gdh*. Additional feeding of biotin.	181	-	3.78	(Xu et al. 2018a)

2.5 Ectoine – high-value amino acid for health and well-being

Ectoine (1,4,5,6-tetrahydro-2-methyl-4-pyrimidinecarboxylic acid) is a natural osmolyte. The compatible solute protects species like *Halomonas elongata* (Cánovas et al. 1997), *Pseudomonas stutzeri* (Stöveken et al. 2011) or *Chromohalobacter salexigens* (Vargas et al. 2006) against environmental stress. Due to the fact that its water binding capability is independent from the salt concentration, ectoine maintains hydration and function of proteins even under conditions of severe osmotic stress (Figure 10) (Czech et al. 2018; Held et al. 2010). On a molecular level, compatible solutes support the clustering of water around hydrophobic proteins while improving their function by e.g. preventing denaturation and mediating overall stability (Graf et al. 2008).

The substance has gained substantial interest in the medical, food, cosmetic, and biotechnological industries (Czech et al. 2018). In dermal lotions, ectoine preserves skin moisture, protects the skin against UVA-induced cell damage and aging (Buenger and Driller 2004). In addition, the chemical chaperone is of great interest for the treatment of diseases, based on protein-misfolding. As example, ectoine blocks the aggregation and the neurotoxicity of Alzheimer's β-amyloid or other amyloidogenic proteins, which contribute to the progression of Parkinson’s and Huntington’s disease, respectively (Dobson 2003; Kanapathipillai et al. 2008; Kanapathipillai et al. 2005; Yang et al. 1999). The application of ectoine offers strong resistance to prion peptide-induced toxicity in human neuroblastoma cells, concluding that such molecules can be potential inhibitors of prion aggregation and toxicity (Kanapathipillai et al. 2008). Furthermore, ectoine serves as a protectant against nanoparticle-induced neutrophilic lung inflammation (Sydlik et al. 2009). Transgenic tomato plants accumulating ectoine, exhibit an increased photosynthetic rate through an enhancement of cell membrane stability under oxidative and salt stress (Moghaieb et al. 2011). Similar results are also observed for tobacco plants (Nakayama et al. 2000).

In biotechnology, the production of biodiesel by enzymatic conversion of triglycerides in cottonseed oil is enhanced by the addition of ectoine to the solvent-free methanolysis system. The additive leads to reduced methanol inhibition on the immobilized lipase (Wang and Zhang 2010). Beneficial effects have also been shown for microbial fermentation processes (Malin and Lapidot 1996).

Due to its favorable properties, ectoine has gained enormous economic interest (Melmer and Schwarz 2009). The purchase cost is approximately 9000 US Dollars kg^{-1} (Acadechem, Hong Kong, China) (Cantera et al. 2018; Czech et al. 2018; Strong et al. 2016). The related osmolyte hydroxyectoine (5-hydroxy-2-methyl-1,4,5,6-tetrahydropyrimidine-6-carboxylic acid) is produced from ectoine by microbes such as *Streptomyces coelicolor* under heat stress. The substance exhibits interesting thermo-protective properties (García-Estepa et al. 2006) and is sold for approximately 17,000 US Dollars kg^{-1} (Merck, Darmstadt, Germany) (Cantera et al. 2018; Czech et al. 2018; Strong et al. 2016). From an evolutionary point of view, producers of both compatible solutes as well as sole ectoine producers have evolved, depending on the respective environmental conditions in their natural habitats (Bursy et al. 2008). In terms of benefits for health, hydroxyectoine is sometimes applied in combination with ectoine in order to e.g. treat inflammatory bowel diseases (Abdel-Aziz et al. 2015).

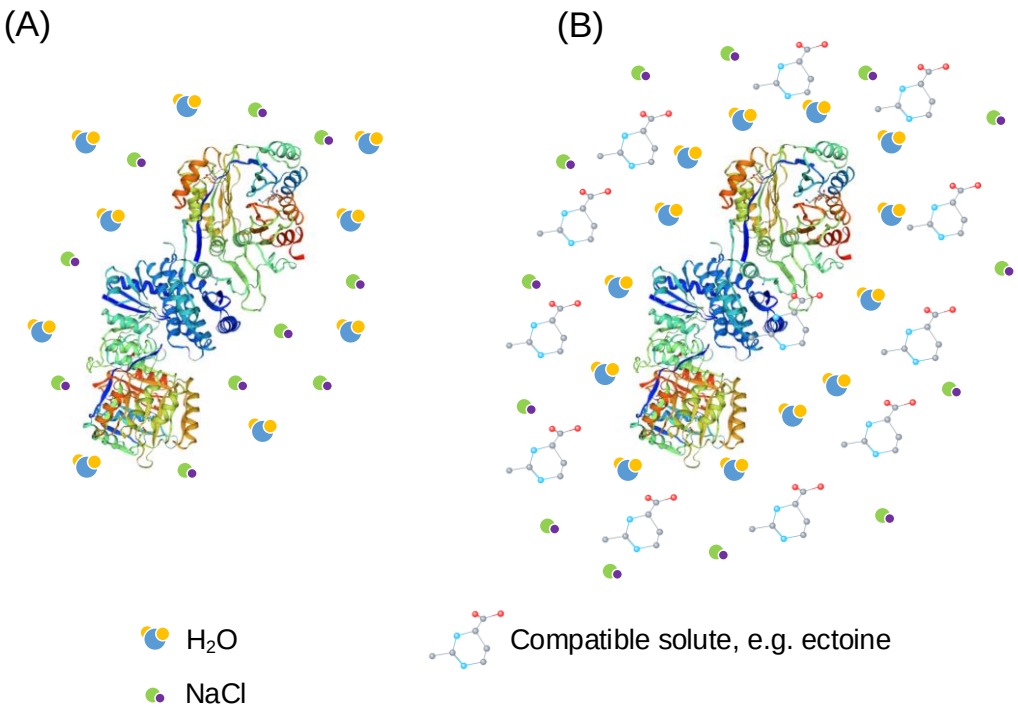

Figure 10. Scheme of protein hydration during salt stress by compatible solutes. During hyperosmotic stress, the protein is denaturized by a decrease in its hydration state (A). In the presence of compatible solutes, salts are excluded from the protein surface, leading to the clustering of water around the protein (B). In this state, the protein is stabilized in its native conformation (Arakawa and Timasheff 1985; Pastor et al. 2010; Qu et al. 1998). For illustration, the protein model structure was obtained from swissmodel.expasy.org (A4QAP5_CORGB).

Most non-halophilic microorganisms, such as *C. glutamicum* are incapable of producing ectoine or hydroxyectoine themselves. Instead, these microbes accumulate intracellular trehalose and L-proline under osmotic pressure (Guillouet and Engasser 1995). However, during the exposition to salt stress, *C. glutamicum* is able to activate osmolyte carriers, in order to promote the uptake of extracellular compatible solutes, like L-proline and ectoine (Peter et al. 1998). So far, a clear regulatory network, as described for oxidative and heat stress, has not been identified for conditions of high osmolarity.

At least, the sigma factor σ^E seems to play a role in the activation of osmoprotection in *C. glutamicum* (Pacheco et al. 2012; Park et al. 2008). In the case of an immediate downshift in osmolarity, mechanosensitive channels are activated within seconds and allow efficient water efflux. The effect of subsequent cell dehydration can be prevented by the accumulation of compatible solutes in the cytoplasm (Wood 1999). ProP and other secondary transporters like BetP, EctP and LcoP promote the influx of the compatible solutes ectoine, betaine or proline (Robertson 2019; Wood et al. 2001). Intracellular solutes are in most cases released by mechanosensitive channels such as the MscL and MscS family or other yet unknown mechanisms (Booth 2014; Börngen et al. 2010; Cox et al. 2018). Mechanisms of these in- and export system of *C. glutamicum* are shown in Figure 11. In contrast to the fast response to high salinity by compatible solute uptake (seconds), the synthesis of the endogenous compatible solutes trehalose and proline happens in a slower range (hours). As a result, the availability of compatible solutes in the cultivation medium promotes the cells resistance against osmotic shifts (Csonka 1989; Kempf and Bremer 1998). However, complex interactions between genome, transcriptome, fluxome, proteome and metabolome, during stress response, like correlations between transcription and translation, as well as the posttranscriptional regulation still remain unclear (Fränzel et al. 2010; Özcan et al. 2005).

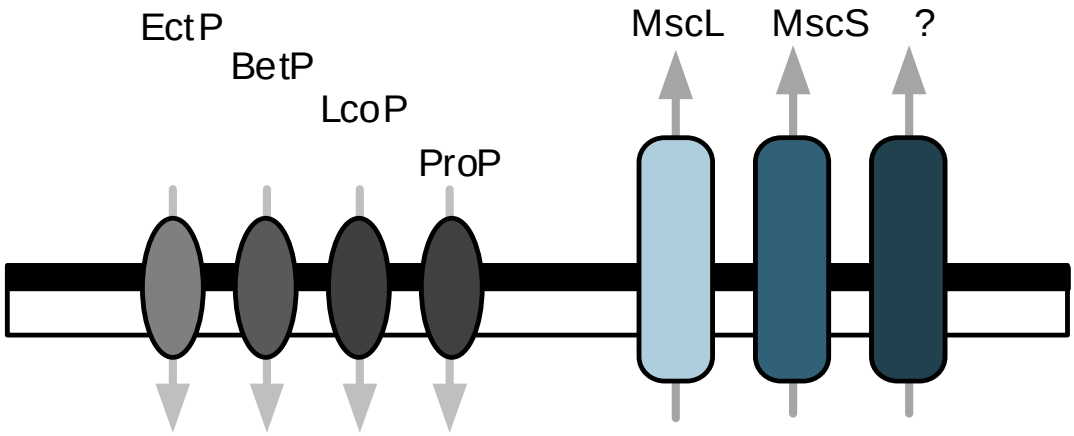

Figure 11. Compatible solute in- and export systems of *C. glutamicum*. Osmoregulated compatible solute import proteins BetP (betaine), EctP (ectoine, betaine, L-proline), LcoP (betaine, ectoine) and ProP (ectoine, L-proline). Mechanosensitive channels MscL and MscS for large and small conductance and unknown export systems for the release of compatible solutes (Morbach and Krämer 2005).

To date, the industrial production of ectoine relies on halophilic microorganisms like *Halomonas elongata* (Cánovas et al. 1997). The cells are grown in high salt media and compatible solute excretion is triggered by an osmotic downshock. This process can be repeated several times, which coined the term “bacterial milking” (Figure 12) (Sauer and Galinski 1998). Unfortunately, it uses highly corrosive media, requires special equipment and reaches relatively low product titers (Fallet et al. 2010; Sauer and Galinski 1998).

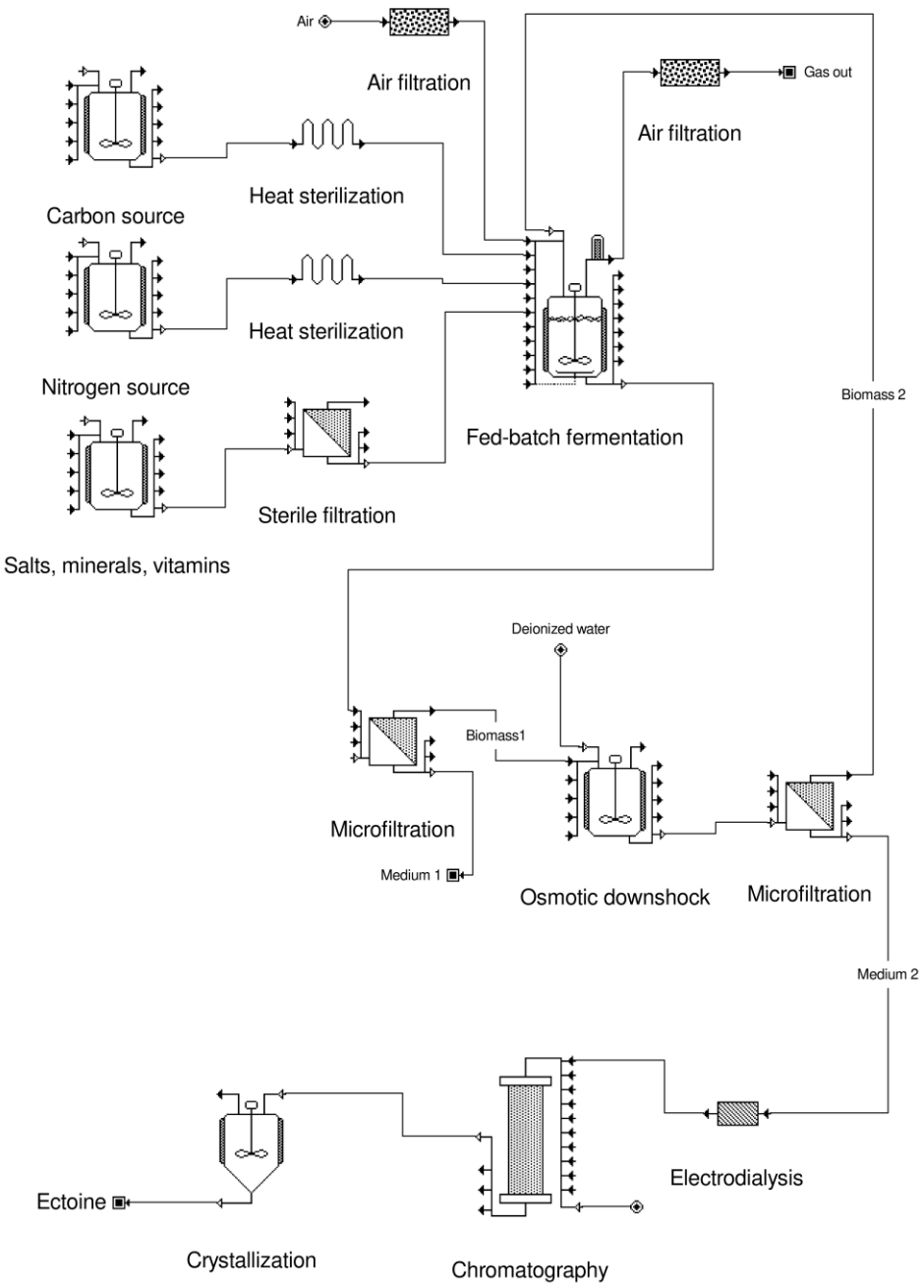

Figure 12. Process scheme of "bacterial milking" of *Halomonas elongata* in industrial processes. After high salinity fermentation of the halophilic *Halomonas elongata*, cells are separated from the medium by filtration and mixed with deionized water in order to release the intracellular compatible solute via osmotic downshock. After the second microfiltration, the biomass can be reused. Salt is removed via electrodialysis and the product is purified via chromatography, prior to crystallization (Kunte et al. 2014)**.**

Another downside of using a natural producer is the complex metabolic regulation cascade, which results in mixtures of ectoine and hydroxyectoine or even in the redirection of both products to catabolism (Schulz et al. 2017). The process requires

an elaborative fermentation-strategy as well as a demanding downstream purification (Sauer and Galinski 1998).

In this regard, heterologous expression of the ectoine genes in well-established industrial production organisms like *E. coli* (Ning et al. 2016) and *C. glutamicum* (Becker et al. 2013; Pérez-García et al. 2017) was successfully demonstrated. These hosts secrete the product directly into the cultivation medium, show growth associated production and can be grown on low salt levels (Becker et al. 2013; Ning et al. 2016; Pérez-García et al. 2017). However, initial approaches suffer from relatively low performance. In addition, undesired production of high amounts of L-lysine was observed (Pérez-García et al. 2017). For heterologous synthesis of ectoine, the genes *ectA* (L-2,4-diaminobutyrate acetyltransferase), *ectB* (L-2,4-diaminobutyrate transaminase) and *ectC* (ectoine synthase), from *Halomonas elongata* were expressed in *E. coli* ECT05 (Ning et al. 2016). The respective genes from *Chromohalobacter salexigens* were expressed in *C. glutamicum* Ecto5 (Pérez-García et al. 2017). By co-expression of the genes *ectA*, *ectB*, *ectC* and *ectD* (ectoine hydroxylase) from *Pseudomonas stutzeri, C. glutamicum* Ect2 was enabled to secrete a mixture of ectoine and hydroxyectoine (Figure 13) (Becker et al. 2013). Previous studies demonstrated a temperature dependent shift in ectoine and hydroxyectoine production for *C. glutamicum* Ect2 (Becker et al. 2013). Especially the increase in hydroxyectoine synthesis at high temperature underlines a temperature dependent activation of ectoine hydroxylase, emphasizing enhanced expression of the protective molecule under heat stress in natural producer strains (Becker et al. 2013; García-Estepa et al. 2006).

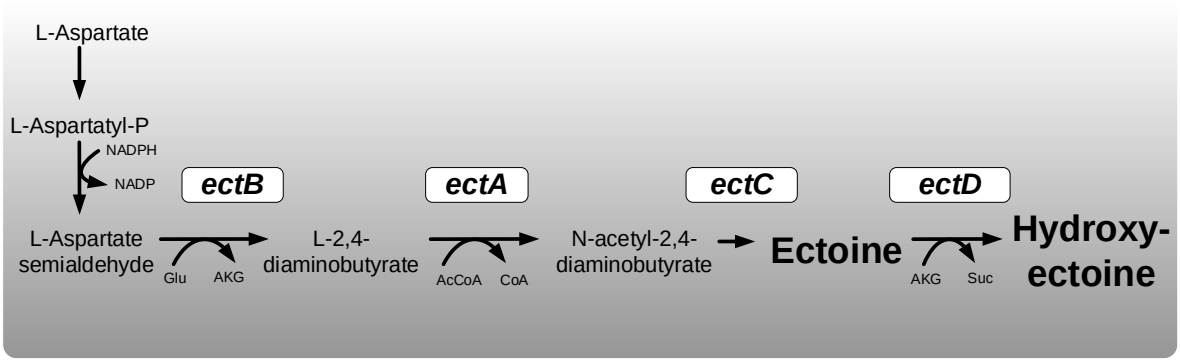

Figure 13. Pathway design for ectoine and hydroxyectoine synthesis in halophilic microorganisms and heterologous hosts. The precursor L-aspartate semialdehyde is synthesized from L-aspartate via aspartokinase and L-aspartate semialdehyde dehydrogenase. The enzyme L-2,4-diaminobutyrate transaminase (*ectB*) forms L-2,4-diaminobutyrate which is converted to N-acetyl-2,4-diamniobutyrate via L-2,4-diaminobutyrate acetyltransferase (*ectA*). The ectoine synthase (*ectC*) catalyzes the reaction from N-acetyl-2,4-diaminobutyrate to ectoine which is then transformed to hydroxyectoine via ectoine hydroxylase (*ectD*) (Mustakhimov et al. 2010).

Characteristics of recent homologous and heterologous ectoine producers are listed in Table 2. One of the first heterologous ectoine producers, *C. glutamicum* Ect2, did not produce significant amounts of by-products, but exhibited a relatively low ectoine titer of 4.5 g L^{-1} (Becker et al. 2013). However, the integration of the ectoine synthesis cassette into the *ddh*-locus, encoding diaminopimelate dehydrogenase of the L-lysine biosynthesis and deletion of the L-lysine export gene *lysE* provided a vital ectoine/ hydroxyectoine producer (Becker et al. 2013). The *ddh* branch of the L-lysine biosynthesis pathway was chosen as integration locus to lower the carbon flux towards L-lysine synthesis under conditions of high ammonium levels in the medium (Becker et al. 2013).

Table 2. Comparison of microorganisms used for the production of ectoine in terms of titer, product yield and productivity.

	Titer [g L^{-1}]	Yield [g g^{-1}]	Productivity [g L^{-1} h^{-1}]	Source
Halomonas elongata DSM142	7.4	-	0.33	(Sauer and Galinski 1998)
Chromohalobacter salexigens DSM3043	32.9*	-	1.35	(Fallet et al. 2010)
C. glutamicum Ect2	4.5	0.23	0.22	(Becker et al. 2013)
E. coli ECT05	25.1	0.11	0.84	(Ning et al. 2016)
C. glutamicum Ecto5	22	0.16	0.32	(Pérez-García et al. 2017)

*continuous cell retention and two continuously operating reactors

The strain *C. glutamicum* Ecto5 was able to accumulate 22 g L^{-1} of ectoine during fed-batch fermentation, but still secreted high amounts of L-lysine and L-glutamic acid into the cultivation medium (Pérez-García et al. 2017). The highest ectoine titer, achieved via heterologous gene expression, was documented for *E. coli* ECT05 (Table 2). The optimization involved the deletion of the competing L-threonine pathway, resulting in an undesired auxotrophy for L-threonine and L-isoleucine (Ning et al. 2016). Consequently, an efficient process in non-natural production of ectoine is still to be developed.

3. Materials and Methods

3.1 Bacterial strains and plasmids

For cloning purposes, *E. coli* DH5α and *E. coli* NM522, were obtained from Invitrogen (Karlsruhe, Germany) and *E. coli* XL1-Blue was obtained from Stratagene (La Jolla, California, USA). *C. glutamicum* ATCC 13032 (American Type Strain and Culture Collection, Manassas, VA, USA) was used as host for genetic engineering and strain development. The strains *C. glutamicum lysC* (Kim et al. 2006), *C. glutamicum* LYS-1, *C. glutamicum* LYS-12 (Becker et al. 2011) and *C. glutamicum* Ect2 (Becker et al. 2013) were obtained from previous work. All strains were stored as cryo-stocks in 60% glycerol at -80°C. Strains used and generated in this work are listed in Table 3.

Genome based modifications in *C. glutamicum* were conducted with the plasmid pClik int*sacB* (Kind et al. 2014). For the episomal overexpression of target genes, the vector pClik 5aMCS was used (Buschke et al. 2013). The plasmids pTc15AcglM expressing the *C. glutamicum* specific DNA-methyltransferase and the *lysE* deletion plasmid (Kind et al. 2011) were obtained from previous work. The plasmid pClik int*sacB ΔmalE* was obtained from BASF SE (BASF SE, Ludwigshafen, Germany). The plasmids used for strain construction are listed in Table 4.

Construction of the ectoine *ectABC* library with the episomal plasmids pCES208 and pCGH was performed by Eun Jeon, Sung Yim and Ki Jun Jeong of the Korea Advanced Institute for Science and Technology, department of Chemical and Biomolecular Engineering.

.

Table 3. Bacterial strains used in this work.

Strain	Description	Source/Reference
E. coli XL1-Blue	Electrocompetent cells for ectoine library construction	Stratagene
E. coli DH5α	Heat shock competent cells for the amplification of the transformation vector	Invitrogen
E. coli NM522	Heat shock competent cells for the amplification and methylation of the transformation vector	Invitrogen
C. glutamicum ATCC 13032	Wild type	American Type Strain and Culture Collection, Manassas, VA, USA
C. glutamicum lysC	*C. glutamicum* ATCC 13032 (Manassas, VA, U.S.A) with a single nucleotide replacement S301Y in the *lysC* (NCgl0247) gene encoding aspartokinase	(Kim et al. 2006)
C. glutamicum LYS-1	L-Lysine producer based on *C. glutamicum* ATCC 13032	(Becker et al. 2011)
C. glutamicum LYS-12	L-Lysine hyper-producer	(Becker et al. 2011)
C. glutamicum Ect1	*C. glutamicum lysC* T311I genomic integration of the codon-optimized biosynthetic ectoine/hydroxyectoine cluster P_{tuf}*ectABCD* of *P. stutzeri*.	(Becker et al. 2013)
C. glutamicum Ect2	*C. glutamicum lysC* T311I genomic integration of the codon-optimized biosynthetic ectoine/hydroxyectoine cluster P_{tuf}*ectABCD* of *P. stutzeri* and deletion of *lysE.*	(Becker et al. 2013)
C. glutamicum LYS-12 *Δ*m*alE*	L-Lysine hyper-producer based on *C. glutamicum* LYS-12 with additional deletion of *malE*	This work
C. glutamicum LYS-12 2x*lysGE*	L-Lysine hyper-producer based on *C. glutamicum* LYS-12 with an additional copy of the gene cluster *lysGE* in the *bioD* locus	This work
C. glutamicum lysC ∆*lysE*	*C. glutamicum lysC* with deletion of the L-lysine exporting gene *lysE* (Ncgl1214)	This work
C. glutamicum lysC ∆*lysE ectABC*^{basic}	*C. glutamicum lysC* ∆*lysE* + pClik 5aMCS P_{tuf}*ectABC*	This work
C. glutamicum PX.Y*	*C. glutamicum lysC* ∆*lysE* + respective ectoine gene cluster library pCES208	This work
C. glutamicum Ect2 ΔNCgl2523	*C. glutamicum* Ect2 with deletion of the transcriptional regulator gene NCgl2523	This work

*The code PX.Y for the library mutants refers to an internal numbering of the strains, reflecting plate number and colony number from original isolation.

Table 4. Bacterial gene expression vectors used in this work. MCS: multiple cloning site, ORI: origin of replication, *kanR*: Kanamycin resistance, *sacB*: levan sucrase.

Plasmids	Description	Source/Reference
pTc15AcglM	Expression of the *C. glutamicum* specific methyltransferase	(Becker et al. 2011)
pClik 5aMCS	Episomal replicating expression vector carrying a MCS for *C. glutamicum*, an ORI for *E. coli*, and *kanR* marker	(Becker et al. 2011)
pClik int*sacB*	Integrative vector carrying a MCS for *C. glutamicum*, an ORI for *E. coli*, and *kanR* and *sacB* as selection markers	(Becker et al. 2011)
pClik int*sacB* Δ*lysE*	Deletion vector for *lysE*	(Kind and Wittmann 2011)
pClik int*sacB* Δ*malE*	Deletion vector for *malE*	(BASF SE, Ludwigshafen, Germany)
pClik int*sacB lysGE* Δ*bioD*	Integrative vector for integration of *lysGE* into *bioD*	This work
pClik 5aMCS P_{tuf}*ectABC*	Episomal vector for expression of *EctABC* under the control of the *tuf* promoter of the elongation factor Tu from *C. glutamicum* Ect1	This work
pCES208 PX.Y*	Ectoine gene cluster library plasmids based on pCES208	This work
pClik int*sacB* ΔNCgl2523	Deletion vector for NCgl2523	This work

*The code PX.Y for the library mutants refers to an internal numbering of the strains, reflecting plate number and colony number from original isolation.

3.2 Genetic engineering

For the design of construction and sequencing primers and the calculation of individual annealing temperatures (T_a) and elongation times (t_e), the software Clone manager (Sci-Ed, Morrisville, USA) was used. Primers used for template amplification or sequencing are listed in Table A 1 (Appendix).

The polymerase chain reaction (PCR) was used for the amplification of genes from genomic or plasmid template DNA, for assembly of plasmids, and strain identification. A standard PCR reaction consisted of 10 µL PCR mastermix, 0.5 µL of each primer (400 nmol), 0.6 µL DMSO, 5-500 ng of template and 8.4 µl H_2O. The PCR was performed with the thermal cycler Peqstar 2 (PEQLAB Biotechnology GmbH, Erlangen, Germany). For the test of single colonies, the 2x Phire Green Hot Start II DNA PCR Mastermix (Thermo Fisher Scientific, Rochester, New York, USA) was used, construction fragments were amplified with the 2x Phusion PCR Mastermix (Thermo Fisher Scientific, Rochester, New York, USA) according to the temperature profile listed in Table 5.

For heterologous expression of the ectoine cluster, the vector pClik 5aMCS was linearized, using the restriction enzyme *Nde*I (FastDigest, Thermo Fischer Scientific), followed by *in vitro* assembly with the codon-optimized construct P_{tuf}*ectABC* (Rohles et al. 2016). After amplification in *E. coli* DH5α, methylation in *E. coli* NM522, and isolation (QIAprep Spin MiniPrep Kit, Quiagen, Hilden, Germany), the functional plasmid was transformed into *C. glutamicum* using electroporation (Kind et al. 2013). Genomic deletion of the gene *lysE*, encoding for the L-lysine exporter (NCgl1214), was performed as described previously (Kind et al. 2011). The integrative vector pClik int*sacB* was linearized with the restriction enzyme *BamH*I for the *LysGE* overexpression plasmid and *Sma*I for the NCgl2523 deletion plasmid. The fragments were assembled *in vitro* and the final products were transformed as described before. Validation of genetic modifications was conducted by PCR and sequencing (GATC Biotech AG, Konstanz, Germany).

Table 5. Temperature profile of the polymerase chain reaction.

Step	Temperature [°C]	Time [min]	Number of Cycles [-]
Initial denaturation	99	15	1
Denaturation	98	0.5	
Annealing	T_a	0.5	30
Elongation	72	t_e	
Final elongation	72	5	1

Construction of the combinatorial ectoine pathway was performed by Eun Jeon, Sung Yim and Ki Jun Jeong of the Korea Advanced Institute for Science and Technology, department of Chemical and Biomolecular Engineering.

For the construction and assembly of the ectoine plasmid library, the shuttle vector pCES208 was used. The primers utilized for construction are listed in Table A 1. *E. coli* XL1-Blue served as transformation host using electroporation. The combinatorial library of *ectA* was constructed, using 19 synthetic promoters (Table 6), three bicistronic designed elements (BCDs), BCD2, BCD8 and BCD21 (Table 7), and the transcriptional terminator rrnBT1T2 (Mutalik et al. 2013; Yim et al. 2013; Yim et al. 2016) . All selected promoters exhibit a different expression strength: H36 (100%), H5 (69%), H3 (68%), H34 (68%), H30 (67%), H28 (65%), H72 (62%), H4 (60%), H17 (58%), I29 (48%), I9 (45%), I12 (40%), I16 (36%), I15 (35%), I64 (33%), I51 (31%), L10 (18%), L80 (16%), L26 (13%).The selected BCDs can also be divided into strong (BCD02, 100%), medium (BCD21, 23%), and weak variants (BCD08, 8%).

In order to construct the initial library, the codon optimized gene *ectA* was amplified by PCR with the primers BCD-F-*BamH*I, *ectA*-R and either BCD2-*ectA*-F, BCD8-*ectA*-F or BCD21-*ectA*-F. The PCR products were mixed and digested with the restriction enzymes *BamH*I and *Not*I, and cloned into the vector pCGH36A containing the synthetic promoter PH36 and the terminator rrnBT1T2. The next step involved the cloning of the 19 synthetic promoters into the *Kpn*I and *BamH*I sites of pCGH36A-*ectA*, resulting in the plasmid pCGH36A-*ectA*-Lib.

The combinatorial libraries for the genes *ectB* (pCGH36A-*ectB*-Lib) and *ectC* (pCGH36A-*ectC*-Lib) were constructed analogously. For the assembly of the whole

module into the vector pCES208, the promoters-BCDs-*ectA*-rrnBT1T2 element was amplified using the primers XhoI-*ectA*-F and *ectA*-R-*Not*I. The resulting PCR products were digested with *Xho*I and *Xba*I and cloned into *Sal*I and *Spe*I sites of pCES208, resulting in the plasmid p*ectA*Lib. For the integration of the other gene libraries, the *ectB* and *ectC* modules were amplified using the primers XhoI-*ectB*-F and *ectB*-*Sal*I-*Xba*I-R, as well as *Sal*I-*ectC*-F and *ectC*-*Xba*I-R, respectively. PCR products were digested with *Xho*I and *Xba*I and cloned into p*ectA*Lib and subsequently p*ectB*Lib. The last assembly did yield the plasmid mixture p*ectABC*-Lib, which was then transformed into *C. glutamicum lysC* Δ*lysE.* All strains are listed in Table 3. The screening and sequencing of the ectoine library transformants was performed by Demian Dietrich during his Master thesis at the Institute of Systems Biotechnology (Saarland University, Saarbrücken, Germany).

Table 6. Promoters used for ectoine library construction.

	Promoter	Sequence
High strength	H36	GGTACCTCTATCTGGTGCCCTAAACGGGGGAATATTAACGGGCCCAGGGTGGTCGCACCTTGGTTGGTAGGAGTAGCATGGGATCC
	H4	GGTACCTGGATTTAGCAATTGGAGTGGCGTATCATGGACGTCCAATTGAGGTATAATAACAGGAGAAGAGGAGAAGCAGGGGATCC
	H5	GGTACCGGTGGTCGTGCTGACTCTACGGGGGAGGAAGTTCAGCTGGTACTGCTCGCGTTGGCTGATAAAGGAGTAGAGTTGGATCC
	H30	GGTACCAAAGTAACTTTTCGGTTAAGGTAGCGCATTCGTGGTGTTGCCCGTGGCCCGGTTGGTTGGGCAGGAGTATATTGGGATCC
	H72	GGTACCGGAGACAATTTGTGCTTCGACGATTTTGTTGGTTAGCACGATCATTTACTGGCGCGCCTCCTAGGAGTATTCTTGGATCC
	H17	GGTACCCCGAGTAGCCGGCCCGAGGGTTAAGGTTAGATTGTTGATCGTCGTGGCACGGTGGGACTTGTAGGAGTAAGTTGGGATCC
	H3	GGTACCTTCGCTTGTAGTTTGGGGGTGTCGCTTATGGTTTAGATCTTCCGTTGCAGACGAGTGATTTGAGGATTAGAGTCGGATCC
	H28	GGTACCGGGGTTTGGCCGATCGGTATTCTCCTTACATTCGGCTTTAAGTTAGCAATTACTTTATGCTTAGGAGTATCGTTGGATCC
	H34	GGTACCCTGCAAGGCAATGTTCGATGTTGGGCTTCATTTTGAGGGTTTGGTTGAGTTTCAAGGGTCGTAGGATAATAATGGGATCC
Medium strength	I29	GGTACCCCTTTTTGAGTGATGAATTTGGTCTTGGTTCGGTTGGTGTTAGTGGGGGTGTATTGGGGTAATAGGAGTATGCTTGGATCC
	I9	GGTACCGACATAGAGAAGGTCTTTTTCTGTTATAGTGTGGAAGCGTATGGACCGCGCTATGGGAGGGTAGGATTTGGATGGGATCC
	I12	GGTACCAGTAGTACAGAGATATAGTTCCGGTGGGCGTGTTTGGGATGTGCTTCTGGTCGTTGCCCAATAGGAGTACGATTGGATCC
	I15	GGTACCGTGGTAGTGCTTTGATCGGCTGTAGATAGTGACTTGGATTTTAGATTGTTGTCGGGTCTCTGAGGATATATTCTGGATCC
	I64	GGTACCGGATTTCTTCGTGGTGTCGGGCTAGTAAGCTACGGTTGGTGGCCTTTTGTTACCCGTCGTTTAGGACTAGAGTCGGATCC
	I51	GGTACCCTGTGTCGTAGGTCTCAAACGGCGTGGAGTTACGGGCTCCCGCATGGCGTGTCACTAGCGTAAGGAGCTAGAGTGGATCC
Low strength	L10	GGTACCGCAGACGGTTATGGTCGCCGCTAGGTCTTGGGGAGTTTTGTTCGGTAGTTATTTATTGTTGAAGGAGATAGATTGGATCC
	L80	GGTACCTTATTGTGGATGTGCTCGTATACCATTGGGGGCATGTCAGCGGCGGTTAGTAGTGTAGATGTAGGAGGGCATTGGGATCC
	L26	GGTACCGTGAGTTTAGAGCAGGGGGGGGGGTTCTTTATGTATGTTCGACGTCGCTTTAGTATGCGTTAGGATTACTATCGGATCC

Table 7. Bicistronic designed elements used for ectoine library construction.

	Bicistronic part	Sequence
High strength	BCD2	GGGCCCAAGTTCACTTAAAAAGGAGATCAACAATGAAAGCAATTTT CGTACTGAAACATCTTAATCATGCTAAGGAGGTTTTCTAATG
Medium strength	BCD21	GGGCCCAAGTTCACTTAAAAAGGAGATCAACAATGAAAGCAATTTT CGTACTGAAACATCTTAATCATGCGAGGGATGGTTTCTAATG
Low strength	BCD8	GGGCCCAAGTTCACTTAAAAAGGAGATCAACAATGAAAGCAATTTT CGTACTGAAACATCTTAATCATGCATCGGACCGTTTCTAATG

3.3 Media and cultivation

The first pre-culture was conducted in liquid BHI medium (37 g L^{-1} Becton Dickson, Heidelberg, Germany). The second pre-culture and the main culture were grown in minimal medium containing per liter: 10 g glucose, 15 g $(NH_4)_2SO_4$, 1 g NaCl, 0.2 g $MgSO_4 \cdot 7H_2O$, 55 mg $CaCl_2$, 20 mg $FeSO_4 \cdot 7H_2O$, 0.5 mg biotin, 1 mg thiamin·HCl, 1 mg calcium pantothenate, 100 mL buffer solution (2 M potassium phosphate, pH 7.8), 10 mL trace element solution (200 mg L^{-1} $FeCl_3 \cdot 6H_2O$, 200 mg L^{-1} $MnSO_4 \cdot H_2O$, 50 mg L^{-1} $ZnSO_4 \cdot 7H_2O$, 20 mg L^{-1} $CuCl_2$ H_2O, 20 mg L^{-1} $Na_2B_4O_7 \cdot 10H_2O$, 10 mg L^{-1} $(NH_4)_6Mo_7O_{24} \cdot 4H_2O$, adjusted to pH 1 with HCl), and 1 mL chelating agent solution (30 mg of 3,4-dihydroxybenzoic acid with 50 µL 6 M NaOH). All solutions were sterilized by autoclaving or sterile filtration. Antibiotics were added from filter sterilized stocks to final concentrations of 50 mg mL^{-1} kanamycin or 12.5 mg mL^{-1} tetracycline, when needed.

3.3.1 Shake flask cultivation

Cultivations in shake flasks were generally carried out at 30°C if not stated differently. After 24 h incubation on BHI agar, a single colony was picked to inoculate the first pre-culture in liquid BHI medium (baffled shake flasks with 10% filling volume) and incubated for 10 h in an orbital shaker at 230 rpm (Multitron, Infors AG, Bottmingen, Switzerland). Cells from the first pre-culture were harvested by centrifugation (4 min, 8800 xg, 30°C), washed twice with medium, and used to inoculate the second pre-culture, which was harvested during the exponential growth phase to inoculate the main culture as described above. All cultures were conducted in triplicates.

3.3.2 Parallel screening in mini-bioreactors

Cells were cultivated in a micro-bioreactor with online optical density measurement (BioLector 1, m2plabs, Baesweiler, Germany), using 48-well flower plates (m2plabs, Baesweiler, Germany). Each well was filled with 500 µL minimal glucose medium as described before. For high throughput screening of ectoine producing strains, single colonies were picked from a fresh agar plate culture and used for direct inoculation of each well. The incubations were conducted at 1,300 rpm, 30 °C, and 85 % humidity.

3.3.3 Production in lab-scale bioreactors

Fed-batch production of ectoine was conducted in 1 L lab-scale bioreactors (SR0700ODLS,DASGIP AG, Jülich, Germany), controlled by a process control software (DASGIP AG, Jülich). The initial batch medium (300 mL) contained per liter: 100 g glucose, 72.4 g sugar cane molasses (Hansa Melasse, Bremen, Germany), 35 g yeast extract (Difco, Becton Dickinson), 20 g $(NH_4)_2SO_4$, 100 mg $MgSO_4$, 11 mg $FeSO_4 \cdot 7H_2O$, 10 mg citrate, 250 µL H_3PO_4 (85 %), 60 mg Ca-pantothenate, 18 mg nicotinamide, 15 mg thiamin HCl, 9 mg biotin, and 200 mg of Antifoam 204 (Sigma-Aldrich, Taufkirchen, Germany). After the initial glucose concentration had dropped below 15 g L^{-1}, feeding was initiated for the *C. glutamicum* P3.4 fed-batch fermentation. The feed was added pulse wise in order to keep the glucose level above 10 g L^{-1}. The feed solution contained per liter: 670 g glucose, 162.5 g sugar cane molasses, 40 g $(NH_4)_2SO_4$ and 2 ml antifoam. The pH value was monitored online (Mettler Toledo, Giessen, Germany) and maintained at pH 7.0 by automatic addition of 25% NH_4OH (MP8 pump system, Eppendorf, Hamburg, Germany).The temperature was kept constant at 30°C. The pO_2 level was monitored online (Hamilton, Höchst, Germany) and maintained above 30% saturation by adjusting stirrer speed, aeration rate and oxygen concentration of the in-gas.

3.4 Analytical Methods

3.4.1 Quantification of cell concentration

Cell concentration was determined via optical density measurement at 660 nm (OD_{660}) (UV1600PC (VWR, Radnor, PA, USA)). Cell dry mass was determined as described previously (Becker et al. 2009; Rohles et al. 2016). The resulting correlation factors between OD_{660} and cell dry mass (CDM) were CDM [g L^{-1}] = 0.32 × OD_{660} (30°C) and CDM [g L^{-1}] = 0.34 × OD_{660} (38-40 °C) (Schäfer 2016).

3.4.2 Quantification of sugars and organic acids

Glucose and trehalose were quantified by HPLC (High Pressure Liquid Chromatography) (Agilent 1260 Infinity Series, Agilent Technologies, Waldbronn, Germany), using a Microguard pre-column (Cation+ H+ 30x4.6, Bio-Rad, Hercules, CA, USA) and an Aminex HPX-87H main column (Bio-Rad) as solid phase. As mobile phase, 5 mM H_2SO_4 (55° C, 0.7 mL min^{-1}) was used. Detection was performed either by refractive index measurement (glucose, trehalose) or by UV absorbance at 210 nm (organic acids).

3.4.3 Quantification of amino acids and ectoine

Ectoine was quantified by HPLC (1290 Infinity, Agilent Technologies, Waldbronn, Germany), using a reversed phase column (Zorbax Eclipse Plus C18, 4.6 x 100 mm, 3.5 µm, Agilent) as stationary phase, demineralized water (0.5 mL min^{-1}, 25°C) as mobile phase and UV detection at 210 nm. Amino acids were quantified by HPLC (Agilent 1200 Series, Agilent Technologies, Waldbronn, Germany) on a reverse phase column (Gemini5u, Phenomenex, Aschaffenburg, Germany) with fluorescence detection, after pre-column derivatization with *o*-phthalaldehyde and fluorenylmethoxycarbonyl (Krömer et al. 2005). Quantification involved α-aminobutyric acid as an internal standard (222.22 µM) (Kind et al. 2010).

3.4.4 Quantification of intracellular amino acids

For the extraction of intracellular amino acids, cells were grown in triplicates in minimal medium until an OD_{660} of 5 was reached. From the growing culture, 2 ml were vacuum filtered using filters with 0.2 µm pore size (Sartorius Stedim Biotech GmbH, Göttingen,

Germany) and washed twice with 15 ml 2.5 % NaCl solution. The filters were incubated for 15 min at 100°C with 2 ml α-aminobutyric acid (222 µM). The resulting solution was centrifuged and the final supernatant was analyzed using HPLC as described in section 3.4.3.

3.4.5 Determination of enzyme activities

Enzyme assays were conducted by Alina Banz during her Master thesis at the Institute of Systems Biotechnology (Saarland University, Saarbrücken, Germany).
Crude cell extract of exponentially growing cells was prepared as previously described (Becker et al. 2009) and used for determination of enzyme activity and protein content. The latter was quantified by the method of Bradford (Kruger 2009) with a reagent solution from BioRad (Quick Start Bradford Dye, BioRad, Hercules, USA). For each enzyme studied, the appropriate washing and disruption buffers were used. Activities of glucose 6-phosphate dehydrogenase (Becker et al. 2007), isocitrate dehydrogenase (Becker et al. 2009), fructose 1,6-bisphosphatase (Becker et al. 2005) and diaminopimelate dehydrogenase (Cremer et al. 1988) were determined as described previously.

3.4.6 RNA sequencing

Biological triplicates of exponentially growing cells were harvested in 2 ml aliquots by centrifugation, and the pellet was immediately frozen in liquid nitrogen. Samples were stored at -80°C until use. Total RNA was extracted using NucleoZol (Macherey-Nagel; Lab Supplies, Athens, Greece) and glass beads (Lysing matrix B, MP Biomedicals, Illkirch-Graffenstaden, France). For cell disruption in the Precellys 24 (Bertin Technologies, Montignyle-Bretonneux, France), samples were homogenized two times at 6500 rpm for 20 s with a 1 min break on ice in between. Further preparations were performed as recommended by the manufacturer. Obtained RNA was DNAse I digested (Invitrogen, Karlsruhe, Germany) and analyzed for integrity with the Agilent Bioanalyzer 2100 using RNA 6000 Pico Kit (Agilent Technologies, Böblingen, Germany) as well as with reducing gel electrophoresis (Aranda et al. 2012). Ribosomal RNA was removed from the total RNA using the Ribo-Zero rRNA removal kit for Gram-positive bacteria (Illumina, San Diego, CA, USA) according to manufacturer's manual. The ribodepleted RNA was then tested for successful removal of rRNA (Agilent 2100

Bioanalyzer RNA 6000 Pico Kit). For the subsequent cDNA library preparation, the NEBNext® Ultra™ Directional RNA Library Prep Kit for Illumina (New England Biolabs, Ipswich, Massachusetts, USA) was used according to manufacturer's recommendation. The libraries were sequenced as single reads on an Illumina HiSeq 2500 platform (Illumina, San Diego, CA, USA) by the Institute for Genetics and Epigenetics at the Saarland University. The obtained sequences were aligned to the reference genome for *C. glutamicum* ATCC13032 (NC_003450.3) obtained from the National Centre for Biotechnology Information (www.ncbi.nlm.nih.gov) using Bowtie2 2.3.4.1 with local alignment settings (Langmead and Salzberg 2012). Visualization and differential expression analysis of the mapped reads were conducted using the software ReadXplorer 2 2.2.3 at default settings (Hilker et al. 2016).

4. Results and Discussion

4.1 Temperature impact on the metabolism of *C. glutamicum* LYS-12

The effect of temperature on L-lysine production and cellular metabolism has been studied for the advanced L-lysine producer *C. glutamicum* LYS-12 (Schäfer 2016). An elevated temperature of 38°C was beneficial for the stoichiometry of the conversion of glucose to L-lysine. The L-lysine yield was enhanced by approximately 40% as compared to 30°C. Previous work has shown that growth was reduced and trehalose yield was increased while metabolic fluxes were significantly affected (see section 2.2) (Schäfer 2016). Next, the influence of the temperature was assessed in more detail to explore the underlying metabolic and regulatory mechanisms.

4.1.1 Enzyme capacity in the central carbon metabolism

To this end, the activity of enzymes from core- and L-lysine biosynthetic metabolism has been quantified. The selected enzymes comprised glucose 6-phosphate dehydrogenase (G6PDH), isocitrate dehydrogenase (ICD), malic enzyme (MalE), fructose 1,6-bisphosphatase (FBP) and diaminopimelate dehydrogenase (DDH) (Table 8).

Table 8. Enzyme activities of *C. glutamicum* LYS-12 at different temperatures. The strain was cultivated at 30°C and 38°C in minimal medium. The results represent mean values and standard deviations from three biological replicates. In addition, each enzyme was assayed at both temperatures. G6PDH: glucose 6-phosphate dehydrogenase, ICD: isocitrate dehydrogenase, MalE: malic enzyme, FBP: fructose 1,6-bisphosphatase, DDH: diaminopimelate dehydrogenase.

		Activity [U $g_{biomass}^{-1}$]	
		Cultivation temperature [°C]	
Enzyme	**Measurement temperature [C°]**	**30**	**38**
DDH	30	301±9	363±11
	38	425±13	525±16
G6PDH	30	198±5	203±8
	38	213±12	201±8
ICDH	30	331±15	269±20
	38	438±42	387±21
FBP	30	292±9	384±12
	38	355±11	513±15
MalE	30	176±13	226±24
	38	253±38	364±5

Most enzymes were significantly activated in cells grown at the higher temperature. As example, the activity of diaminopimelate dehydrogenase and of fructose 1,6-bisphosphatase was increased by 24% and 45% respectively, when cultivated at 38°C. In comparison, glucose 6-phosphate dehydrogenase remained unaffected. Measurements and cultivations were conducted at both temperatures in order to elucidate to which extent a change in activity is based on specific enzyme properties or the enzyme concentration.

Figure 14 highlights the metabolic potential of *C. glutamicum* at 38°C normalized to the reference temperature of 30°C. Diaminopimelate dehydrogenase and fructose 1,6-bisphosphatase showed the strongest increase in their specific activity. Besides, the activity of glucose 6-phosphate dehydrogenase and isocitrate

dehydrogenase remained nearly unchanged while the malic enzyme exhibited an upregulated specific activity.

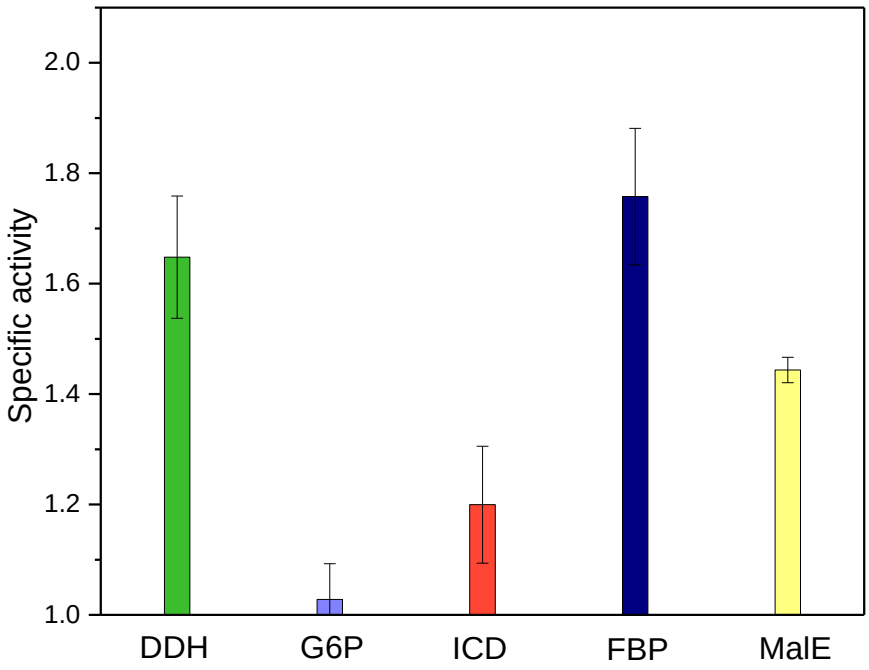

Figure 14. Specific enzyme activity of *C. glutamicum* LYS-12 cultivated at 38°C, normalized to 30°C as reference temperature. Cells were cultivated in minimal medium. The results represent mean values and standard deviations from three biological replicates. G6PDH: glucose 6-phosphate dehydrogenase, ICD: isocitrate dehydrogenase, MalE: malic enzyme, FBP: fructose 1,6-bisphosphatase, DDH: diaminopimelate dehydrogenase**.**

Malic enzyme is linked to L-lysine biosynthesis. On one hand, the decarboxylation from malate to pyruvate is coupled to the generation of NADPH, but results in the loss of carbon in form of CO_2 (Gourdon et al. 2000). The elevated activity of malic enzyme displays, at least to some extent, a potential target for strain optimization towards improved L-lysine production.

The enzymatic activity matches with the respective carbon flux changes, previously identified via metabolic flux analysis (Schäfer 2016). Likewise, the activated fructose 1,6-bisphosphatase is driving powerfully the PP pathway flux. The increased flux into the L-lysine biosynthesis branch was supported by diaminopimelate dehydrogenase activity (Figure 4). Both enzymes have been overexpressed during the creation of *C. glutamicum* LYS-12, resulting in an increased L-lysine production performance (Becker et al. 2011; Schäfer 2016).

4.1.2 Establishment of protocols for transcriptome analysis

Next, differential gene expression analysis was conducted in order to elucidate to which extent the observed change in fluxes and enzyme activities originates from a change in gene expression. For this purpose, the entire workflow for RNA sequencing was adapted from previous work (Pfeifer-Sancar et al. 2013). This included protocols for RNA extraction, ribosomal RNA (rRNA) removal, and quality control. To prevent size selection of mRNAs, which were anticipated by most column based techniques, a one-phase protocol for RNA extraction from *C. glutamicum* was adapted. It included cell disruption of the frozen cell-pellet, using glass beads and NucleoZol buffer (30-60% phenol, 30-60% guanidinium thiocyanate).

First tests with TRIzol reagent (30-60% phenol, 15-40% guanidinium thiocyanate, 7-13% ammonium rhodanide) in a two–phase extraction resulted in a slight contamination of the obtained RNA with phenol as indicated by an absorbance ratio 260/230 nm of 1.04 (Figure 15). The absorbance ratio at 260/280 nm indicated, that no significant protein contamination occurred in the samples (260/280 nm < 2). Consequently, one-phase extraction system was preferred. It should be noted, that the extraction of a 2 mL culture sample (OD_{660}= 5) led to sufficient RNA concentrations for subsequent gene expression analysis in both cases.

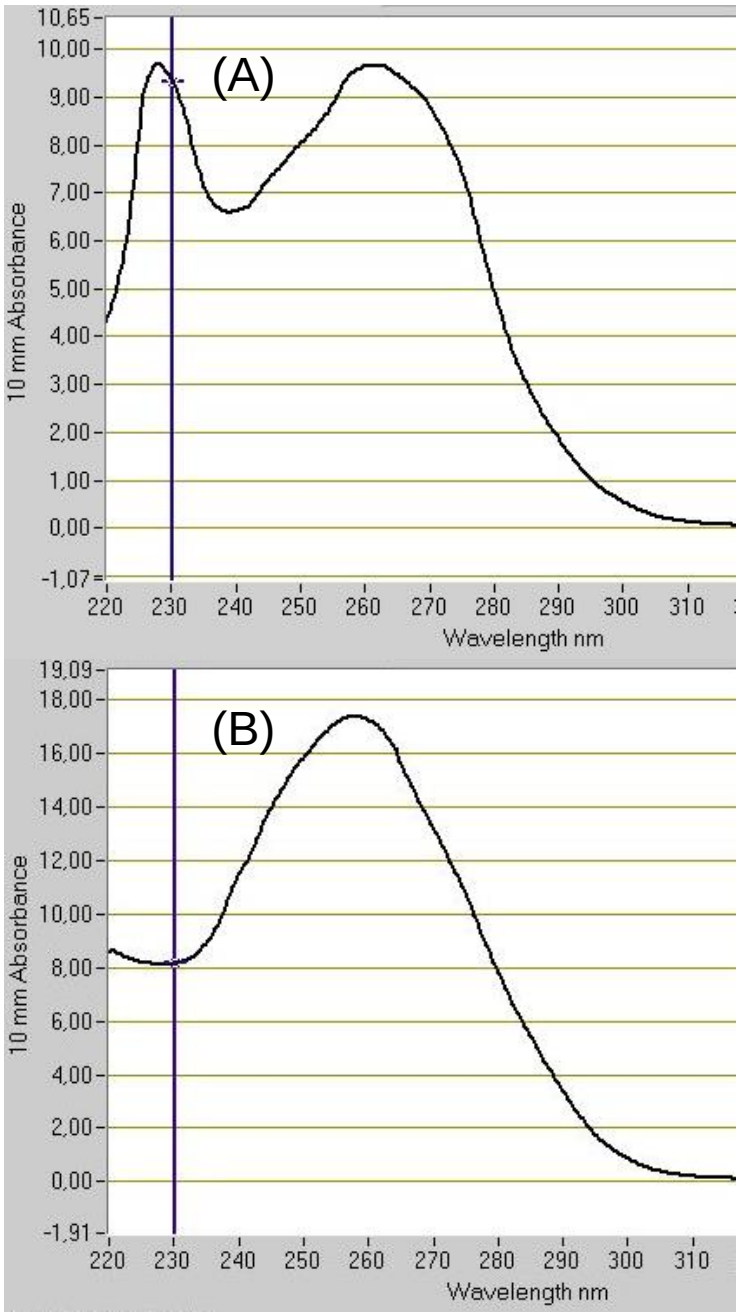

260/280: 2
260/230: 1.04
ng µL^{-1} : 385

260/280: 2.2
260/230: 2.1
ng µL^{-1} : 689

Figure 15. Quality control of extracted total RNA of *C. glutamicum* LYS-12. Plot of absorbance against wavelength for TRIzol extracted RNA (A) and NucleoZol (B) extracted RNA from *C. glutamicum* LYS-12. Ratios of approximately 2 for 260/230 and 260/280 indicate a clean sample for the NuceloZol extracted RNA (B). The ratio of 260/230 of 1.04 is caused by a possible phenol contamination (A).

In order to assess the quality of the extracted total RNA, a denaturing gel electrophoresis was performed. Hereby, the formation of distinct bands for the ribosomal subunits of *C. glutamicum* helped to evaluate possible sample degradation by RNAse activity (Aranda et al. 2012). A frequent protocol for this type of denaturing gel electrophoresis includes the application of formaldehyde. Formaldehyde is added to the respective agarose gel in order to inactivate RNAse activity during the

electrophoresis process (Mansour and Pestov 2013). Due to the inconsistency and health risks for the operator of running formaldehyde gels, a bleach gel based protocol was used instead (Aranda et al. 2012). Agarose gels with a sodium hypochlorite concentration of 0.06% (v/v) were found to sufficiently deactivate RNAse activity (Figure 16 B). Formaldehyde based gels were apparently not sufficient for quality assessment (Figure 16 A) (Marker et al. 2010). In addition, the use of sodium hypochlorite resulted in high resolution of the gel electrophoresis as compared to the formaldehyde based method. The newly adapted protocol allowed a reliable initial quality control prior to further RNA processing and RNAseq sample preparation steps.

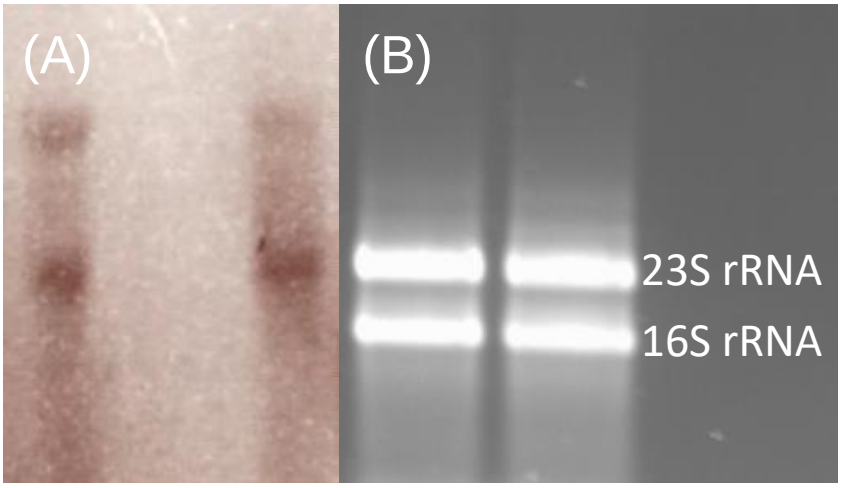

Figure 16. Formaldehyde (A) and sodium hypochlorite (B) based agarose gel with 1 µL of total RNA extracted from biological duplicates of *C. glutamicum* LYS-12 at an OD_{660} of 5. Samples were loaded on an agarose gel, containing formaldehyde (A) and 0.06% of sodium hypochlorite (B). Visible ribosomal subunits 23S (2906 nt) and 16S (1542 nt) were only detected for the sodium hypochlorite based gel. The single bands did not show any signs of degradation. Missing bands in the formaldehyde gel (A) were caused by potential RNAse activity.

Ribosomal RNA has to be removed from the samples due to the low concentration of mRNA compared to the rRNA share (He et al. 2010). For the removal of the ribosomal RNA fraction from the samples prior to library preparation, two commercially available protocols were compared. As shown in Figure 17 B, ribodepletion using the RiboMinus Transcriptome isolation kit for bacteria resulted in insufficient removal of ribosomal RNA. In contrast, the Ribo-Zero rRNA removal kit for bacterial RNA resulted in efficient removal of ribosomal RNA from the total RNA sample (Figure 17 C). In the next step, a cDNA library was prepared, including reverse transcription of mRNA to adapter and linker equipped DNA fragments for subsequent Illumina sequencing.

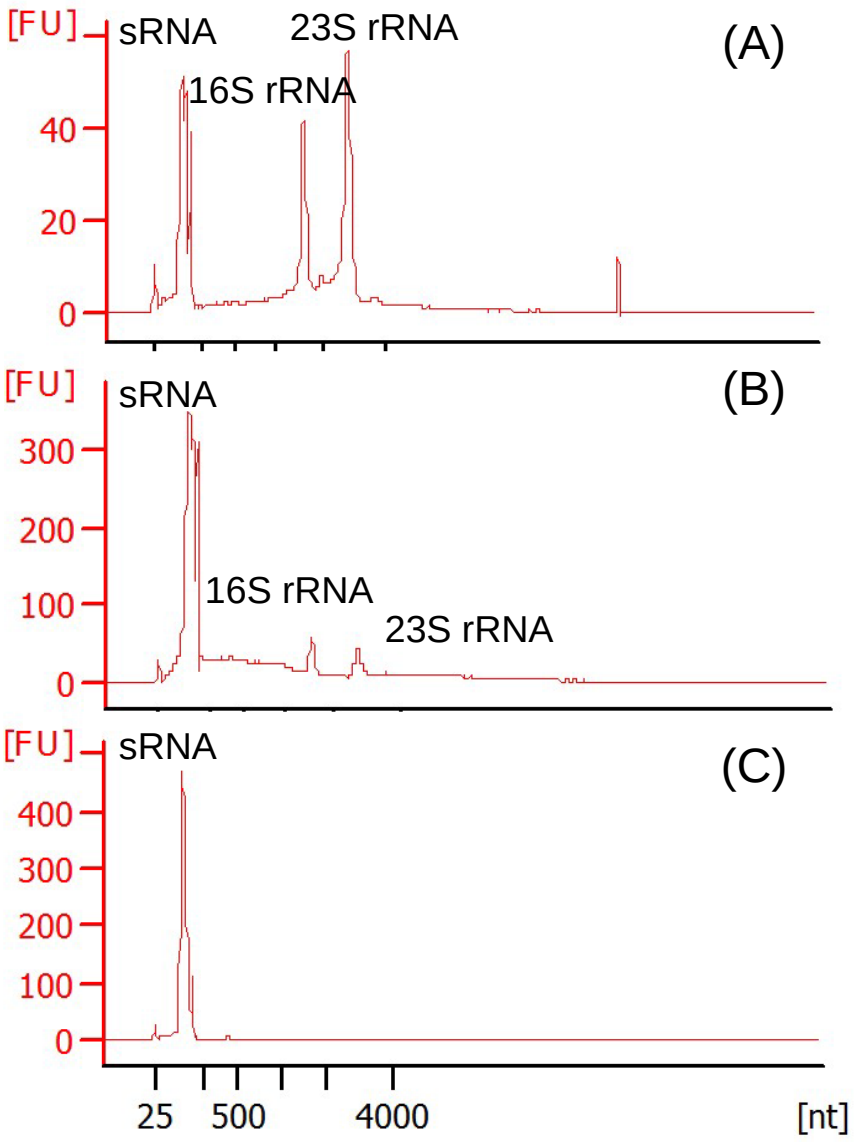

Figure 17. BioAnalyzer plots for total and ribodepleted RNA from *C. glutamicum* LYS-12. The original sample (A) shows the undepleted mRNA with ribosomal subunits (16S RNA, 23S RNA) and small RNA fraction (sRNA) of *C. glutamicum* LYS-12. The depletion with RiboMinus (B) shows a decrease in ribosomal subunits concentration, indicated by the comparable increase in the small fraction. Ribodepletion with Ribo-Zero (C) shows a total depletion of ribosomal RNA by the absence of the respective peaks and a high concentration of the small fraction.

During library preparation, 10-12 amplification cycles were found sufficient to achieve a cDNA library concentration of 5-20 ng μL^{-1}. The desired average fraction length of 300 bps was confirmed using a BioAnalyzer HS DNA chip (Figure 18). This is critical for the success of the sequencing procedure, as fragments of shorter or longer length do not cluster on the flow cell during the sequencing process (Illumina, San Diego, CA, USA). The analysis and sequencing of the cDNA library was performed by the Institute for Genetics and Epigenetics at the Saarland University.

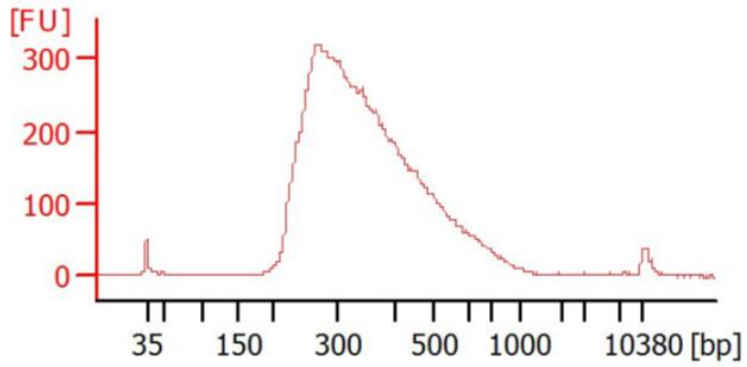

Figure 18. BioAnalyzer plot for cDNA library sample of *C. glutamicum* LYS-12. The graph shows the size distribution of the cDNA library from *C. glutamicum* LYS-12. The majority of cDNA fragments, created during library synthesis, has a length of 300 bps. Shorter or longer fragments are not included during sequencing due to the selective clustering on the flow cell.

4.1.3 Transcriptome at different temperatures

The developed protocol was used for genome wide comparative transcription analysis of *C. glutamicum* LYS-12 grown at 30°C and 38°C. The sequencing of the duplicates resulted in an average of 7 million reads with a coverage of 90-95% for both conditions. Data was processed using the differential gene expression function of the ReadXplorer (Hilker et al. 2016) via Diseq2 analysis and default settings. For the resulting table of differentially expressed genes, the accepted mean base coverage per gene was set to 30. Genes with a lower base mean value were not taken into account during data evaluation in order to increase the significance of the final data. Figure 19 illustrates an example of the ReadXplorer data visualization. A major part of the gene *pepck*, encoding for the enzyme phosphoenolpyruvate carboxykinase (NCgl2765), was deleted in *C. glutamicum* LYS-12 (Becker et al. 2011). As a result, the sequenced RNA lacked reads for the deleted fragment (Figure 19 B).

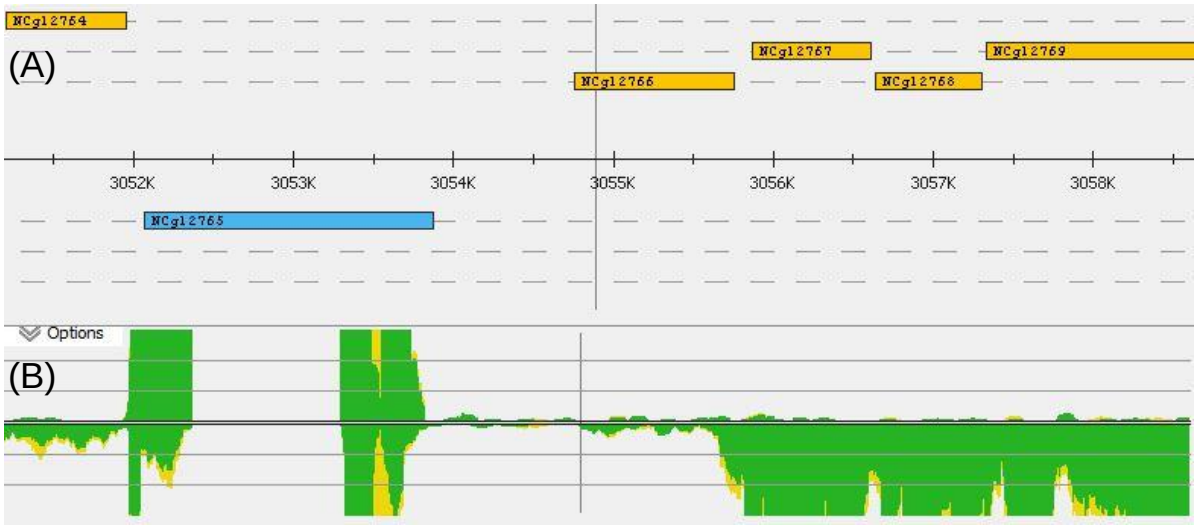

Figure 19. ReadXplorer data visualization, showing the reference genome (A) and the respective mRNA reads (B). The color indicates the quality of matches, with green representing perfect matches. The blue bar represents the gene *pepck* (NCgl2765), which has been deleted in *C. glutamicum* LYS-12. Consequently, no reads were found for the removed fragment (B).

Only selected genes were significantly affected in expression by the elevated temperature (Table 9 and Table 10). In total 150 genes were found to be downregulated whereas 360 genes were upregulated when the temperature was increased to 38°C. Genes with a $\log_2$fold change of > 1.0 were considered significantly upregulated, while genes with a $\log_2$fold change of lower than -1.0 were considered

significantly downregulated. The frame was set in order to identify the most significant regulatory differences. The total list of all up-and downregulated genes can be found in the Appendix in Table A 2 and Table A 3.

The expression changes were much weaker as compared to heat shock experiments with *C. glutamicum* incubated under heat stress at 45°C (Ehira et al. 2009). An interesting picture was yielded, when integrating the gene expression response with the previously obtained data on metabolic flux (Schäfer 2016) (Figure 20). Most reactions were significantly affected in flux, which, however, were not triggered substantially by a change in gene expression.

The observed increase in malic enzyme flux was not caused by elevated expression of the *malE* gene. As an exception, diaminopimelate decarboxylase (LysA), an enzyme of the L-lysine biosynthetic pathway, showed increased flux while the expression level of the corresponding gene was strongly decreased. In a previous study, the inhibition of the gene expression by L-lysine has been demonstrated (Cremer et al. 1988). In this case, the observed flux increase was apparently controlled on the metabolic level and even compensated the decreased amount of *lysA* transcript.

In general, the list of strongly affected genes included a high number of hypothetical proteins, transcriptional regulators and a few enzymes of core metabolism (Table 9). The gene NCgl2739, encoding 3-methyladenine DNA glycosylisomerase, was one of the most prominently upregulated ones. The enzyme is responsible for DNA damage recognition and repair (Wyatt et al. 1999). Therefore, the upregulation points to increased cellular maintenance activity, imposed by temperature induced damage (Metz et al. 2007) (Table 9).

Temperature induced DNA damage could also explain the observed upregulation of NCgl2901, putatively encoding a methylated DNA-protein cysteine methyltransferase, together with two additional upregulated genes (NCgl0737, NCgl0604), involved in DNA repair mechanisms (Ikeda and Nakagawa 2003; Kalinowski et al. 2003). The strong expression of six transcriptional regulators (NCgl2941, NCgl2840, NCgl0655, NCgl0405, NCgl1900 and NCgl1401) points to an overall adaption of the microbe to the elevated temperature. However, typical heat-shock related genes were not affected (Ehira et al. 2009).

Table 9. Significantly upregulated genes in *C. glutamicum* LYS-12 grown in standard minimal medium at 38°C as compared to 30°C. Genes were identified by comparative transcription analysis via ReadXplorer (Hilker et al. 2016), base mean > 30, log_2fold change > 1.0.

Gene-identifier	Gene name	log_2fold Change	Description	Function
NCgl0132		4.1	Hypothetical protein	Unknown
NCgl0131		3	Hypothetical protein	
NCgl2246		2.9	Hypothetical protein	
NCgl0148		2.3	Hypothetical protein	
NCgl2739		3.8	3-Methyladenine DNA glycosylase	Repair
NCgl1040		2.6	Excinuclease ATPase subunit	Unknown
NCgl1485		2.2	Nucleoside-diphosphate-sugar epimerase	
NCgl0200		1.8	NADPH:quinone reductase or related Zn-dependent oxidoreductase	
NCgl0198		1.7	ABC transporter permease	Transport
NCgl0213		1.4	ABC transporter ATPase	
NCgl0915		1.0	ABC transporter ATPase and permease	
NCgl2406		1.0	Major facilitator superfamily permease	
NCgl1214	*lysE*	1.0	L-Lysine efflux permease	
NCgl2871		1.3	Cation transport ATPase	
NCgl1379	*zupT*	1.2	Zinc transporter ZupT	
NCgl0602		1.1	Lipocalin	
NCgl2901		1.7	Methylated DNA-protein cysteine methyltransferase	Repair
NCgl0737		1.0	Helicase	
NCgl0604		1.0	Deoxyribodipyrimidine photolyase	
NCgl2028		3	Hydroxypyruvate isomerase	Catabolism
NCgl2029		3	Dehydrogenase	
NCgl1584		2.6	Glycerol-3-phosphate dehydrogenase	
NCgl2000		1.4	Glycerate kinase	
NCgl0650		1.2	D-Alanyl-D-alanine carboxypeptidase	
NCgl1932	*map*	1.2	Methionine aminopeptidase	
NCgl0322		1.1	5'-Nucleotidase	
NCgl2487	*mshD*	1.1	Histone acetyltransferase HPA2-like protein	
NCgl0233	*gluQ*	1.8	Glutamyl-Q tRNA(Asp) synthetase	Translation
NCgl0991		1.3	Acetyltransferase	
NCgl1974	*rimM*	1.3	16S rRNA-processing protein RimM	
NCgl2941		1.7	Transcriptional regulator	Regulation
NCgl2840		1.6	Transcriptional regulator	
NCgl0655		1.5	Transcriptional regulator	
NCgl0405		1.4	Transcriptional regulator	
NCgl1900	*pnp*	1.3	Polynucleotide phosphorylase	
NCgl1401		1.1	Transcriptional regulator	

Table 9 continued

Gene-identifier	Gene name	log_2fold Change	Description	Function
NCgl1354		1.5	TPR repeat-containing protein	
NCgl2041		1.5	Coenzyme F420-dependent N5,N10-methylene tetrahydromethanopterin Reductase	
NCgl0549		1.4	Hypothetical protein	
NCgl0800		1.4	Hypothetical protein	
NCgl1038		1.4	Hypothetical protein	
NCgl1082		1.3	Hypothetical protein	
NCgl0750		1.3	Hypothetical protein	
NCgl0920		1.3	Hypothetical protein	
NCgl0191		1.2	Hypothetical protein	
NCgl0621		1.2	Hypothetical protein	
NCgl1837		1.2	Hypothetical protein	
NCgl2334		1.2	Hypothetical protein	
NCgl2631		1.2	Hypothetical protein	Unknown
NCgl1741		1.2	Hypothetical protein	
NCgl2577		1.2	Hypothetical protein	
NCgl1147		1.1	Hypothetical protein	
NCgl2305		1.1	Hypothetical protein	
NCgl2144		1.1	Hypothetical protein	
NCgl1672		1.1	Hypothetical protein	
NCgl2355		1.1	Hypothetical protein	
NCgl2252		1.1	Hypothetical protein	
NCgl1838		1.1	Hypothetical protein	
NCgl2972		1.0	Hypothetical protein	
NCgl1047		1.0	Hypothetical protein	
NCgl0732		1.0	Hypothetical protein	
NCgl2583		1.0	Hypothetical protein	
NCgl1083		1.0	Hypothetical protein	
NCgl0953	*coaA*	1.4	Pantothenate kinase	
NCgl2516	*bioD*	1.7	Dithiobiotin synthetase	
NCgl1163	*atpA*	1.5	ATP Synthase F0F1 subunit alpha	
NCgl1189		1.5	Spermidine synthase	
NCgl2173		1.4	Hydrolase/acyltransferase	
NCgl0797		1.4	Acetyl-CoA carboxylase beta subunit	
NCgl2405	*acpS*	1.4	4'-Phosphopantetheinyl transferase	
NCgl1347	*argH*	1.4	Argininosuccinate lyase	
NCgl1073	*glgC*	1.3	Glucose-1-phosphate adenylyltransferase	Anabolism
NCgl2243	*rbsk*	1.3	Sugar kinase	
NCgl1340	*argC*	1.2	N-Acetyl-gamma-glutamyl-phosphate reductase	
NCgl1827	*dxs*	1.1	1-Deoxy-D-xylulose-5-phosphate synthase	
NCgl0959		1.1	Sortase or related acyltransferase	
NCgl1216		1.1	Glutathione S-transferase	
NCgl0550		1.0	Subtilisin-like serine protease	
NCgl0666	*prpC1*	1.0	Citrate synthase	
NCgl0119		1.0	Carbonic anhydrase/acetyltransferase	

The most strongly downregulated gene at 38°C was an ABC-type transport system permease (NCgl0394). This gene is putatively involved in lipoprotein release (Ikeda and Nakagawa 2003; Kalinowski et al. 2003). The response potentially hints to changes in cell morphology. Likewise, diaminopimelate decarboxylase (*lysA*) (NCgl1133) and the coexpressed arginyl-tRNA synthase (*argS*) (NCgl1132) are significantly downregulated (Table 10, Figure 20). The *lysA*/*argS* operon is occurring two times in the genome of *C. glutamicum* LYS-12 (Becker et al. 2011). Both genes are transcribed simultaneously (Oguiza et al. 1993). Due to this, the previous duplication of the operon preserved the natural transcriptional regulation pattern.

As mentioned before, it has been reported that the expression of diaminopimelate decarboxylase in *C. glutamicum* is inhibited by L-lysine (Cremer et al. 1988). Altogether, most genes of the central carbon metabolism and L-lysine synthesis were almost exclusively affected on the metabolic level but did show insignificant differential expression.

Table 10. Significantly downregulated genes in *C. glutamicum* LYS-12 grown in standard minimal medium at 38 °C as compared to 30°C. Genes were identified by comparative transcription analysis via ReadXplorer (Hilker et al. 2016), base mean > 30, log_2fold change < -1.

Gene-identifier	Gene name	log_2fold Change	Description	Function
NCgl0394		-2.4	ABC-type transport system permease	Transport
NCgl2740		-1.9	Hemoglobin-like flavoprotein	Unknown
NCgl1133	*lysA*	-1.9	Diaminopimelate decarboxylase	Anabolism
NCgl1132	*argS*	-1.9	Arginyl-tRNA synthetase	
NCgl0662		-1.4	G3E family GTPase	
NCgl0184		-1.3	Arabinosyl transferase	Cell envelope synthesis
NCgl2982		-1.1	Virulence factor	
NCgl0340		-1.0	Nucleoside-diphosphate sugar epimerase	
NCgl2800		-1.1	Amidase	Translation
NCgl1567		-1.1	Shikimate 5-dehydrogenase	Catabolism
NCgl0030		-1.0	ABC transporter permease	Transport
NCgl1965		-1.0	Thiamine biosynthesis protein ThiF	Anabolism
NCgl2100		-1.0	Hypothetical protein	Unknown

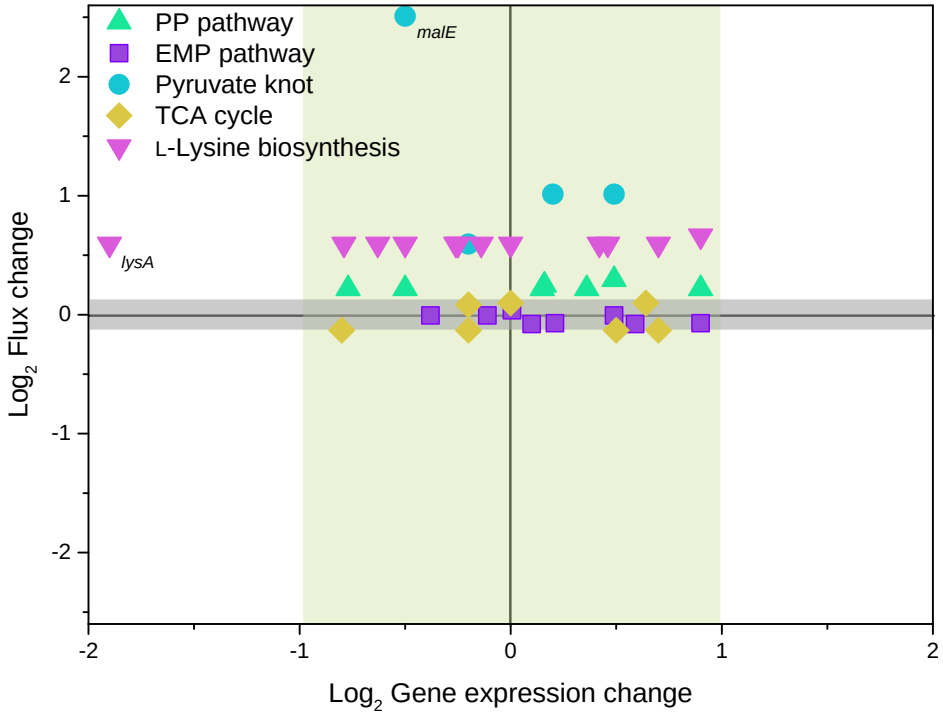

Figure 20. Flux expression change plotted versus gene expression change. Change of the carbon flux (Schäfer 2016) plotted against the expression change of the respective genes of central carbon- and L-lysine metabolism from experiments at 30°C and 38°C. Genes with insignificant changes on the expression level are located in the green area, genes with insignificant changes on the metabolic level are located in the grey area.

The apparent mismatch between the different omics levels is a well-known phenomenon (Jessop-Fabre et al. 2019; Nie et al. 2007). Transcribed mRNA undergoes posttranscriptional regulation processes, e.g. evoked by small RNAs, which eventually results in the same amount of mRNAs, but changed fluxes, when comparing data of two experiments (Kang et al. 2014). Due to this, posttranscriptional and posttranslational mechanisms seem crucial for *C. glutamicum* to maintain its metabolic stability at elevated temperatures (Becker et al. 2016).

The integrative inspection of transcriptome and fluxome revealed the gene *lysA,* encoding for the diaminopimelate decarboxylase, as potential candidate. The increased flux together with a significant downregulation at the mRNA level exposes temperature induced inhibition. In order to study this effect in more detail, the intracellular L-lysine concentration was measured (Figure 21). It was proven to be the case that the intracellular L-lysine pool was significantly increased at elevated temperatures. This finding further supported the view of metabolic inhibition of *lysA* expression.

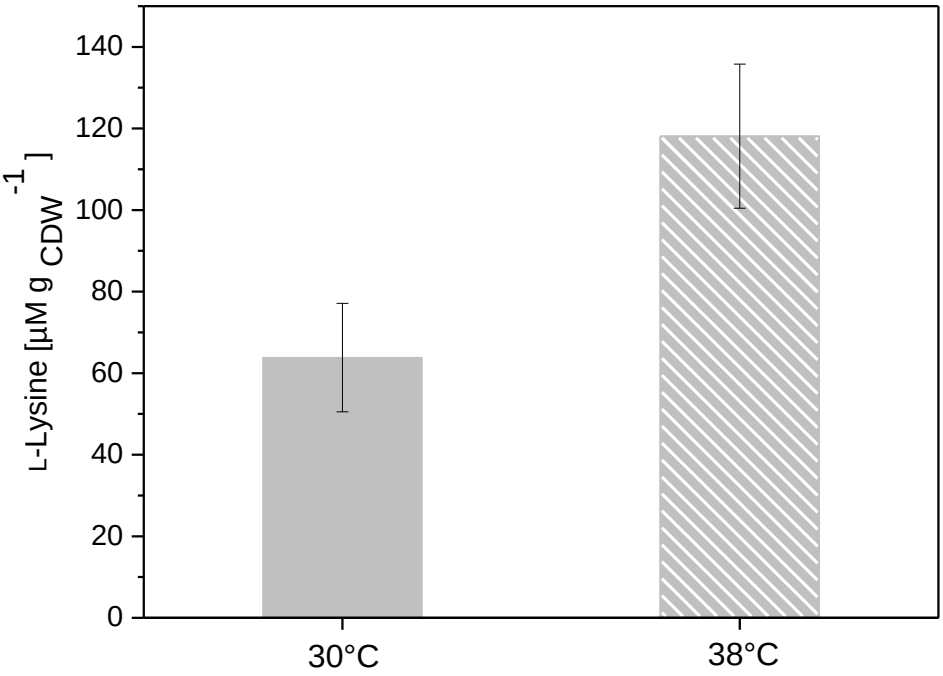

Figure 21. Intracellular L-lysine concentration in *C. glutamicum* LYS-12 grown in minimal medium at 30°C and 38°C. The data was obtained from exponentially growing cells. The results represent mean values and standard deviations from three biological replicates. CDW: cell dry weight.

The direct precursor of L-lysine is *meso*-diaminopimelic acid. The intermediate is further an important building block for cell wall synthesis (Wehrmann et al. 1998). The cell naturally relies on an efficient control of its turnover into L-lysine in order to prevent growth inhibition by a shortage of *meso*-diaminopimelic acid (Wehrmann et al. 1998). A promising strategy to overcome the inhibition mechanism is the enhanced efflux of L-lysine. The L-lysine permease (*lysE*) was identified as target for strain optimization at elevated temperature. The gene *lysE* is controlled by its positive regulator *lysG*, which itself is induced by intracellular L-lysine (Bellmann et al. 2001). In order to promote an auto-regulative L-lysine export and to deregulate *lysA* expression, the gene cluster *lysGE* should be duplicated in the genome of *C. glutamicum* LYS-12. In addition, deletion of *malE* should be tested.

4.1.4 Physiological response to malic enzyme deletion in *C. glutamicum* LYS-12

In order to prevent carbon loss due to metabolically upregulated malic enzyme, *malE* was deleted from the chromosome via homologous recombination. The deletion was verified by PCR and enzyme activity measurement. The new strain was designated *C. glutamicum* LYS-12 *ΔmalE.* It did not exhibit improved L-lysine production. Cell vitality was decreased as indicated by the reduced growth rate (Table 11).

Table 11. Growth and production characteristics of *C. glutamicum* LYS-12 Δ*malE*. The data comprise the specific rate for growth (μ) and the yields for biomass ($Y_{X/Glc}$), L-lysine ($Y_{Lys/Glc}$), trehalose ($Y_{Tre/Glc}$) and the specific glucose uptake rate (q_S). The results represent mean values and standard deviations from three biological replicates. Values for *C. glutamicum* LYS-12 (Schäfer 2016) are shown in brackets.

Temp. [°C]	μ [h^{-1}]	$Y_{X/Glc}$ [g mol^{-1}]	q_S [mmol g^{-1} h^{-1}]	$Y_{Lys/Glc}$ [mmol mol^{-1}]	$Y_{Tre/Glc}$ [mmol mol^{-1}]
30	0.14±0 (0.24±0.01)	60±3 (58±3)	2.3±0.1 (4.1±0.2)	270±6 (270±2)	6±1 (6±1)
38	0.06±0 (0.13±0.01)	32±2 (33±1)	2.0±0.0 (3.9±0.2)	418±3 (430±4)	13±1 (14±1)

Another indicator for the negative effect of malic enzyme deletion is the persistent production of trehalose. One possible reason for this observation is the redirection of the fluxes in order to replace the missing reaction of the malic enzyme by a persistent reverse flux from pyruvate to oxaloacetate. Metabolic imbalances are likely to be a burden, resulting in impaired growth and reduced L-lysine production at elevated temperatures. Similar kinds of bypass reactions have been shown for pyruvate kinase deletion mutants where malic enzyme replaced the reaction from phosphoenolpyruvate to pyruvate (Becker et al. 2008).

For previous strains, overexpression of malic enzyme was not beneficial for L-lysine production from glucose, as well (Georgi et al. 2005; Gourdon et al. 2000; Wendisch et al. 2006a). It seems that the natural level of this enzyme is somewhat crucial for the cell.

4.1.5 Overexpression of *lysGE* for increased L-lysine yield

In order to improve L-lysine production performance of *C. glutamicum* LYS-12, the L-lysine exporting operon *lysGE* was duplicated. The integration was realized by inserting an additional copy of the cluster into the *bioD* locus. At 30°C the new strain showed a slight increase in growth rate while the L-lysine yield was kept high. At 38°C, the L-lysine yield was increased by 7% (Table 12 and Figure 22). The yield for L-lysine was more than 40% higher when comparing it to *C. glutamicum* LYS-12 grown at 30°C. Moreover, the genetic modification led to a significant decrease of trehalose accumulation, which was nearly abolished at both temperatures (Table 12).

Table 12. Growth and production characteristics of *C. glutamicum* LYS-12 2x*lysGE*. The data comprise the specific rate for growth (μ) and the yields for biomass ($Y_{X/Glc}$), L-lysine ($Y_{Lys/Glc}$), trehalose ($Y_{Tre/Glc}$) and the specific glucose uptake rate (q_S). The results represent mean values and standard deviations from three biological replicates. Values for *C. glutamicum* LYS-12 (Schäfer 2016) are shown in brackets.

Temp. [°C]	μ [h^{-1}]	$Y_{X/Glc}$ [g mol^{-1}]	q_S [mmol g^{-1} h^{-1}]	$Y_{Lys/Glc}$ [mmol mol^{-1}]	$Y_{Tre/Glc}$ [mmol mol^{-1}]
30	0.25±0.02 (0.24±0.01)	60±1 (58±3)	4.1±0.3 (4.1±0.2)	265±7 (270±2)	0±0 (6±1)
38	0.052±0.002 (0.13±0.01)	24±5 (33±1)	2.2±0.2 (3.9±0.2)	460±1 (430±4)	0.01±0 (14±1)

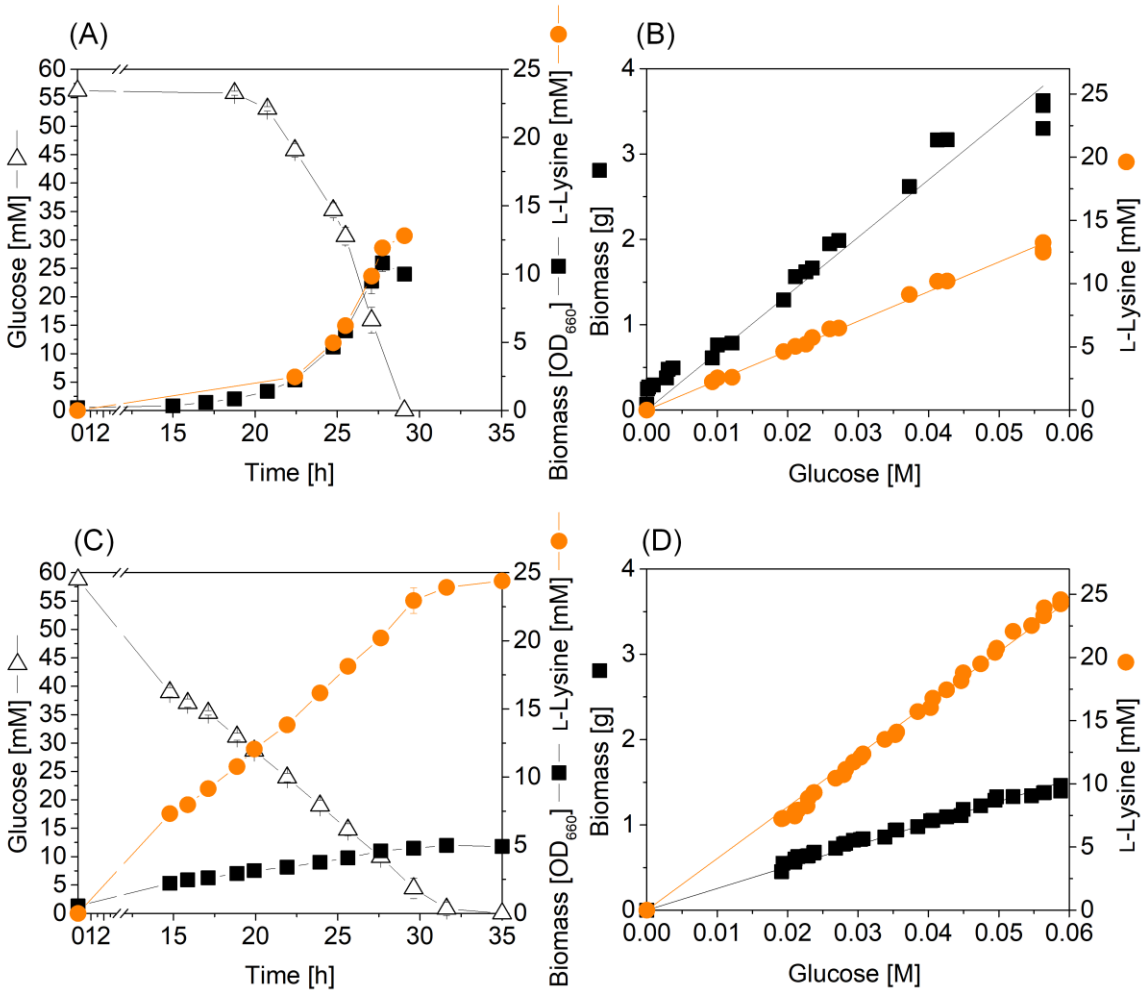

Figure 22. Cultivation profiles of *C. glutamicum* LYS-12 2x*lysGE* at 30°C (A,B) and 38°C (C,D) in minimal medium. The results represent mean values and standard deviations from three biological replicates.

The new strain *C. glutamicum* LYS-12 2x*lysGE* and the parent strain *C. glutamicum* LYS-12 were tested for intracellular L-lysine concentration during cultivations at 30°C and 38°C. As shown in Table 13, no decrease of intracellular L-lysine concentration at 30°C was observed. However, at 38°C, the new strain exhibited a slightly reduced intracellular L-lysine concentration.

Table 13. Intracellular L-lysine concentration of *C. glutamicum* LYS-12 and *C. glutamicum* LYS-12 2x*lysGE* at 30°C and 38°C. The data were obtained from intracellular measurements of exponentially growing cells in minimal medium at 30°C and 38°C. The results represent mean values and standard deviations from three biological replicates. CDW: cell dry weight.

Strain	Temperature [°C]	Intracellular L-lysine [µM g_{CDW}^{-1}]
C. glutamicum LYS-12	30	64±13
C. glutamicum LYS-12 2x*lysGE*	30	64±14
C. glutamicum LYS-12	38	118±18
C. glutamicum LYS-12 2x*lysGE*	38	113±17

These observations can be explained by the auto inductive nature of L-lysine export, mainly active at elevated temperatures due to high intracellular L-lysine levels. The increased growth rate of *C. glutamicum* LYS-12 2x*lysGE* appears to be a sign of a reduced metabolic burden. The deletion of the *bioD* gene does not add additional stress to the organism as shown in recent publications (Rohles et al. 2016; Rohles et al. 2018). The slight decrease in intracellular L-lysine concentration points to a change in the export behavior at 38°C, while at 30°C the activation threshold for the increased export was not exceeded. The increased amount of exporter and regulator did promote the export, as shown by the increased L-lysine yield, thus a new intracellular L-lysine balance has been set to keep homeostasis (Bellmann et al. 2001). During cultivation at 38°C the strain showed a significantly lower growth rate as compared to the parent strain. Changes in cell wall composition and fluidity described for the mycobacterial cell wall as well as altered precursor supply may have synergetic effects on lowering cell growth (Liu et al. 1996). This assumption is supported by the downregulation of three genes (NCgl0184, NCgl2982 and NCgl0340), involved in the synthesis of the cell envelope, identified by differential expression analysis of *C. glutamicum* LYS-12 (Table 10). Subsequent measurements of the intracellular level of *meso*-diaminopimelate showed a slight decrease at 38°C (Table 14, Figure 23).

Table 14. Intracellular *meso*-diaminopimelate concentration of *C. glutamicum* LYS-12 and *C. glutamicum* LYS-12 2x*lysGE* at 30°C and 38°C. The data were obtained from intracellular measurements of exponentially growing cells in minimal medium at 30°C and 38°C. CDW: cell dry weight. The results represent mean values and standard deviations from three biological replicates.

Strain	Temp. [°C]	Intracellular *meso*-diaminopimelate [µM g_{CDW}^{-1}]
C. glutamicum LYS-12	30	25±1
C. glutamicum LYS-12 2x*lysGE*	30	23±0
C. glutamicum LYS-12	38	5±0
C. glutamicum LYS-12 2x*lysGE*	38	< 0.005

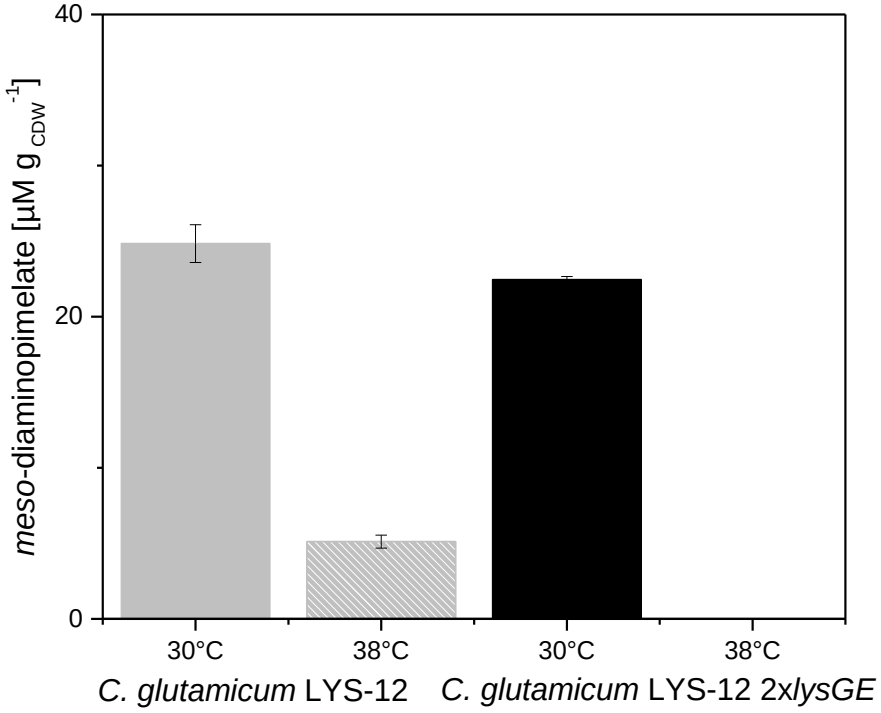

Figure 23. Intracellular *meso*-diaminopimelate concentration of *C. glutamicum* LYS-12 and *C. glutamicum* LYS-12 2x*lysGE* at 30 and 38°C. The data were obtained from intracellular measurements of exponentially growing cells in minimal medium at 30°C and 38°C. The results represent mean values and standard deviations from three biological replicates. CDW: cell dry weight.

The integrative overexpression of the export mechanism allowed a convenient self-regulation of product export. Since *lysG* shows high sensitivity for L-lysine, it has also been used as an intracellular L-lysine sensor when fused to a fluorescent protein gene

(Schendzielorz et al. 2013). The kind of genetic modification applied here, appeared less invasive than the utilization of constitutive promoters, potentially leading to a balanced expression. Compared to the parent strain *C. glutamicum* LYS-12 cultivated at both temperatures, *C. glutamicum* LYS-12 2x*lysGE*'s L-lysine yield at 38°C further advances the genealogy of L-lysine producers (Figure 24).

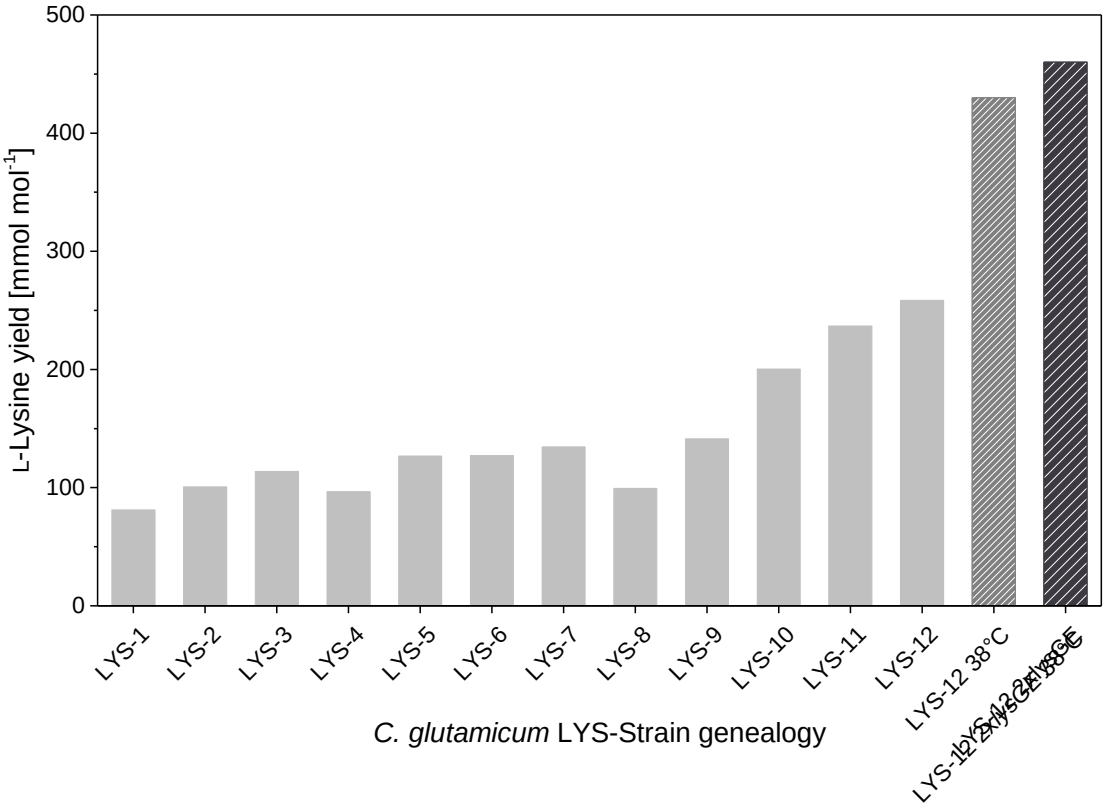

Figure 24. Comparison of L-lysine yields in streamlined producer strains, cultivated in standard glucose minimal medium. The strains *C. glutamicum* LYS-1 to 12 were developed by Becker et al. 2011 showing the streamlined metabolic strain engineering (grey) (Becker et al. 2011). *C. glutamicum* LYS-12 and *C. glutamicum* LYS-12 2x*lysGE* cultivated at 38°C, are displayed in striped columns (Schäfer 2016)**.**

4.1.6 *C. glutamicum* LYS-12 reveals new target and production possibilities at high temperature

The application of a cultivation temperature above the usual value of 30°C revealed a solid temperature robustness of *C. glutamicum.* The L-lysine hyper-producer *C. glutamicum* LYS-12 was able to increase its L-lysine yield at 38°C, underlining the genetic and metabolic stability of the rationally designed strain (Becker et al. 2011). Due to the increased yield, the higher temperature could be attractive for L-lysine manufacturing. Since production is based on the sugar industry, it is necessary to locate the respective factories in close proximity to the raw materials (Leuchtenberger et al. 2005; Wittmann et al. 2004). One of the cost factors for production is the cooling of the fermenter, especially during hot seasonal periods (Abe et al. 1967; Kelle et al. 2005). As a result, the temperature stability and beneficial behavior of *C. glutamicum* LYS-12 was approved straightforward. New insights into the regulatory interplay between L-lysine export and pathway control revealed *lysA* as an important target for enzyme engineering. The implementation of inducible release of the enzyme activity from L-lysine feedback inhibition in combination with promoted export could yield a synthetic switch from growth to production.

Integration of a second, feedback resistant copy of the *lysA* gene with an inducible promoter or a more desensitized variant of the enzyme might help to further drain the L-lysine production pathway. In *Bacillus subtilis* for instance, *meso*-diaminopimelate decarboxylase can be desensitized to L-lysine by lowering the pH (Rosner 1975). However, care must be taken to avoid a decrease in cell vitality due to the close interaction between cell wall formation and L-lysine production. Additional enhancements at the initial steps of the L-lysine pathway could help to balance this node even better.

4.2 Metabolically engineered *C. glutamicum* for high-level ectoine production

4.2.1 Increase of ectoine pathway flux through transcriptional balancing

In order to generate a competitive ectoine producing strain without the drawbacks of former heterologous hosts, the ectoine pathway itself was optimized. So far, this pathway has mainly been implemented from other hosts without further optimization (Becker et al. 2013; Ning et al. 2016; Pérez-García et al. 2017). At this point, it appeared promising to aim at increased pathway flux, utilizing novel concepts of transcriptional balancing (Rytter et al. 2014). Using a set of synthetic transcription and translation elements, a large variety of different ectoine pathway modules should be created (Mutalik et al. 2013; Rytter et al. 2014; Yim et al. 2013).

For the generation of a by-product free expression host as chassis for metabolic engineering, the basic L-lysine producer *C. glutamicum lysC* was chosen (Kim et al. 2006). It expresses a feedback resistant aspartokinase and, due to the mutation (S301Y), is able to accumulate the ectoine precursor L-aspartate semialdehyde (Figure 13). In order to prevent undesired carbon loss via synthesis and export of L-lysine, the *lysE* gene, encoding for the L-lysine export protein LysE was deleted (Becker et al. 2013). The deletion was verified by a shortened PCR product (893 bp) while the wild type showed a fragment size of 1468 bp (Figure 25).

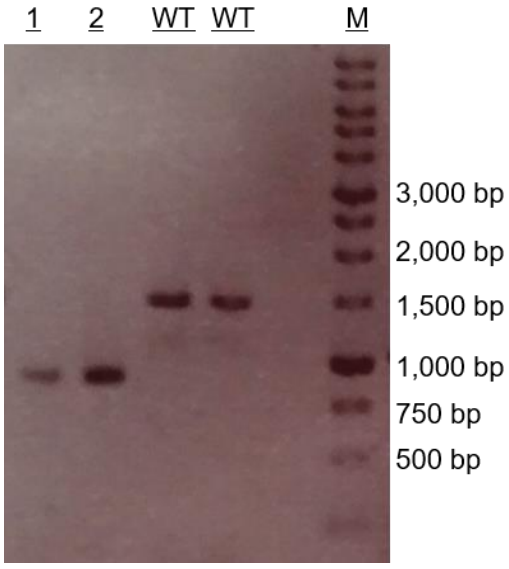

Figure 25. Confirmation of deletion of the gene *lysE* in *C. glutamicum lysC*. Lines 1 and 2 show the successful deletion of the gene *lysE*, still existing in the wild type (WT) controls. A DNA ladder was used to infer fragment size (M).

The resulting strain *C. glutamicum lysC ΔlysE* did not excrete L-lysine anymore (Table 15). Further, the deletion of *lysE* slightly decreased the growth rate. By-products like L-glycine and L-glutamate only occurred in negligible amounts (Table 15). Next, an episomal plasmid for the expression of the *ectABC* cluster was created. After transformation of the episomal plasmid, which carried the genes *ectABC* under the control of the constitutive *tuf* promoter in a polycistronic design, the resulting strain *C. glutamicum lysC ΔlysE ectABC*^{basic} produced ectoine at a yield of about 30 mmol mol^{-1} of glucose. Ectoine was produced almost exclusively. The introduced ectoine pathway did not fully use the available carbon for product synthesis. The parent strain *C. glutamicum lysC* secreted L-lysine at a yield of about 90 mmol mol^{-1} (Table 15). Apparently, expression of the native polycistronic ectoine cluster *P*$_{tuf}$*ectABC* in *C. glutamicum lysC ΔlysE* failed to drain all carbon available from L-lysine synthesis, similar to other studies (Pérez-García et al. 2017).

Table 15. Kinetics and stoichiometry of L-lysine and ectoine producing strains of *C. glutamicum*. The data comprise the specific rate for growth (μ) and the yields for biomass ($Y_{X/S}$), ectoine ($Y_{Ectoine/S}$), L-lysine ($Y_{Lysine/S}$), L-glutamate ($Y_{Glutamate/S}$), and L-glycine ($Y_{Glycine/S}$). Errors represent standard deviations from three biological replicates in minimal glucose medium.

	C. glutamicum lysC	*C. glutamicum lysC ΔlysE*	*C. glutamicum lysC ΔlysE ectABC*^{basic}
μ [h^{-1}]	0.35±0.00	0.34±0.02	0.33±0.01
$Y_{X/S}$ [g mol^{-1}]	83.4±3.9	78.2±0.4	74.2±1.5
$Y_{Ectoine/S}$ [mmol mol^{-1}]	n.d.*	n.d.	31.8±3
$Y_{Lysine/S}$ [mmol mol^{-1}]	94.5±1.0	n.d.	n.d.
$Y_{Glutamate/S}$ [mmol mol^{-1}]	n.d.	8.1±0.9	10.3±0.3
$Y_{Glycine/S}$ [mmol mol^{-1}]	n.d.	4.3±0.7	4.0±0.23

*not detected.

4.2.2 Modulated *ectABC* expression via synthetic pathway design

In order to allow the investigation of different levels of ectoine gene expression for the modulated pathway flux, a library of synthetic modules was constructed. The modular layout comprised the three codon optimized genes *ectA*, *ectB* and *ectC*, obtained from previous work (Becker et al. 2013). The genes were cloned in a conserved order, each randomly linked to one out of nineteen synthetic promoters (Table 6), one out of three bicistronic linkers (Table 7) and one terminator *rrnB*T1T2 as shown in Figure 26.

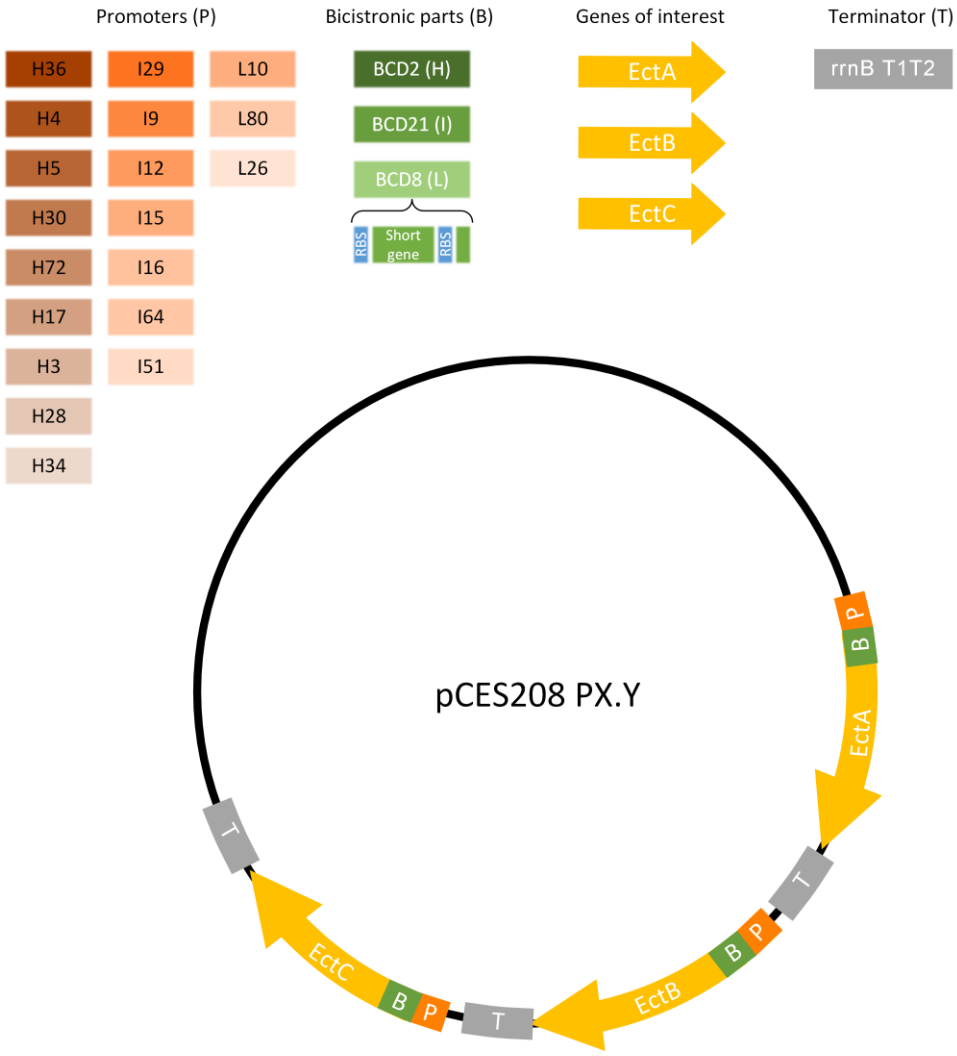

Figure 26. Schematic diagram of the constructed ectoine plasmid library. The synthetic ectoine library consisted of three expression modules for the ectoine genes *ectA*, *ectB* and *ectC* (yellow). Each gene is randomly linked to one of 19 synthetic promoters (orange), one of three bicistronic design elements (BCDs) (green), and one transcriptional terminator (grey). The created synthetic cluster was assembled into the expression vector pCES208. The varying expression strength of the individual elements is visualized by the color intensity.

After synthesis and assembly of the elements, the obtained mixture of different ectoine pathway modules was cloned into the episomal vector pCES208. This yielded a pool of differently composed plasmids with 185,193 possible combinations. The plasmid library was transformed into *E. coli* XL1-Blue for confirmation of correct assembly by sequencing of twenty randomly picked clones. The synthetic plasmids were then transformed into the chassis strain *C. glutamicum lysC ΔlysE*. More than 350 positive clones were selected on kanamycin containing agar plates for further investigation. Each clone was numbered internally, referring to the corresponding selection agar plate and an individual clone number. For example, clone 40 from plate 3 was designated P3.40. In order to enable fast analysis of the screened clones, a precise short-time quantification method for ectoine was developed. As displayed in Figure 27, the method enabled ectoine measurement within a total analysis time of three minutes per sample. Clones of *C. glutamicum lysC ΔlysE*, transformed with the synthetic *ectABC* plasmid library, were cultivated in a miniaturized cultivation system at 500 µL scale in standard minimal glucose medium. Similar to the performed shake flask experiments, *C. glutamicum lysC ΔlysE ectABC*^{basic} accumulated 0.5 g L^{-1} of ectoine. With this strain as reference, about 400 synthetic ectoine producer strains were characterized. Nearly 30% of the strains tested revealed higher ectoine titers as compared to the reference (Figure 28). While around 10% of the tested strains did not excrete ectoine at all or below the threshold, around 60% of the screened mutants produced less than the reference strain. The screening of about 0.2% of the possible library size already led to the identification of high-titer mutants, outscoring the initial strain almost five-fold. All obtained mutants were able to excrete ectoine without elaborative and expensive extraction and without the need for high salinity conditions (Becker et al. 2013; Fallet et al. 2010).

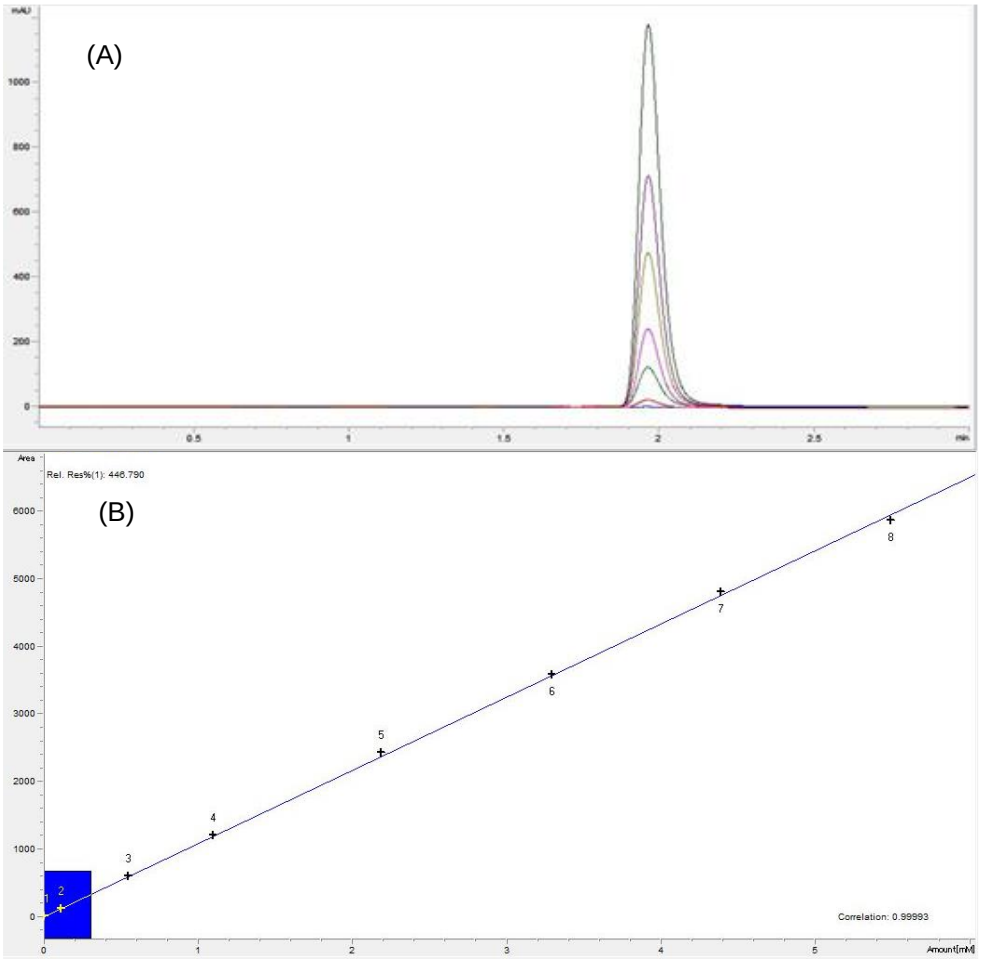

Figure 27. Established HPLC analysis method for fast quantification of ectoine concentration. Spectrum of the HPLC analysis of different ectoine concentrations, ranging from 0.01 mM to 5 mM (A) and the corresponding calibration graph (B). The target substance elutes after 2 minutes with deionized water as mobile phase and can be clearly identified for direct quantification via an UV-detector at 210 nm wavelength**.**

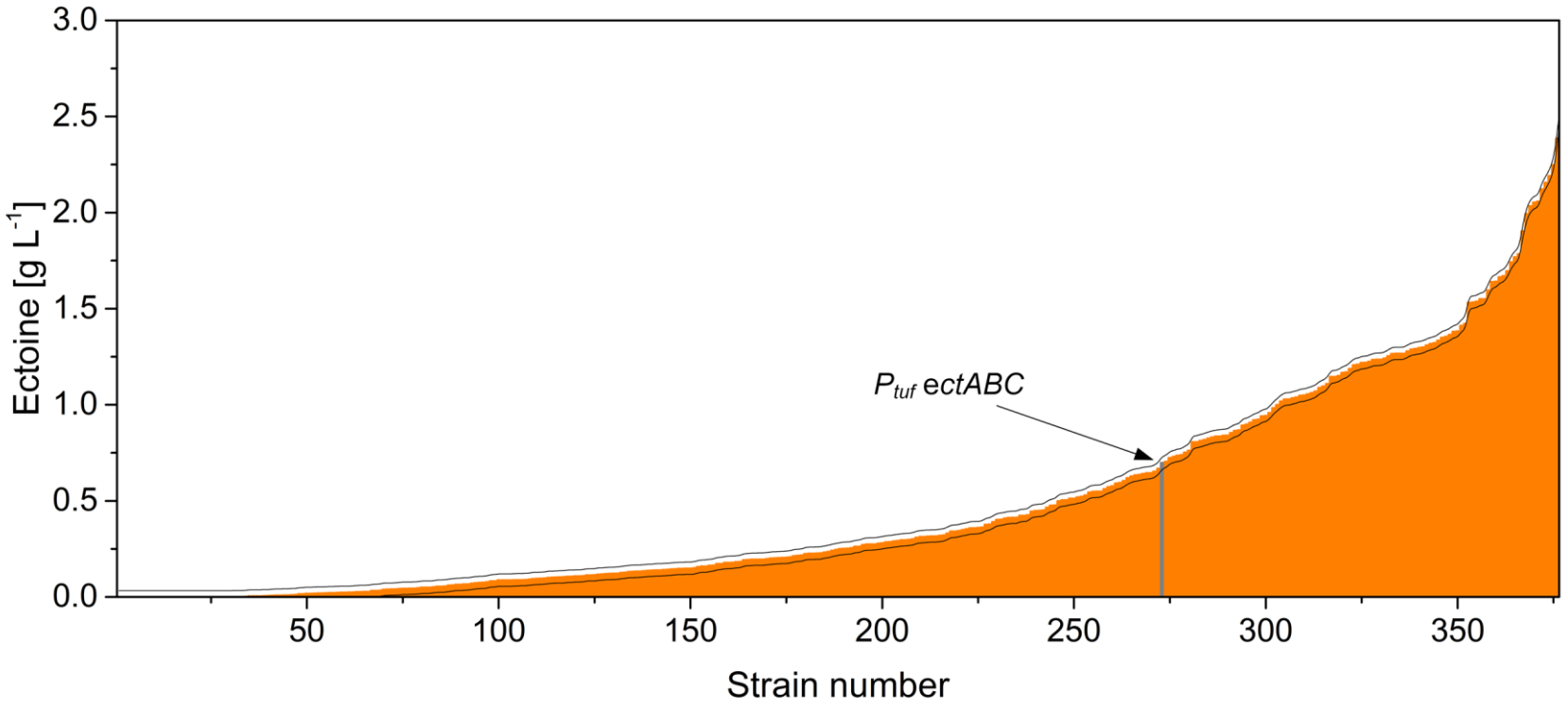

Figure 1. Characterization of synthetic ectoine library transformants. Strains were grown in miniaturized scale for high throughput screening. The plasmid *P*$_{tuf}$*ectABC* of *C. glutamicum lysC ΔlysE ectABC*^{basic} served as reference. Errors (double line) were calculated from the mean of errors of 25 in triplicates cultivated clones in the same miniaturized experimental setup.

4.2.3 Optimal flux relies on specific combination of genetic control elements in the ectoine operon

In order to elucidate optimal expression patterns for the ectoine clusters, the genetic elements, promoters, and bicistronic parts, were sequenced in selected strains (Figure 29).

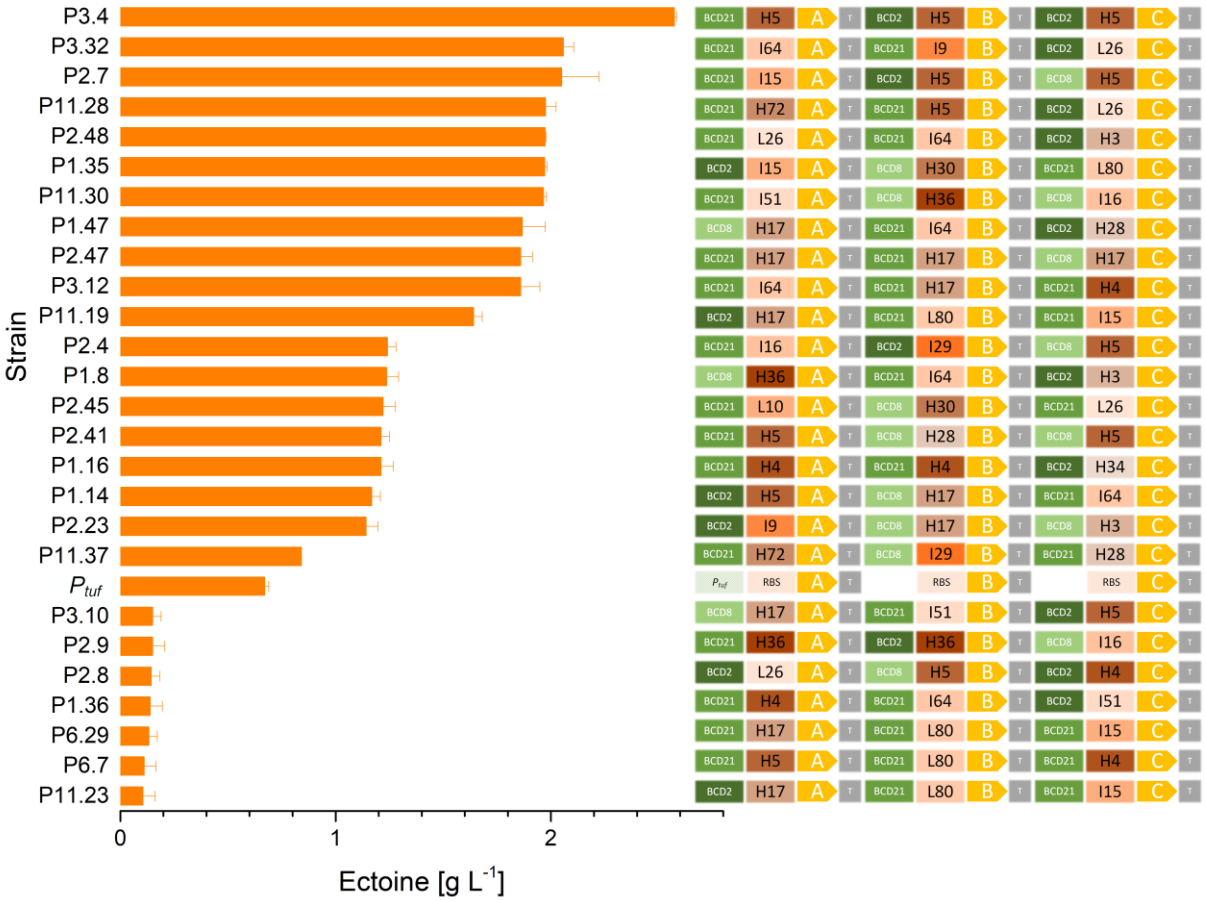

Figure 29. Genotypic and phenotypic comparison of different synthetic mutants of *C. glutamicum* for ectoine production. The plasmid of *C. glutamicum lysC ΔlysE ectABC*^{basic} served as polycistronically designed reference (P_{tuf}).

Sequencing of the ectoine synthesis clusters revealed different characteristics linked to the ectoine titer. The three genes, *ectA*, *ectB* and *ectC* seemed to require balanced expression. Interestingly, the approximately strongest promoter was not found in the top producers. In addition, expression of the gene *ectB* required a high level of expression and translation for optimal production. The genes *ectA* and *ectC* revealed

weaker promoters instead. For these two genes, a lower expression level or the combination with a weaker bicistronic element enabled high production performance. In order to draw a more precise picture of kinetics and stoichiometrics, several strains of different production performances were cultivated in shake flasks (Table 16, Figure 30).

Table 16. Kinetics and stoichiometry of low, medium and high producing strains. The data shown comprise the specific growth rate [μ], the biomass yield [$Y_{X/S}$], the product yield [$Y_{P/S}$], the specific ectoine production rate [q_P] and the specific substrate uptake rate [q_S]. The results represent mean values and standard deviations from three biological replicates.

	P3.4	P3.32	P11.28	P11.37
$Y_{Ectoine/S}$ [mol mol^{-1}]	0.26±0.01	0.20±0.00	0.16±0.00	0.08±0.00
$Y_{X/S}$ [g $mmol^{-1}$]	0.05±0.00	0.07±0.00	0.09±0.00	0.08±0.00
$q_{Ectoine}$ [mmol g^{-1} h^{-1}]	0.85±0.03	0.71±0.03	0.57±0.02	0.33±0.01
μ [h^{-1}]	0.16±0.01	0.26±0.00	0.29±0.02	0.34±0.03
q_s [mmol g^{-1} h^{-1}]	3.2±0.1	3.5±0.1	3.5±0.2	4.2±0.1

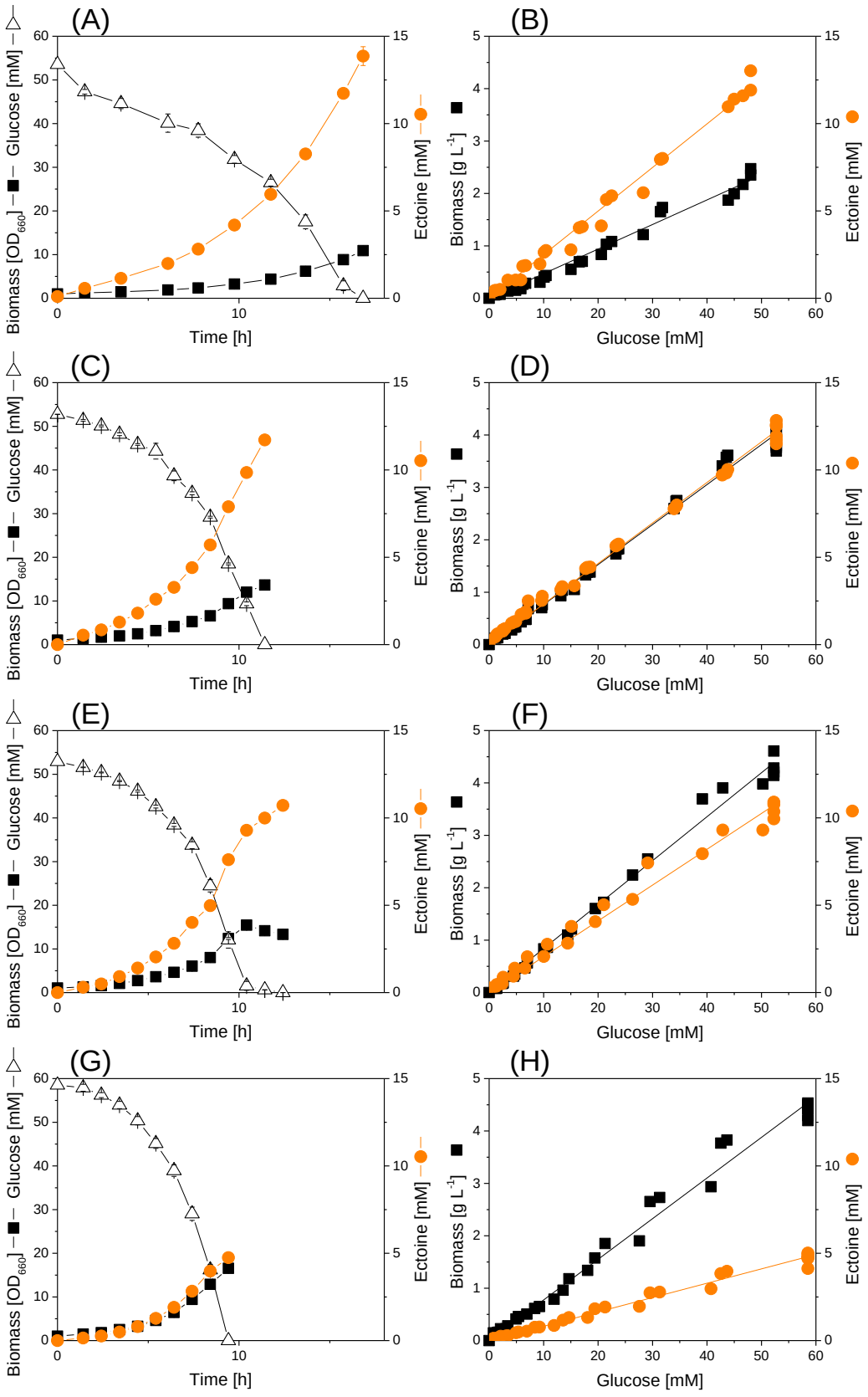

Figure 30. Growth and production characteristics of different synthetic *C. glutamicum* mutants for ectoine production. The strains shown are *C. glutamicum* P3.4 (A, B), P3.32 (C, D), P11.28 (E, F), and P11.37 (G, H). Errors represent standard deviations from three biological replicates.

The strain P11.37 accumulated ectoine with a yield of 0.08 mol mol^{-1} of glucose. The strain P3.4 even exhibited a threefold higher value (0.26 mol mol^{-1}). The increased ectoine yield in comparison to the L-lysine yield of the parent strain indicates an active channeling of carbon from the central metabolism towards ectoine synthesis.

The limitations of the polycistronic reference design used in *C. glutamicum ectABC*^{basic}, with the inability of independent gene expression in an operon-like structure, were widely exposed by the findings of this study, allowing only the channeling of a limited amount of carbon towards ectoine biosynthesis (Becker et al. 2013). Further attempts to use improved L-lysine producing strains with an abolished L-lysine export as chassis for ectoine producers failed so far, due to a potentially incomplete precursor utilization for ectoine synthesis, resulting in mutants with poor growth and low vitality (Pérez-García et al. 2017). Previous studies, suffering from low titers, by-products or auxotrophies did exclusively use a polycistronic design with a single promoter upstream of the first gene in the cluster. These methods were obviously not able to consider gene regulations on transcriptional and translational level, marking the polycistronic design as the final bottleneck (Becker et al. 2013; Ning et al. 2016; Pérez-García et al. 2017). Since the genes of the ectoine cluster were individually controlled in this study, an optimal enzymatic capacity for the different steps was created. Metabolic imbalances of previous producers were reduced, resulting in increased flux towards the ectoine pathway. The best performing strain P3.4 was designated *C. glutamicum ectABC*^{opt} and benchmarked under industrial conditions in a fed-batch process.

4.2.4 Benchmarking of the best producer *C. glutamicum ectABC^{opt}*

In order to assess the performance of *C. glutamicum ectABC^{opt}* under industrial conditions, the strain was fermented in a fed-batch process with molasses based medium (Figure 31). The strain was able to deplete the initial 125 g L^{-1} of sugar within 15 h, resulting in a concentration of 20 g L^{-1} of ectoine after the batch-phase. The concentrated feed solution was added pulse wise when the concentration of glucose dropped below 5 g L^{-1}. By the end of the batch-phase, a final concentration of 65 g L^{-1} of ectoine was achieved, during the feeding-phase, the molar yield peaked at 0.17 mol mol $^{-1}$. The only observed by-product was trehalose which accumulated to a concentration of 3 g L^{-1}. At the beginning of the feeding-phase, a maximum space-time yield for ectoine of 2.3 g L^{-1} h^{-1} was achieved, while throughout the whole process production occurred with 1.2 g L^{-1} h^{-1}.

The mutant strain *C. glutamicum ectABC^{opt}* was able to overcome previous limitations with its optimized flux through the ectoine pathway. Pathway balancing, achieved by the use of specific synthetic promoter- and bicistronic elements created an industrially competitive production process. Previously reported ectoine titers were surpassed nearly twofold (Table 2). Cell vitality and productivity were kept constant during the whole fermentation, indicating a low metabolic burden. The persistent secretion of ectoine into the medium makes this process interesting for industrial application. The export of ectoine into the low salinity culture medium would simplify an adaption of the process to large scale, overcoming the weaknesses of “bacterial milking” (Sauer and Galinski 1998).

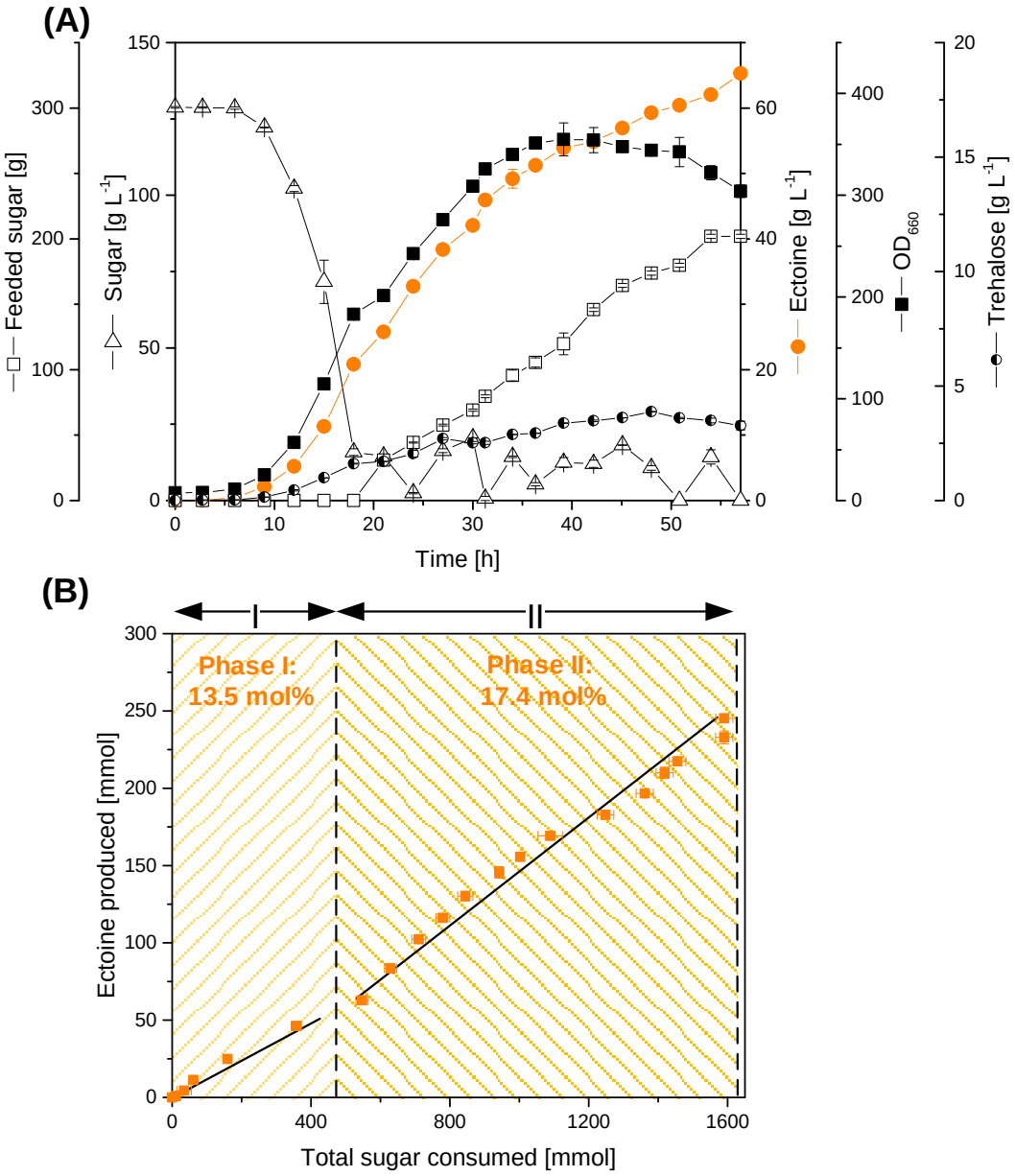

Figure 31. Fed-batch growth (A) and ectoine production (B) characteristic of metabolically engineered *C. glutamicum ectABC^{opt}*. The substrate is given as total sugars (sum of glucose, sucrose or fructose as pure substance or molasses-based). After depletion of the initial sugar, the batch-phase ended and feed pulses were added manually in order to maintain the sugar concentration (A). The molar amount of sugar (B) is reflected by hexose units, implying that sucrose consists of two hexose molecules (glucose and fructose). The data represent mean values and standard deviations of two fermentation experiments.

4.2.5 Impact of transcriptional balancing on ectoine production performance

The findings of this work correlate with results from transcriptional balancing of a heterologous violacein synthesis pathway in *E. coli* (Jeschek et al. 2016; Jones et al. 2015). By correlating promoters, identified in the production strains via sequencing (Figure 29), according to their putative expression strength (Yim et al. 2013), reasons for high level ectoine production in *C. glutamicum* were pinpointed. The strongest promoter H36 was only found in 4% of all plasmids from high level producers.
In fact, the high ectoine production was achieved with plasmids containing promoters of medium strength. The observation matches with previous findings, which reported improved metabolic activity for heterologous pathways at limited expression (Kim et al. 2018; Oh et al. 2015). Furthermore, the increased expression of *ectB* in comparison to *ectA* seemed to be of high importance, as this relationship was observed to be reversed in weaker producers (Figure 29). A similar trend has been observed for the bicistronic designed elements, being slightly stronger for *ectB* than for *ectA* and vice versa for mutants with lower production performance. Previous studies of the ectoine synthesis in various hosts match with the observation made here, identifying the enzyme L-2,4-diaminobutyric acid aminotransferase as rate limiting enzyme in halophilic organisms like *Halomonas elongata* and the heterologous host *E. coli* (Chen et al. 2015; He et al. 2015; Mustakhimov et al. 2010; Ono et al. 1999).

4.2.6 Driving industrial ectoine production at low salinity

So far, the production of the compatible solute ectoine with heterologous hosts under mild conditions suffered from low product yields and titers. Especially in terms of productivity, previous attempts lacked efficiency in space-time yield (Table 2). Fermentations with *Chromohalobacter salexigens* resulted in slightly higher productivities but rely on complex production techniques and high salinity (Fallet et al. 2010). A main advantage of heterologous synthesis is the independency from high salinity media and “bacterial milking” (Becker et al. 2013; Kuhlmann and Bremer 2002; Louis and Galinski 1997; Ning et al. 2016; Pérez-García et al. 2017). The obligatory change from high to low salt to induce an osmotic down shock and release ectoine from the cells, is no more necessary when using the heterologous production system (Sauer and Galinski 1998). The streamlined ectoine pathway in *C. glutamicum* also

reduces or even abolishes the production of side products like L-lysine and trehalose, resulting in decreased carbon loss. In addition, ectoine is not used as energy source by *C. glutamicum*, as it is the case for *Chromohalobacter salexigens* (Vargas et al. 2006). Production of the natural compatible solute trehalose is reduced drastically by the production of ectoine, which may act as a replacement compatible solute. Many production processes still suffer from the high carbon loss into the synthesis of side products (Pérez-García et al. 2017; Rohles et al. 2016; Vassilev et al. 2018). In contrast to the traditional production system, heterologous hosts are able to excrete the majority of product into the medium without external pressure and therefore offer more flexibility for the use in well-established industrial processes (Becker et al. 2013; Becker and Wittmann 2012; Ning et al. 2016; Ruffert et al. 1997).

4.2.7 Metabolic engineering of ectoine export

An important feature of *C. glutamicum* is the efficient export of the product of interest. As example, a permease has been identified as a 1,5-diaminopentane exporter, leading to highly enhanced export of the desired product via overexpression (Kind et al. 2011). With regard to compatible solutes, numerous import mechanisms are known in *C. glutamicum* (Morbach and Krämer 2005). Moreover, active export mechanisms, independent from mechanosensitive release have not been identified so far. In order to gain insight into the export of ectoine in *C. glutamicum*, the basic ectoine producer *C. glutamicum* Ect1 (Becker et al. 2013) and its parent strain *C. glutamicum* LYS-1 (Becker et al. 2011) were analysed via comparative transcriptome analysis. In particular, comparative transcription analysis aimed to identify a possible compatible solute exporter in *C. glutamicum*. The two strains genomically differed in the deletion of the gene *ddh* and the integration of the *ectABCD* cluster. Surprisingly, the two producers varied only slightly in gene expression (Table 17). All significant expression changes are listed in the supplement (Table A 4 and Table A 5). With regard to the identification of a potential ectoine export protein, the gene NCgl2524 appeared to be the most promising candidate. It was upregulated in the ectoine producer and encoded a major facilitator superfamily permease.

Table 17. Significantly upregulated genes in *C. glutamicum* Ect1 grown in standard minimal medium as compared to *C. glutamicum* LYS-1. Genes were identified by comparative transcription analysis via ReadXplorer (Hilker et al. 2016), base mean > 30, log_2fold change > 0.5.

Gene-identifier	Gene name	log_2fold Change	Description	Function
NCgl2941		1.2	Transcriptional regulator	Regulator
NCgl0829		0.5	Transcriptional regulator	
NCgl2311		0.6	DNA-Binding HTH domain-containing protein	
NCgl1485		1.0	Nucleoside-diphosphate-sugar epimerase	Anabolism
NCgl1484		0.8	Glutamine amidotransferase	
NCgl2524		**0.8**	**Major facilitator superfamily permease**	**Transport**
NCgl2732		0.8	ABC transporter duplicated ATPase	
NCgl1214	*lysE*	0.7	L-Lysine efflux permease	
NCgl2246		0.9	Hypothetical protein	Unknown
NCgl0859		0.9	Hypothetical protein	
NCgl1985		0.8	Hypothetical protein	
NCgl0092		0.8	Hypothetical protein	
NCgl1138		0.8	Hypothetical protein	
NCgl2790	*glpK*	0.6	Glycerol kinase	Anabolism
NCgl2110	*qcrA*	0.5	Rieske Fe-S protein	
NCgl2800		0.8	Amidase	Translation
NCgl0463		0.8	NAD-dependent aldehyde dehydrogenase	Catabolism
NCgl0363		0.7	Hypothetical protein	Unknown
NCgl2004		0.6	Hypothetical protein	
NCgl2778		0.6	Hypothetical protein	
NCgl1734		0.6	Hypothetical protein	
NCgl2987		0.6	Hypothetical protein	
NCgl1733		0.6	Hypothetical protein	
NCgl2864		0.5	Hypothetical protein	
NCgl2357		0.5	Hypothetical protein	
NCgl1675		0.5	Hypothetical protein	
NCgl0274		0.5	Membrane carboxypeptidase	Cell envelope synthesis

According to previous work, the gene NCgl2524 is controlled by the transcriptional regulator NCgl2523 (Itou et al. 2005). The transcriptional regulator NCgl2523 exhibits similarity to the multidrug resistance related transcription factor QacR in *Staphylococcus aureus*, which represses transcription of the gene *quacA* similar to NCgl2524 (Brown and Skurray 2001; Itou et al. 2005). In *Staphylococcus aureus*, expression of *quacA* mediates resistance against intercalating dyes and antiseptic compounds (Rouch et al. 1990). A regulator deficient mutant (ΔNCgl2523) of *C. glutamicum* showed increased resistance against substances like norfloxacin, ethidium bromide and benzalkonium chloride (Itou et al. 2005). This indicated a putative compound exporter.

In order to assess the influence of deregulated expression of NCgl2524 in an ectoine producing strain, the repressor NCgl2523 was deleted from the genome of *C. glutamicum* Ect2. The deletion was verified by PCR (Figure 32). It should be noted, that within the approximately 100 screened clones, no mutants could be obtained which lacked the gene NCgl2524. In all cases, the second recombination event resulted in a back-mutation to the wild type.

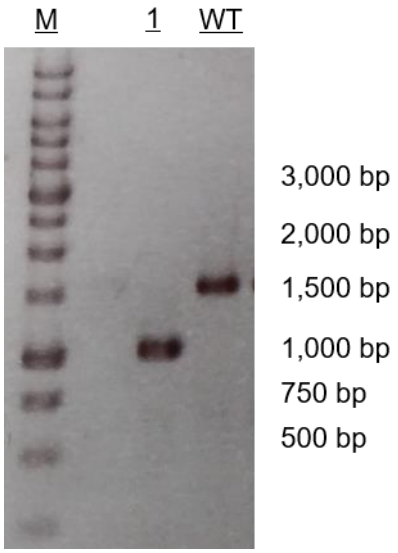

Figure 32. Confirmation of the deletion of NCgl2523 in *C. glutamicum* Ect2 via PCR. Position one shows the successful deletion of NCgl2523, still existent in the wild type (WT) control. The 1 kb ladder was used for size distinction (M).

C. glutamicum Ect2 ΔNCgl2523 showed a 30% increase in ectoine yield and reduced hydroxyectoine excretion on minimal glucose medium (Table 18). Additional by-products were not detected. Consequently, the increase of ectoine yield does not seem to be caused by an overall leakiness of the cell. The deregulation did not significantly influence the biomass yield. Overall, the novel ectoine exporter displays an interesting target for metabolic engineering of *C. glutamicum* for ectoine production.

Table 18. Comparison of growth and production characteristics of *C. glutamicum* Ect2 and *C. glutamicum* Ect2 ΔNCgl2523 in glucose minimal medium. The results represent mean values and standard deviations from three biological replicates.

	C. glutamicum Ect2	*C. glutamicum* Ect2 ΔNCgl2523
μ_{max} [h^{-1}]	0.26±0.00	0.20±0.00
$Y_{X/S}$ [g $mmol^{-1}$]	0.083±0.03	0.084±0.00
$Y_{Ectoine/S}$ [mmol mol^{-1}]	42±1	59±2
$Y_{Hydroxyectoine/S}$ [mmol mol^{-1}]	2.5±0	0.2±0.0

Moreover, the permease NCgl2524 enabled selective export of ectoine. We here identified a highly selective export mechanism for ectoine. The transporter might support the passive system, i.e. mechanosensitive export of ectoine. Taken together, this study contributes to the elucidation of yet unknown compatible solute transport systems in *C. glutamicum* (Booth 2014; Börngen et al. 2010; Cox et al. 2018).

4.2.8 *C. glutamicum* as promising production host for ectoine

This work demonstrates the suitability of *C. glutamicum* as a host for the production of compatible solutes, independent from high salt concentrations. Transcriptional balancing of the ectoine synthesis cluster resulted in an ectoine production strain, which surpassed previously known producers in product titer (Table 2).

The observed excretion of ectoine to the medium without the need for osmotic pressure enables a constant and sole production of the high value substance at low salt levels (Czech et al. 2018). The application of the ectoine overproducer strain, developed in this work, would simplify the currently costly and elaborate downstream processing.

In particular, it would allow to omit steps of an osmotic downshock and electrodialysis (Kunte et al. 2014; Sauer and Galinski 1998). A potential process scheme for such a process is shown in Figure 33. RNA sequencing allowed the identification of an active ectoine export mechanism. The exporter NCgl2524 was found to be selective for ectoine, laying the foundation for further strain development. The identification of an ectoine export mechanism might also contribute to the development of hydroxyectoine producing strains.

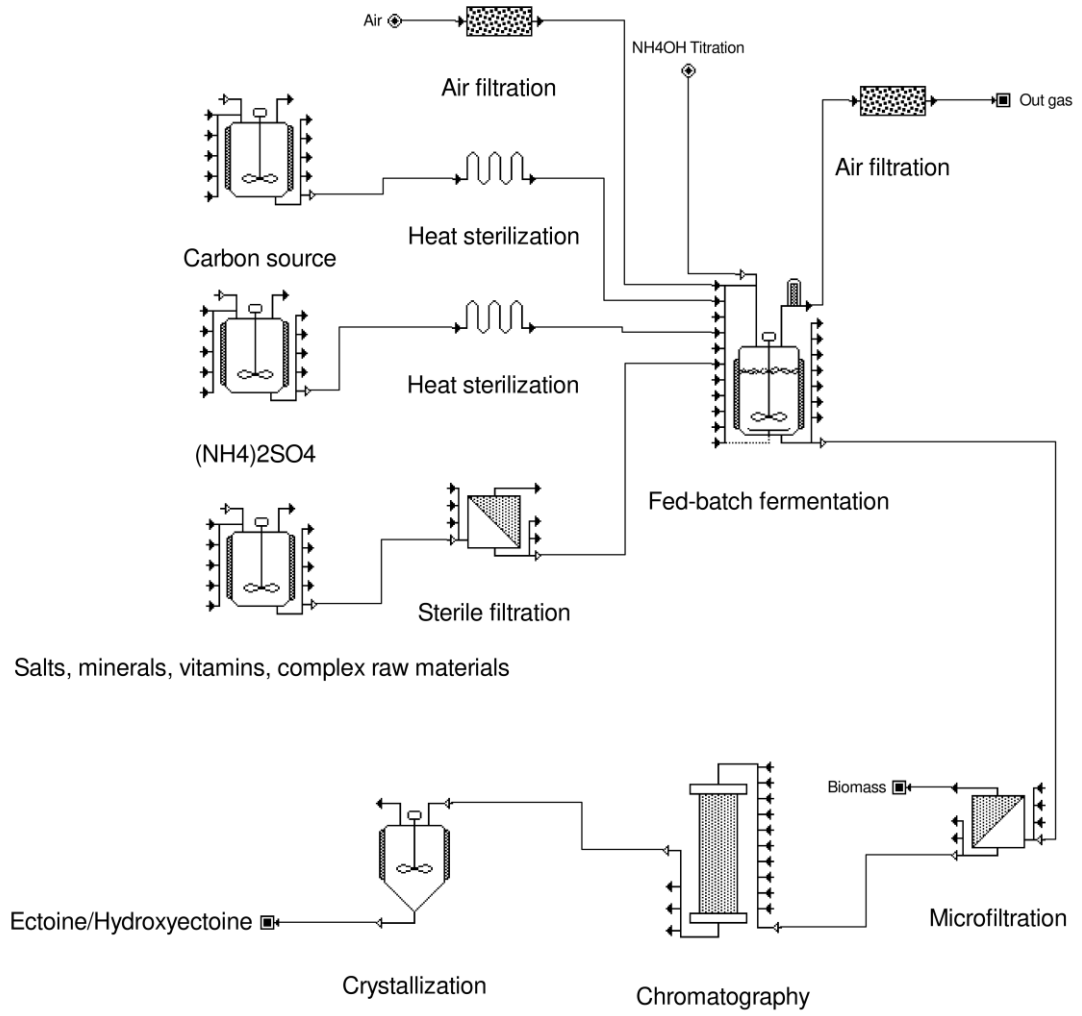

Figure 33. Ectoine process flow diagram for *C. glutamicum* as heterologous ectoine producer. Fed-batch fermentation of the heterologous expression host in low salt medium. Shortened downstream process with microfiltration, extraction of ectoine/ hydroxyectoine from supernatant via preparative chromatography and crystallization of the final product. Corrosive media, biomass recycling, osmotic downshock and electrodialysis are not required in the process (Kunte et al. 2014).

5. Conclusion and Outlook

Continuous efforts in metabolic engineering of *C. glutamicum* have turned the microbe into a most versatile and relevant catalyst in industrial biotechnology. In a relatively short period of time, the bacterium has been optimized towards the production and consumption of numerous natural and non-natural products and substrates (Becker et al. 2018b). The development and application of next generation techniques like advanced genome editing via CRISPR and next generation sequencing opened the door towards the development of new sustainable and highly profitable processes (Cho et al. 2017; Jiang et al. 2017; Pfeifer-Sancar et al. 2013). These developments appear important to face the constant changes of environmental and market requirements and to provide future proof solutions.

This study focused on metabolic engineering of *C. glutamicum* for the enhanced production of L-lysine and ectoine. In order to identify genomic targets for an increased L-lysine yield, the metabolism of the advanced L-lysine producer *C. glutamicum* LYS-12, was analyzed in depth during exposition to temperature stress. The integration of data from transcriptome, fluxome, and functional proteome analysis provided a detailed insight into the adaption of *C. glutamicum* LYS-12 to 38°C. The data helped to identify a remaining bottleneck in L-lysine biosynthesis at the level of the gene *lysA* at high temperature, which was obviously triggered by an increased intracellular level of L-lysine. An optimized producer, which expressed a second copy of the genes *lysE* and *lysG*, exhibited an increased L-lysine yield. The strategy of systems level analysis appears promising for future strain development, e.g. for the production of L-lysine and L-lysine derivatives, such as the biopolymer building block 5-aminovalerate (Rohles et al. 2016) and health-related products such as L-pipecolic acid (Pérez-García et al. 2016). Insights into the regulatory mechanisms of industrial producer strains will help to push the producing cells towards their limit.

Apart from L-lysine, the production of the heterologous compatible solute ectoine was optimized. The application of a combinatorial pathway design enabled an optimal balance for transcription and translation between the three genes *ectA*, *ectB* and *ectC* in *C. glutamicum*. While earlier strains suffered from low productivity and high by-product levels, most likely caused by regulatory imbalances, the strain designed in this work surpassed natural and non-natural ectoine producers obtained so far. Low salt production as demonstrated here, could replace current industrial processes

depending on “bacterial milking” (Sauer and Galinski 1998) due to the possibility of a simplified downstream processing. Furthermore, the identification of an ectoine exporter protein in *C. glutamicum* via next generation sequencing enabled the development of a more advanced producing strain. Due to the increasing demand for ectoine, the findings seem promising to finally obtain sole producers for ectoine and hydroxyectoine, further decreasing the costs for elaborate product separation systems. (Czech et al. 2018). By taking the discoveries to industrial scale in the future, competitive processes might be developed, which could lead to a worldwide increase in market volume at reduced costs (Cantera et al. 2018; Czech et al. 2018; Strong et al. 2016).

6. Appendix

Table A 1. Primers used in this work.

Primer	5'-Sequence-3'
L-Lysine strain construction and verification	
*bioD*_Downstream_FW	AATCCCGGGTCTAGAGGATCACGCATGAGTGTGCTTGTGGAA
*bioD*_Downstream_RV	TCGAGGGATTGCGGCCTTAGGGTTTATTTCCCTTTAACTGCAGC
*lysGE*_FW	CTGCGTTAATTAACAATTGGTAAGCAATGGCCTACAACCAGAC
*lysGE*_RV	AACTGATGTTGATGGGTTAGTCGTGAACACCGTGCCTTCG
*bioD*_Upstream_FW	CAGTTAAAGGGAAATAAACCCTAAGGCCGCAATCCCTCGA
*bioD*_Upstream_FW	CGAAGGCACGGTGTTCACGACTAACCCATCAACATCAGTTTGATG
Δ*malE*_TS1_FW	GCGAAAGAGCTAAACAGCTG
Δ*malE*_TS1_RV	CAGCTGTTTAGCTCTTTCGCAGGACGCTCTCAAACTCATG
Δ*malE*_TS2_FW	GATCAACGCGTCTGAAGTAGCAGCCCAAATTC
Δ*malE*_TS2_RV	ATCTACGTCGACCATTACTCCAAGGCAAGAGAG

Table A 1 continued

Primer	5'-Sequence-3'
Ectoine library construction	
BCD-F-*BamH*I	ATTAATGGATCCGGGCCCAAGTTCACTTAAAAAGGAGATCAA CAATGAAAGCAATTTTCGTACTGAAAC
BCD2-*ectA*-F1	GAAAGCAATTTTCGTACTGAAACATCTTAATCATGCTAAGGAG GTTTTCTAATGCCAACCCTGAAGCGCAACT
BCD21-*ectA*-F1	GAAAGCAATTTTCGTACTGAAACATCTTAATCATGCGAGGGA TGGTTTCTAATGCCAACCCTGAAGCGCAACT
BCD8-*ectA*-F1	GAAAGCAATTTTCGTACTGAAACATCTTAATCATGCATCGGAC CGTTTCTAATGCCAACCCTGAAGCGCAACT
BCD2-*ectB*-F1	GAAAGCAATTTTCGTACTGAAACATCTTAATCATGCTAAGGAG GTTTTCTAATGAAAACCTTCGAACTGAACGAATCC
BCD21-*ectB*-F1	GAAAGCAATTTTCGTACTGAAACATCTTAATCATGCGAGGGA TGGTTTCTAATGAAAACCTTCGAACTGAACGAATCC
BCD8-*ectB*-F1	GAAAGCAATTTTCGTACTGAAACATCTTAATCATGCATCGGAC CGTTTCTAATGAAAACCTTCGAACTGAACGAATCC
BCD2-*ectC*-F1	GAAAGCAATTTTCGTACTGAAACATCTTAATCATGCTAAGGAG GTTTTCTAATGATCGTGCGCACCCTG
BCD21-*ectC*-F1	GAAAGCAATTTTCGTACTGAAACATCTTAATCATGCGAGGGA TGGTTTCTAATGATCGTGCGCACCCTG
BCD8-*ectC*-F1	GAAAGCAATTTTCGTACTGAAACATCTTAATCATGCATCGGAC CGTTTCTAATGATCGTGCGCACCCTG
ectA-R-NotI	ATTAATGCGGCCGCTCATTATGCGTGTTCTTTCAGTTCTTCTT CCAG
ectB-R-NotI	ATTAATGCGGCCGCTCATTAGGATGCCTGGTTTTCGGTCT
ectC-R-NotI	ATTAATGCGGCCGCTCATTACACGGTTTCTGCTTCCAGT
*Xho*I-*ectA*-F	GCTCCTCGAGAAAGGGAACAAAAGCTGGGTAC
ectA-*Sal*I-*Xba*IR	CGAGTCTAGAGTCGACTCACCGACAAAACAACAGATAAAA
*Xho*I-*ectB*-F	GCTCCTCGAGAAAGGGAACAAAAGCTGGGTAC
ectB-*Sal*I-*Xba*IR	CGAGTCTAGATTGTCGACTCACCGACAAACAACAGATAAAA
*Sal*I-*ectC*-F	GCTCGTCGACAAAGGGAACAAAAGCTGGGTAC
ectC-*Xba*I-R	CGAGTCTAGATCACCGACAAACAACAGATAAAA

Table A 1 continued

Primer	5'-Sequence-3'
Ectoine strain construction and verification	
Pr1_*tufectABC*_FW	GGGCCCGGTACCACGCGTCATGGCCGTTACCCTGCGAA
Pr2_*tufectABC*_RV	CCCTAGGTCCGAACTAGTCATATTACACGGTTTCTGCTTCCAGTG
Pr1_seq_*ectA*	CGAGCTGGTGCAGGTTGTAG
Pr2_seq_*ectB*	TCGATGTAGCGCTTGCCATCC
Pr3_seq_*ectC*	GAAGGAGAAGCCCACCTTATC
Pr1_TS1_FW_ ΔNCgl2523	TTAACAATTGGGATCCTCTAGACCCTATCGGTGGTGCAAACCTG
Pr2_TS1_RV_ΔNCgl2523	TATTGGCTCCCTTCGGATTT
Pr3_TS2_FW_ΔNCgl2523	CGCGGAAATCCGAAGGGAGCCAATAATTTCTACCTTAAAGTCTTGAG
Pr4_TS2_RV_ΔNCgl2523	GCAGCCCGCTAGCGATTTAAATCCCGAAACCAGAAACTCGGCCCAC

Table A 2. Upregulated genes of *C. glutamicum* LYS-12 cultivated at 38°C in comparison to *C. glutamicum* LYS-12 cultivated at 30°C. Genes were identified by comparative transcription analysis via ReadXplorer (Hilker et al. 2016), base mean > 30.

Gene-identifier	log2fold Change	Feature
NCgl0132	4.1	Hypothetical protein
NCgl2739	3.8	3-Methyladenine DNA glycosylase
NCgl2028	3.0	Hydroxypyruvate isomerase
NCgl2029	3.0	Dehydrogenase
NCgl0131	3.0	Hypothetical protein
NCgl2246	2.9	Hypothetical protein
NCgl1040	2.6	Excinuclease Atpase subunit
NCgl1584	2.6	Glycerol-3-phosphate dehydrogenase
NCgl0148	2.3	Hypothetical protein
NCgl1485	2.2	Nucleoside-diphosphate-sugar epimerase
NCgl2061	2.1	Hypothetical protein
NCgl0200	1.8	NADPH:quinone reductase or related Zn-dependent oxidoreductase
NCgl0363	1.8	Hypothetical protein
NCgl0642	1.8	Hypothetical protein
NCgl0890	1.8	Hypothetical protein
NCgl0233	1.8	Glutamyl-Q tRNA (Asp) synthetase
NCgl0198	1.7	ABC transporter permease
NCgl1060	1.7	Hypothetical protein
NCgl1323	1.7	Hypothetical protein
NCgl1707	1.7	Hypothetical protein
NCgl2516	1.7	Dithiobiotin synthetase
NCgl2901	1.7	Methylated DNA-protein cysteine methyltransferase
NCgl2941	1.7	Transcriptional regulator
NCgl2840	1.6	Transcriptional regulator
NCgl1588	1.6	Hypothetical protein
NCgl1163	1.5	ATP synthase F0F1 subunit alpha
NCgl1354	1.5	TpR repeat-containing protein
NCgl2041	1.5	Coenzyme F420-dependent N5,N10-methylene tetrahydromethanopterin reductase
NCgl1189	1.5	Spermidine synthase
NCgl0655	1.5	Transcriptional regulator
NCgl1046	1.5	Hypothetical protein
NCgl1185	1.5	Hypothetical protein
NCgl0953	1.4	Pantothenate kinase
NCgl0736	1.4	Hypothetical protein
NCgl0405	1.4	Transcriptional regulator
NCgl0549	1.4	Hypothetical protein
NCgl2173	1.4	Hydrolase/acyltransferase
NCgl2000	1.4	Glycerate kinase
NCgl0800	1.4	Hypothetical protein
NCgl0797	1.4	Acetyl-CoA carboxylase beta subunit
NCgl2405	1.4	4'-Phosphopantetheinyl transferase
NCgl1038	1.4	Hypothetical protein
NCgl1347	1.4	Argininosuccinate lyase
NCgl1078	1.4	ATPase
NCgl0213	1.4	ABC transporter ATPase
NCgl1082	1.3	Hypothetical protein
NCgl0991	1.3	Acetyltransferase
NCgl1900	1.3	Polynucleotide phosphorylase
NCgl0750	1.3	Hypothetical protein
NCgl0920	1.3	Hypothetical protein
NCgl1974	1.3	16S rRNA-processing protein rimm
NCgl1073	1.3	Glucose-1-phosphate adenylyltransferase

Table A 2 continued

Gene-identifier	log2fold Change	Feature
NCgl2243	1.3	Sugar kinase
NCgl2871	1.3	Cation transport atpase
NCgl1741	1.2	Hypothetical protein
NCgl1340	1.2	N-acetyl-gamma-glutamyl-phosphate reductase
NCgl2577	1.2	Hypothetical protein
NCgl0650	1.2	D-alanyl-D-alanine carboxypeptidase
NCgl2631	1.2	Hypothetical protein
NCgl1932	1.2	Methionine aminopeptidase
NCgl1379	1.2	Zinc transporter zupT
NCgl0191	1.2	Hypothetical protein
NCgl0621	1.2	Hypothetical protein
NCgl1837	1.2	Hypothetical protein
NCgl2334	1.2	Hypothetical protein
NCgl1827	1.1	1-Deoxy-D-xylulose-5-phosphate synthase
NCgl1147	1.1	Hypothetical protein
NCgl2305	1.1	Hypothetical protein
NCgl0959	1.1	Sortase or related acyltransferase
NCgl1216	1.1	Glutathione S-transferase
NCgl0602	1.1	Lipocalin
NCgl2144	1.1	Hypothetical protein
NCgl1672	1.1	Hypothetical protein
NCgl2355	1.1	Hypothetical protein
NCgl2252	1.1	Hypothetical protein
NCgl0322	1.1	5'-Nucleotidase
NCgl1401	1.1	Transcriptional regulator
NCgl2487	1.1	Histone acetyltransferase Hpa2-like protein
NCgl1838	1.1	Hypothetical protein
NCgl0915	1.0	ABC transporter ATPase and permease
NCgl0550	1.0	Subtilisin-like serine protease
NCgl2972	1.0	Hypothetical protein
NCgl2406	1.0	Major facilitator superfamily permease
NCgl0737	1.0	Helicase
NCgl1083	1.0	Hypothetical protein
NCgl0604	1.0	Deoxyribodipyrimidine photolyase
NCgl0666	1.0	Citrate synthase
NCgl1047	1.0	Hypothetical protein
NCgl0732	1.0	Hypothetical protein
NCgl2583	1.0	Hypothetical protein
NCgl0119	1.0	Carbonic anhydrase/acetyltransferase
NCgl1214	1.0	L-Lysine efflux permease
NCgl2187	0.9	Hypothetical protein
NCgl2660	0.9	Hypothetical protein
NCgl2987	0.9	Hypothetical protein
NCgl2447	0.9	Hypothetical protein
NCgl1908	0.9	Exopolyphosphatase
NCgl1194	0.9	Major facilitator superfamily permease
NCgl2022	0.9	Hypothetical protein
NCgl0808	0.9	Hypothetical protein
NCgl1319	0.9	Hypothetical protein
NCgl0727a	0.9	Hypothetical protein
NCgl0139	0.9	Hrpa-like helicase
NCgl0433	0.9	1,4-Dihydroxy-2-naphthoate octaprenyltransferase
NCgl1050	0.9	Hypothetical protein

Table A 2 continued

Gene-identifier	log2fold Change	Feature
NCgl0620	0.9	Bifunctional 5,10-methylene-tetrahydrofolate dehydrogenase/ 5,10-methylene-tetrahydrofolate cyclohydrolase
NCgl0791	0.9	rRNA methylase
NCgl0904	0.9	Hypothetical protein
NCgl1255	0.8	Glucan phosphorylase
NCgl2125	0.8	Hypothetical protein
NCgl0922	0.8	Hypothetical protein
NCgl0357	0.8	Hypothetical protein
NCgl1026	0.8	Hypothetical protein
NCgl2640	0.8	Carboxylate-amine ligase
NCgl0735	0.8	Hypothetical protein
NCgl2053	0.8	Dehydrogenase
NCgl0488	0.8	50S ribosomal protein l4
NCgl2461	0.8	Hypothetical protein
NCgl1508	0.8	Cytochrome oxidase assembly protein
NCgl2295	0.8	Molecular chaperone
NCgl1646	0.8	Hypothetical protein
obgE	0.8	GTPase obgE
NCgl2083	0.8	UDP-N-acetylmuramoylalanyl-D-glutamate--2, 6-diaminopimelate ligase
NCgl2762	0.8	Glycosyltransferase
NCgl0809	0.8	Dihydrofolate reductase
NCgl0795	0.8	Type II citrate synthase
NCgl0544	0.8	Acetyltransferase
NCgl0772	0.8	Hypothetical protein
NCgl2298	0.8	Transcriptional regulator
NCgl1067	0.8	Glucosyl-3-phosphoglycerate synthase
NCgl1978	0.8	ABC transporter permease
rho	0.7	Transcription termination factor Rho
NCgl2171	0.7	Hypothetical protein
NCgl0474	0.7	Transcriptional regulator
NCgl1929	0.7	Hypothetical protein
NCgl1747	0.7	Hypothetical protein
NCgl2253	0.7	Hypothetical protein
NCgl1574	0.7	Metalloprotease
NCgl1734	0.7	Hypothetical protein
NCgl2581	0.7	Hypothetical protein
NCgl0901	0.7	Peptidyl-tRNA hydrolase
NCgl2720	0.7	Hypothetical protein
NCgl2286	0.7	Hypothetical protein
NCgl2576	0.7	DNA integrity scanning protein DisA
NCgl0812	0.7	Lhr-like helicase
NCgl2074	0.7	Hypothetical protein
NCgl1583	0.7	L-serine deaminase
NCgl2537	0.7	Trehalose-6-phosphatase
NCgl1548	0.7	Carbamoyl phosphate synthase small subunit
NCgl1479	0.7	Phosphoribosylaminoimidazole-succinocarboxamide synthase
NCgl2124	0.7	Leucyl aminopeptidase
NCgl1237	0.7	3-isopropylmalate dehydrogenase
NCgl1742	0.7	Hypothetical protein
NCgl1074	0.7	Hypothetical protein
NCgl2986	0.7	N-acetylmuramoyl-l-alanine amidase
NCgl1921	0.7	Mg-chelatase subunit ChlD
NCgl0380	0.7	ABC transporter atpase
NCgl1831	0.7	Hypothetical protein
NCgl0348	0.6	Transposase

Table A 2 continued

Gene-identifier	log2fold Change	Feature
NCgl2813	0.6	Flavoprotein
NCgl2150	0.6	Hypothetical protein
NCgl1959	0.6	ABC transporter periplasmic component
NCgl2438	0.6	Ribonucleotide-diphosphate reductase subunit beta
NCgl1570	0.6	Alanyl-tRNA synthetase
NCgl0931	0.6	Hypothetical protein
NCgl0884	0.6	Hypothetical protein
NCgl0250	0.6	RNA polymerase sigma factor
NCgl2671	0.6	Hypothetical protein
NCgl2186	0.6	Hypothetical protein
NCgl2302	0.6	Major facilitator superfamily permease
NCgl2900	0.6	Hypothetical protein
NCgl2839	0.6	Inner membrane protein translocase YidC
NCgl1478	0.6	Hypothetical protein
NCgl2694	0.6	Hypothetical protein
NCgl2908	0.6	Mercuric reductase
NCgl0796	0.6	FKBP-type peptidylprolyl isomerase
NCgl2404	0.6	Transcriptional regulator
NCgl1410	0.6	Cyclopropane fatty acid synthase
NCgl0463	0.6	NAD-dependent aldehyde dehydrogenase
NCgl0615	0.6	Hypothetical protein
NCgl1070	0.6	SAM-dependent methyltransferase
NCgl2658	0.6	Ferredoxin/ferredoxin-NADP reductase
NCgl2290	0.6	Hypothetical protein
NCgl0335	0.6	Hypothetical protein
NCgl0866	0.6	Adenine-specific DNA methylase
NCgl0667	0.5	Hypothetical protein
NCgl1658	0.5	Hypothetical protein
NCgl2743	0.5	Hypothetical protein
NCgl2526	0.5	Succinate dehydrogenase/fumarate reductase, flavoprotein subunit
NCgl0964	0.5	Hypothetical protein
NCgl0112	0.5	Pantoate--beta-alanine ligase
NCgl2777	0.5	Esterase
NCgl0502	0.5	Hypothetical protein
NCgl1483	0.5	Transcriptional regulator
NCgl2387	0.5	Hypothetical protein
NCgl1876	0.5	Glutamate ABC transporter periplasmic component
NCgl0032	0.5	Hypothetical protein
NCgl2836	0.5	Hypothetical protein
NCgl1482	0.5	Aconitate hydratase
NCgl2201	0.5	Hypothetical protein
NCgl1093	0.5	Major facilitator superfamily permease
NCgl1213	0.5	Oxidoreductase
NCgl1365	0.5	ABC transporter duplicated ATPase
NCgl2143	0.5	Hypothetical protein
NCgl2303	0.5	Permease
NCgl2832	0.5	Membrane transport protein
NCgl2241	0.5	ABC transporter duplicated ATPase
NCgl1670	0.5	Hypothetical protein
NCgl2101	0.5	Hypothetical protein
NCgl2472	0.5	Regulatory-like protein
NCgl0829	0.5	Transcriptional regulator
NCgl0355	0.5	Dihydrolipoamide dehydrogenase
NCgl1348	0.5	Hypothetical protein
NCgl2219	0.5	Zn-dependent oligopeptidase
NCgl1393	0.5	Hypothetical protein

Table A 2 continued

Gene-identifier	log2fold Change	Feature
NCgl1641	0.5	Hypothetical protein
NCgl0230	0.5	Hypothetical protein
NCgl1755	0.5	Hypothetical protein
NCgl2110	0.5	Rieske Fe-S protein
NCgl0029	0.5	ABC transporter periplasmic component
NCgl2360	0.5	Cystathionine gamma-synthase
NCgl2004	0.5	Hypothetical protein
NCgl0633	0.5	Hypothetical protein
NCgl0638	0.5	ABC transporter permease
NCgl0924	0.4	Transcription-repair coupling factor
NCgl1492	0.4	Integrase
NCgl1756	0.4	Hypothetical protein
NCgl0864	0.4	Hypothetical protein
NCgl2661	0.4	Hypothetical protein
NCgl2669	0.4	Adenylosuccinate synthetase
NCgl2130	0.4	Permease
NCgl0479	0.4	Hypothetical protein
NCgl1973	0.4	Hypothetical protein
NCgl2940	0.4	Hypothetical protein
NCgl2876	0.4	Transmembrane transport protein
NCgl2276	0.4	Xanthine/uracil permease
NCgl1371	0.4	16S rRNA uridine-516 pseudouridylate synthase
NCgl1416	0.4	Hypothetical protein
NCgl0455	0.4	Oxidoreductase
NCgl1697	0.4	Hypothetical protein
NCgl2050	0.4	Permease
NCgl0606	0.4	ABC transporter permease
NCgl1431	0.4	Hypothetical protein
NCgl1847	0.4	Hypothetical protein
NCgl0133	0.4	Aspartate alpha-decarboxylase
NCgl0212	0.4	Hypothetical protein
NCgl2441	0.4	Mn-dependent transcriptional regulator
NCgl1283	0.4	Hypothetical protein
NCgl2781	0.4	Prenyltransferase
NCgl1662	0.4	Transposase
NCgl1021	0.4	Transposase
NCgl2191	0.4	Glucosamine--fructose-6-phosphate aminotransferase
NCgl2167	0.4	Pyruvate dehydrogenase subunit E1
NCgl1484	0.4	Glutamine amidotransferase
NCgl1705	0.4	Stress-sensitive restriction system protein 2
NCgl2091	0.4	5,10-methylenetetrahydrofolate reductase
NCgl2111	0.4	Cytochrome C
NCgl0658	0.4	Flavoprotein disulfide reductase
NCgl1170	0.4	Lactoylglutathione lyase
NCgl0639	0.3	ABC transporter periplasmic component
NCgl1852	0.3	HrpA-like helicase
NCgl2698	0.3	NAD-dependent aldehyde dehydrogenase
NCgl0665	0.3	PEP phosphonomutase or related enzyme
NCgl1039	0.3	Hypothetical protein
NCgl2052	0.3	Co/Zn/Cd cation transporter
NCgl2090	0.3	Hypothetical protein
NCgl2060	0.3	ABC transporter ATPase
NCgl0480	0.3	Elongation factor Tu
NCgl1062	0.3	Gamma-aminobutyrate permease

Table A 2 continued

Gene-identifier	log2fold Change	Feature
NCgl2688	0.3	Cystathionine gamma-synthase
NCgl0726	0.3	Preprotein translocase subunit seca
NCgl1071	0.3	Beta-fructosidase
NCgl2247	0.3	Malate synthase G
NCgl1626	0.3	Phosphopantothenoylcysteine synthetase/decarboxylase
NCgl2926	0.3	Hypothetical protein
NCgl1411	0.3	Major facilitator superfamily permease
NCgl1616	0.3	Hypothetical protein
NCgl2529	0.3	Hypothetical protein
NCgl2070	0.3	Cell division initiation protein
NCgl0106	0.3	Lactoylglutathione lyase or related lyase
NCgl2103	0.3	Hypothetical protein
NCgl0481	0.3	Hypothetical protein
NCgl1633	0.3	Hypothetical protein
NCgl1733	0.3	Hypothetical protein
NCgl2306	0.3	Acyl-CoA:acetate CoA transferase beta subunit
NCgl2749	0.3	Hypothetical protein
NCgl2359	0.3	Transcriptional regulator
NCgl1920	0.3	Hypothetical protein
NCgl1939	0.3	Membrane-associated Zn-dependent protease 1
NCgl2894	0.3	Myo-inositol-1-phosphate synthase
NCgl2729	0.3	ABC transporter permease
NCgl1910	0.3	Translation initiation factor IF-2
NCgl1300	0.3	Major facilitator superfamily permease
NCgl1452	0.3	K+ transport flavoprotein
NCgl0436	0.3	Hypothetical protein
NCgl1018	0.3	Hypothetical protein
NCgl0199	0.3	Selenocysteine lyase
NCgl1687	0.3	Hypothetical protein
NCgl0013	0.3	Hypothetical protein
NCgl1451	0.3	Hypothetical protein
NCgl1754	0.2	Hypothetical protein
NCgl2341	0.2	Type IV restriction endonuclease
NCgl1322	0.2	Excinuclease ABC subunit A
NCgl0120	0.2	Transcriptional regulator
NCgl1240	0.2	DNA polymerase III epsilon subunit
NCgl0203	0.2	Na+/alanine symporter
NCgl1945	0.2	Hypothetical protein
NCgl0717	0.2	Hypothetical protein
NCgl2863	0.2	Two-component system, response regulator
NCgl2467	0.2	Dehydrogenase
NCgl1085	0.2	ABC transporter duplicated ATPase
NCgl1176	0.2	ABC transporter periplasmic component
NCgl2242	0.2	2'-5' RNA ligase
NCgl1378	0.2	ABC-type transport system atpase
NCgl1740	0.2	Hypothetical protein
NCgl2363	0.2	Chromate transport protein chra
NCgl1094	0.2	5-Methyltetrahydropteroyltriglutamate-- homocysteine S-methyltransferase
NCgl2491	0.2	4-Amino-4-deoxychorismate lyase
NCgl1902	0.2	Inosine-uridine nucleoside N-ribohydrolase
NCgl2789	0.2	Hypothetical protein
NCgl1826	0.2	Ribonuclease D
NCgl0435	0.2	O-succinylbenzoic acid-CoA ligase
NCgl1518	0.2	Hypothetical protein
NCgl2675	0.2	rRNA methylase

Table A 2 continued

Gene-identifier	log2fold Change	Feature
NCgl1867	0.2	Hypothetical protein
NCgl0802	0.2	Fatty-acid synthase
NCgl2495	0.2	Amidophosphoribosyltransferase
NCgl0167	0.2	Transcriptional regulator
NCgl2916	0.2	Hypothetical protein
NCgl0746	0.2	Hypothetical protein
NCgl1631	0.2	Hypothetical protein
NCgl1222	0.2	Acetolactate synthase large subunit
NCgl2284	0.2	Transposase
NCgl1928	0.2	Mycothione reductase
NCgl0518	0.2	30S ribosomal protein S5
rpsA	0.2	30S ribosomal protein S1
NCgl0752	0.2	Hypothetical protein
NCgl1625	0.2	Hypothetical protein
NCgl2902	0.2	Hypothetical protein
NCgl1669	0.2	ATPase
NCgl2218	0.2	ABC transporter ATPase and permease
NCgl2318	0.2	Chloromuconate cycloisomerase
NCgl0860	0.1	Hypothetical protein
NCgl2779	0.1	Esterase
NCgl0691	0.1	Hypothetical protein
NCgl0092	0.1	Hypothetical protein
NCgl1575	0.1	Helicase
NCgl0916	0.1	Gamma-glutamyltranspeptidase
NCgl0353	0.1	Cell wall biogenesis glycosyltransferase
NCgl1749	0.1	Hypothetical protein
NCgl0821	0.1	ABC transporter permease
NCgl2154	0.1	Hypothetical protein
NCgl0012	0.1	DNA gyrase subunit A
NCgl1931	0.1	Hypothetical protein
NCgl0749	0.1	Hypothetical protein
NCgl2702	0.1	Molecular chaperone DnaK
NCgl0069	0.1	Phosphoglycerate dehydrogenase or related dehydrogenase
NCgl1655	0.1	Hypothetical protein
NCgl2474	0.1	Serine acetyltransferase
NCgl1145	0.1	Serine protease
NCgl0274	0.1	Membrane carboxypeptidase
NCgl0659	0.1	Pyruvate carboxylase
NCgl2285	0.1	Pirin

Table A 3. Downregulated genes of *C. glutamicum* LYS-12 cultivated at 38°C in comparison to *C. glutamicum* LYS-12 cultivated at 30°C. Genes were identified by comparative transcription analysis via ReadXplorer (Hilker et al. 2016), base mean > 30.

Gene-identifier	log2fold Change	Feature
NCgl0394	-2.4	ABC-type transport system permease
NCgl2740	-1.9	Hemoglobin-like flavoprotein
NCgl1133	-1.9	Diaminopimelate decarboxylase
NCgl1132	-1.9	Arginyl-tRNA synthetase
NCgl0662	-1.4	G3e family GTPase
NCgl0184	-1.3	Arabinosyl transferase
NCgl2982	-1.1	Virulence factor
NCgl2800	-1.1	Amidase
NCgl0409	-1.1	Shikimate 5-dehydrogenase
NCgl2100	-1.0	Hypothetical protein
NCgl1965	-1.0	Thiamine biosynthesis protein ThiF
NCgl0030	-1.0	ABC transporter permease
NCgl0202	-0.9	Hypothetical protein
NCgl0340	-0.9	Nucleoside-diphosphate sugar epimerase
NCgl0911	-0.9	Two-component system sensory transduction histidine kinase
NCgl2409	-0.9	3-oxoacyl-ACP synthase
NCgl0194	-0.8	Hypothetical protein
NCgl2713	-0.8	Permease
NCgl2460	-0.8	Transposase
NCgl0912	-0.7	Two-component system, response regulator
NCgl0687	-0.7	Nitrilotriacetate monooxygenase
NCgl2936	-0.7	ABC transporter permease
NCgl1200	-0.7	Siderophore-interacting protein
NCgl0504	-0.7	Hypothetical protein
NCgl0601	-0.6	MarR family transcriptional regulator
NCgl2152	-0.6	Galactokinase
NCgl0978	-0.6	Hypothetical protein
NCgl0391	-0.6	Signal transduction histidine kinase
NCgl1294	-0.6	Hypothetical protein
NCgl0828	-0.6	Citrate lyase beta subunit
NCgl2229	-0.6	Coenzyme F420-dependent N5,N10-methylene tetrahydromethanopterin reductase
NCgl0673	-0.6	Hypothetical protein
NCgl1868	-0.5	Diaminopimelate epimerase
NCgl0047	-0.5	Hypothetical protein
NCgl2914	-0.5	Hypothetical protein
NCgl2325	-0.5	Benzoate transporter
NCgl2809	-0.5	Pyruvate kinase
NCgl0285	-0.5	Zn-dependent hydrolase
NCgl0503	-0.5	Aldo/keto reductase
NCgl1134	-0.5	Hypothetical protein
NCgl0705	-0.5	Helicase
NCgl1031	-0.5	Major facilitator superfamily permease
NCgl2222	-0.5	Hypothetical protein
NCgl0700	-0.5	Helicase
NCgl0656	-0.5	Phosphomannomutase
NCgl0108	-0.5	Mannitol-1-phosphate/altronate dehydrogenase
NCgl2668	-0.5	Two-component system, response regulator
NCgl0024	-0.5	Transcriptional regulator
NCgl0068	-0.5	Two-component system response regulator
NCgl0229	-0.5	Queuine/archaeosine tRNA-ribosyltransferase
NCgl0429	-0.5	YjgF translation initiation inhibitor
NCgl1354a	-0.5	Hypothetical protein
NCgl0699	-0.5	Hypothetical protein
NCgl1417	-0.4	Sulfate permease
NCgl0146	-0.4	Methylated DNA-protein cysteine methyltransferase

Table A 3 continued

Gene-identifier	log2fold Change	Feature
NCgl2340	-0.4	Aminopeptidase
NCgl2139	-0.4	Threonine synthase
NCgl2895	-0.4	Hypothetical protein
NCgl0375	-0.4	Cation transport ATPase
NCgl2833	-0.4	Transcriptional regulator
NCgl0278	-0.4	Major facilitator superfamily permease
NCgl2964	-0.4	Helicase
NCgl0625	-0.4	O-acetylhomoserine aminocarboxypropyltransferase
NCgl2195	-0.4	Chromosome segregation ATPase
NCgl0095	-0.4	Hypothetical protein
NCgl2774	-0.4	Acyl-CoA synthetase
NCgl0694	-0.4	ABC transporter permease
NCgl2400	-0.4	Hypothetical protein
NCgl0596	-0.4	C50 carotenoid epsilon cyclase
NCgl1627	-0.4	Hypothetical protein
NCgl0926	-0.4	ABC transporter atpase
NCgl0994	-0.4	Diguanylate cyclase
NCgl0729	-0.3	Hypothetical protein
NCgl0831	-0.3	30S ribosomal protein S18
NCgl1566	-0.3	ABC transporter ATPase
NCgl2064	-0.3	DNA polymerase IV
NCgl2525	-0.3	Hypothetical protein
NCgl2788	-0.3	UDP-galactopyranose mutase
NCgl2648	-0.3	Na+/phosphate symporter
NCgl0603	-0.3	Nucleoside-diphosphate-sugar epimerase
NCgl0050	-0.3	Phenol 2-monooxygenase
NCgl0351	-0.3	UDP-glucose 6-dehydrogenase
NCgl0611	-0.3	DNA polymerase III subunit alpha
NCgl2746	-0.3	ABC transporter ATPase
NCgl0891	-0.3	Hypothetical protein
NCgl2864	-0.3	Hypothetical protein
NCgl0728	-0.3	Hypothetical protein
NCgl2528	-0.3	D-2-hydroxyisocaproate dehydrogenase
NCgl0599	-0.3	RND superfamily drug exporter
NCgl0747	-0.3	Hypothetical protein
NCgl2639	-0.3	Hypothetical protein
NCgl0706	-0.3	Type II restriction enzyme, methylase subunits
NCgl0701	-0.2	Hypothetical protein
NCgl0854	-0.2	Dolichyl-phosphate-mannose--protein O-mannosyl transferase PMT1
NCgl0155	-0.2	5-Dehydro-2-deoxygluconokinase
NCgl2291	-0.2	Hypothetical protein
NCgl1084	-0.2	Alpha-ketoglutarate decarboxylase
NCgl0820	-0.2	Helicase
NCgl2680	-0.2	Multidrug resistance protein
NCgl2456	-0.2	Hypothetical protein
NCgl2915	-0.2	Leucyl-tRNA synthetase
NCgl0598	-0.2	Phytoene synthase
NCgl1637	-0.2	Hypothetical protein
NCgl2905	-0.2	Sugar kinase
NCgl2356	-0.2	Hypothetical protein
NCgl1985	-0.2	Hypothetical protein

Table A 3 continued

Gene-identifier	log2fold Change	Feature
NCgl2188	-0.2	DNA primase
NCgl1969	-0.2	Adenylosuccinate lyase
NCgl1924	-0.2	Hypothetical protein
NCgl0704	-0.2	Helicase
NCgl0107	-0.2	Phosphohistidine phosphatase SixA
NCgl0960	-0.2	Allophanate hydrolase subunit 2
NCgl2672	-0.2	Hypothetical protein
NCgl0703	-0.2	Hypothetical protein
NCgl1116	-0.2	Na+/proline, Na+/panthothenate symporter
NCgl0049	-0.2	NAD-dependent aldehyde dehydrogenase
NCgl2959	-0.1	Hypothetical protein
NCgl0707	-0.1	SNF2 family helicase
NCgl2017	-0.1	Major facilitator superfamily permease
NCgl0360	-0.1	Succinate dehydrogenase flavoprotein subunit
NCgl2181	-0.1	Hypothetical protein
NCgl1640	-0.1	Hypothetical protein
NCgl2946	-0.1	Hypothetical protein
NCgl2503	-0.1	Extracellular nuclease
NCgl0579	-0.1	Inosine 5-monophosphate dehydrogenase
NCgl2816	-0.1	Integral membrane transport protein
NCgl1336	-0.1	Phenylalanyl-tRNA synthetase subunit beta
NCgl2311	-0.1	DNA-binding HTH domain-containing protein
NCgl1169	-0.1	Hypothetical protein
NCgl1983	-0.1	Ammonia permease
NCgl2488	-0.1	Hypothetical protein
NCgl0031	-0.1	ABC transporter atpase
NCgl0815	-0.1	Hypothetical protein
NCgl2230	-0.1	EctP protein
NCgl2003	-0.1	Metal-dependent amidase/aminoacylase/carboxypeptidase
NCgl0605	-0.1	Cell wall biogenesis glycosyltransferase
NCgl0147	-0.1	Hypothetical protein
NCgl2790	-0.1	Glycerol kinase
NCgl2896	-0.1	Hypothetical protein
NCgl0111	-0.1	Sugar (pentulose and hexulose) kinase
NCgl0104	-0.1	Acyl-CoA synthetase
NCgl1628	-0.1	Hypothetical protein
NCgl1042	-0.1	Hypothetical protein
NCgl2392	-0.1	Transposase
NCgl0241	-0.1	Recombination protein RecR
NCgl0358	-0.1	Transcriptional regulator
NCgl2433	-0.1	Rad3-related DNA helicase
NCgl2693	-0.1	Hypothetical protein
NCgl2233	-0.1	FAD/FMN-containing dehydrogenase
NCgl0352	-0.1	Hypothetical protein
NCgl2589	-0.1	Hypothetical protein
NCgl1950	-0.1	30S ribosomal protein S2

Table A 4. Upregulated genes of *C. glutamicum* Ect1 in comparison to *C. glutamicum* LYS-1. Genes were identified by comparative transcription analysis via ReadXplorer (Hilker et al. 2016), base mean > 30.

Gene-identifier	log2fold Change	Feature
NCgl2941	1.2	Transcriptional regulator
NCgl1485	1.0	Nucleoside-diphosphate-sugar epimerase
NCgl2246	0.9	Hypothetical protein
NCgl0859	0.9	Hypothetical protein
NCgl1985	0.8	Hypothetical protein
NCgl0092	0.8	Hypothetical protein
NCgl2800	0.8	Amidase
NCgl1138	0.8	Hypothetical protein
NCgl2524	0.8	Major facilitator superfamily permease
NCgl1484	0.8	Glutamine amidotransferase
NCgl2732	0.8	ABC transporter duplicated ATPase
NCgl0463	0.8	NAD-dependent aldehyde dehydrogenase
NCgl1214	0.7	L-Lysine efflux permease
NCgl0363	0.7	Hypothetical protein
NCgl2004	0.6	Hypothetical protein
NCgl2778	0.6	Hypothetical protein
NCgl1734	0.6	Hypothetical protein
NCgl2790	0.6	Glycerol kinase
NCgl2987	0.6	Hypothetical protein
NCgl1733	0.6	Hypothetical protein
NCgl2311	0.6	DNA-binding HTH domain-containing protein
NCgl2864	0.5	Hypothetical protein
NCgl0829	0.5	Transcriptional regulator
NCgl2110	0.5	Rieske Fe-S protein
NCgl2357	0.5	Hypothetical protein
NCgl1675	0.5	Hypothetical protein
NCgl0732	0.5	Hypothetical protein
NCgl0274	0.5	Membrane carboxypeptidase
NCgl2739	0.5	3-Methyladenine DNA glycosylase
NCgl1931	0.5	Hypothetical protein
NCgl0549	0.4	Hypothetical protein
NCgl0673	0.4	Hypothetical protein
NCgl0884	0.4	Hypothetical protein
NCgl2303	0.4	Permease
NCgl0230	0.4	Hypothetical protein
NCgl0736	0.4	Hypothetical protein
NCgl2876	0.4	Transmembrane transport protein
NCgl1237	0.4	3-Isopropylmalate dehydrogenase
NCgl2796	0.4	Hypothetical protein
NCgl0111	0.4	Sugar (pentulose and hexulose) kinase
NCgl2125	0.4	Hypothetical protein
NCgl2234	0.4	Transcriptional regulator
NCgl2171	0.4	Hypothetical protein
NCgl0932	0.4	Hypothetical protein
NCgl2424	0.4	Hypothetical protein
NCgl2516	0.4	Dithiobiotin synthetase
NCgl2840	0.4	Transcriptional regulator
NCgl0434	0.4	Hypothetical protein
NCgl0436	0.4	Hypothetical protein
NCgl2694	0.4	Hypothetical protein
NCgl0373	0.4	Hypothetical protein
NCgl0474	0.4	Transcriptional regulator
NCgl0667	0.4	Hypothetical protein
NCgl0809	0.4	Dihydrofolate reductase
NCgl1566	0.4	ABC transporter ATPase
NCgl1285	0.4	Hypothetical protein
NCgl0273	0.4	Hypothetical protein

Table A 4 continued

Gene-identifier	log2fold Change	Feature
NCgl0031	0.4	ABC transporter atpase
NCgl0007	0.4	Hypothetical protein
NCgl2695	0.3	Amidohydrolase
NCgl1416	0.3	Hypothetical protein
NCgl1194	0.3	Major facilitator superfamily permease
NCgl0614	0.3	Mn-dependent transcriptional regulator
NCgl2729	0.3	ABC transporter permease
NCgl2341	0.3	Type IV restriction endonuclease
NCgl2001	0.3	Hypothetical protein
NCgl2355	0.3	Hypothetical protein
NCgl0876	0.3	Pyridoxal/pyridoxine/pyridoxamine kinase
NCgl0358	0.3	Transcriptional regulator
NCgl0635	0.3	Hypothetical protein
NCgl1921	0.3	Mg-chelatase subunit ChlD
NCgl0729	0.3	Hypothetical protein
NCgl1077	0.3	Sec-independent translocase
NCgl2299	0.3	Transcriptional regulator
NCgl1627	0.3	Hypothetical protein
NCgl0410	0.3	Hypothetical protein
NCgl1418	0.3	Hypothetical protein
NCgl1583	0.3	L-Serine deaminase
NCgl2222	0.3	Hypothetical protein
NCgl0912	0.3	Two-component system, response regulator
NCgl2358	0.3	Short chain dehydrogenase
NCgl0925	0.3	ABC transporter ATP-binding component
NCgl1868	0.3	Diaminopimelate epimerase
NCgl2785	0.3	Membrane-associated phospholipid phosphatase
NCgl2688	0.3	Cystathionine gamma-synthase
NCgl2270	0.3	Nicotinic acid mononucleotide adenylyltransferase
NCgl0167	0.3	Transcriptional regulator
NCgl0804	0.3	Hypothetical protein
NCgl2173	0.3	Hydrolase/acyltransferase
NCgl2909	0.3	D-amino acid dehydrogenase subunit
NCgl2489	0.3	Hypothetical protein
NCgl0828	0.3	Citrate lyase beta subunit
NCgl0897	0.3	ABC transporter ATP-binding protein
NCgl2021	0.3	Histidinol dehydrogenase
rpsA	0.3	30S ribosomal protein S1
NCgl1220	0.3	Hypothetical protein
NCgl2318	0.3	Chloromuconate cycloisomerase
NCgl1318	0.3	Nucleoside-diphosphate-sugar epimerase
NCgl0191	0.3	Hypothetical protein
NCgl0202	0.3	Hypothetical protein
NCgl2472	0.3	Regulatory-like protein
NCgl0139	0.3	HrpA-like helicase
NCgl0250	0.3	RNA polymerase sigma factor
NCgl1323	0.3	Hypothetical protein
NCgl2364	0.2	Hypothetical protein
NCgl0931	0.2	Hypothetical protein
NCgl2144	0.2	Hypothetical protein
NCgl0322	0.2	5'-Nucleotidase
NCgl0132	0.2	Hypothetical protein
NCgl2243	0.2	Sugar kinase
NCgl0050	0.2	Phenol 2-monooxygenase
NCgl0900	0.2	Glyceraldehyde-3-phosphate dehydrogenase

Table A 4 continued

Gene-identifier	log2fold Change	Feature
NCgl0454	0.2	Ubiquinone/menaquinone biosynthesis methyltransferase
NCgl0796	0.2	FKBP-type peptidylprolyl isomerase
NCgl2525	0.2	Hypothetical protein
NCgl2529	0.2	Hypothetical protein
NCgl2660	0.2	Hypothetical protein
NCgl1018	0.2	Hypothetical protein
NCgl0800	0.2	Hypothetical protein
NCgl0662	0.2	G3E family GTPase
NCgl1760	0.2	Hypothetical protein
NCgl2028	0.2	Hydroxypyruvate isomerase
NCgl0728	0.2	Hypothetical protein
NCgl1188	0.2	Acetyltransferase
NCgl0580	0.2	Hypothetical protein
NCgl0095	0.2	Hypothetical protein
NCgl2460	0.2	Transposase
NCgl1027	0.2	Hypothetical protein
NCgl1508	0.2	Cytochrome oxidase assembly protein
NCgl1050	0.2	Hypothetical protein
NCgl0991	0.2	Acetyltransferase
NCgl1951	0.2	Membrane metalloendopeptidase
NCgl2404	0.2	Transcriptional regulator
NCgl1920	0.2	Hypothetical protein
NCgl0915	0.2	ABC transporter atpase and permease
NCgl0344	0.2	O-antigen and teichoic acid membrane export protein
NCgl0808	0.2	Hypothetical protein
NCgl0544	0.2	Acetyltransferase
NCgl0147	0.2	Hypothetical protein
NCgl2908	0.2	Mercuric reductase
NCgl2900	0.2	Hypothetical protein
NCgl1584	0.2	Glycerol-3-phosphate dehydrogenase
NCgl1354	0.2	TPR repeat-containing protein
NCgl2090	0.2	Hypothetical protein
NCgl0433	0.2	1,4-Dihydroxy-2-naphthoate octaprenyltransferase
NCgl1308	0.2	Hypothetical protein
NCgl0068	0.2	Two-component system response regulator
NCgl1974	0.2	16S rRNA-processing protein rimm
NCgl2488	0.2	Hypothetical protein
NCgl1067	0.2	Glucosyl-3-phosphoglycerate synthase
NCgl2863	0.2	Two-component system, response regulator
NCgl1042	0.2	Hypothetical protein
NCgl1031	0.2	Major facilitator superfamily permease
NCgl2915	0.1	Leucyl-tRNA synthetase
NCgl0391	0.1	Signal transduction histidine kinase
NCgl2538	0.1	Transcriptional regulator
NCgl2490	0.1	Hypothetical protein
NCgl1040	0.1	Excinuclease ATPase subunit
NCgl1147	0.1	Hypothetical protein
NCgl0509	0.1	Hypothetical protein
NCgl0479	0.1	Hypothetical protein
NCgl1245	0.1	Transcriptional regulator
NCgl1478	0.1	Hypothetical protein
NCgl2916	0.1	Hypothetical protein
NCgl0704	0.1	Helicase

Table A 4 continued

Gene-identifier	log2fold Change	Feature
NCgl0803	0.1	Hypothetical protein
NCgl0705	0.1	Helicase
NCgl1078	0.1	ATPase
NCgl1697	0.1	Hypothetical protein
NCgl1479	0.1	Phosphoribosylaminoimidazole-succinocarboxamide synthase
NCgl1082	0.1	Hypothetical protein
NCgl1633	0.1	Hypothetical protein
NCgl2139	0.1	Threonine synthase
NCgl0649	0.1	Hypothetical protein
NCgl0821	0.1	ABC transporter permease
NCgl1047	0.1	Hypothetical protein
NCgl0706	0.1	Type II restriction enzyme, methylase subunits
NCgl2869	0.1	Copper chaperone
NCgl0650	0.1	D-alanyl-D-alanine carboxypeptidase
NCgl0864	0.1	Hypothetical protein
NCgl2306	0.1	Acyl-CoA:acetate CoA transferase beta subunit
NCgl0911	0.1	Two-component system sensory transduction histidine kinase
NCgl2781	0.1	Prenyltransferase
NCgl0960	0.1	Allophanate hydrolase subunit 2
NCgl0409	0.1	Shikimate 5-dehydrogenase
NCgl2713	0.1	Permease
NCgl0069	0.1	Phosphoglycerate dehydrogenase or related dehydrogenase
NCgl1176	0.1	ABC transporter periplasmic component
NCgl0924	0.1	Transcription-repair coupling factor
NCgl2187	0.1	Hypothetical protein
NCgl0435	0.1	O-succinylbenzoic acid--CoA ligase
NCgl1170	0.1	Lactoylglutathione lyase
NCgl2905	0.1	Sugar kinase
NCgl2295	0.1	Molecular chaperone
NCgl1093	0.1	Major facilitator superfamily permease
NCgl2631	0.1	Hypothetical protein
NCgl1300	0.1	Major facilitator superfamily permease
NCgl2839	0.1	Inner membrane protein translocase yidc
NCgl2788	0.1	UDP-galactopyranose mutase
NCgl0089	0.1	Urease accessory protein ureh
NCgl2359	0.1	Transcriptional regulator
NCgl2671	0.1	Hypothetical protein
NCgl0746	0.1	Hypothetical protein
NCgl2375	0.1	ABC transporter periplasmic component
NCgl2053	0.1	Dehydrogenase
NCgl2296	0.1	Rossmann fold nucleotide-binding protein
NCgl0335	0.1	Hypothetical protein
NCgl2670	0.1	Hypothetical protein
NCgl0199	0.1	Selenocysteine lyase
NCgl2188	0.1	DNA primase
NCgl0666	0.1	Citrate synthase
NCgl2877	0.1	Hypothetical protein
NCgl1452	0.1	K+ transport flavoprotein
NCgl2809	0.1	Pyruvate kinase
NCgl1616	0.1	Hypothetical protein
NCgl2109	0.1	Cytochrome b subunit of the bc complex

Table A 4 continued

Gene-identifier	log2fold Change	Feature
NCgl2503	0.1	Extracellular nuclease
NCgl1492	0.1	Integrase
NCgl0599	0.1	RND superfamily drug exporter
NCgl1431	0.1	Hypothetical protein
NCgl1847	0.1	Hypothetical protein

Table A 5. Downregulated genes of *C. glutamicum* Ect1 in comparison to *C. glutamicum* LYS-1. Genes were identified by comparative transcription analysis via ReadXplorer (Hilker et al. 2016), base mean > 30.

Gene-identifier	log2fold Change	Feature
NCgl1672	-0.9	Hypothetical protein
NCgl0904	-0.8	Hypothetical protein
NCgl2101	-0.8	Hypothetical protein
NCgl2668	-0.8	Two-component system, response regulator
NCgl0901	-0.8	Peptidyl-tRNA hydrolase
NCgl2285	-0.8	Pirin
NCgl1908	-0.7	Exopolyphosphatase
NCgl1932	-0.7	Methionine aminopeptidase
NCgl1742	-0.6	Hypothetical protein
NCgl0104	-0.6	Acyl-CoA synthetase
NCgl2103	-0.6	Hypothetical protein
NCgl0350	-0.6	Acyltransferase
NCgl1707	-0.6	Hypothetical protein
NCgl1290	-0.6	Hypothetical protein
NCgl2284	-0.6	Transposase
NCgl2084	-0.6	Cell division protein FtsI
NCgl2832	-0.5	Membrane transport protein
NCgl2003	-0.5	Metal-dependent amidase/aminoacylase/carboxypeptidase
NCgl1368	-0.5	Acetyltransferase
NCgl1705	-0.5	Stress-sensitive restriction system protein 2
NCgl1380	-0.5	NhaP-type Na+/H+ and K+/H+ antiporter
NCgl2441	-0.5	Mn-dependent transcriptional regulator
NCgl1411	-0.5	Major facilitator superfamily permease
NCgl0639	-0.5	ABC transporter periplasmic component
NCgl0622	-0.5	Flotillin-like protein
NCgl2017	-0.5	Major facilitator superfamily permease
NCgl2895	-0.5	Hypothetical protein
NCgl1625	-0.5	Hypothetical protein
NCgl0606	-0.5	ABC transporter permease
NCgl1959	-0.5	ABC transporter periplasmic component
NCgl0922	-0.5	Hypothetical protein
NCgl1588	-0.5	Hypothetical protein
NCgl1928	-0.5	Mycothione reductase
NCgl1189	-0.5	Spermidine synthase
NCgl0604	-0.5	Deoxyribodipyrimidine photolyase
NCgl0429	-0.5	YjgF translation initiation inhibitor
NCgl1624	-0.5	ABC transporter permease
NCgl2325	-0.4	Benzoate transporter
NCgl1973	-0.4	Hypothetical protein
NCgl0455	-0.4	Oxidoreductase
NCgl0347	-0.4	Cell wall biogenesis glycosyltransferase
NCgl0351	-0.4	UDP-glucose 6-dehydrogenase

Table A 5 continued

Gene-identifier	log2fold Change	Feature
NCgl1659	-0.4	Hypothetical protein
NCgl2926	-0.4	Hypothetical protein
NCgl1454	-0.4	Protein-tyrosine-phosphatase
NCgl1670	-0.4	Hypothetical protein
NCgl2392	-0.4	Transposase
NCgl2286	-0.4	Hypothetical protein
NCgl1756	-0.4	Hypothetical protein
NCgl1145	-0.4	Serine protease
NCgl0926	-0.4	ABC transporter atpase
NCgl0789	-0.4	Hypothetical protein
rho	-0.4	Transcription termination factor Rho
NCgl1706	-0.4	Hypothetical protein
NCgl2964	-0.4	Helicase
NCgl1213	-0.4	Oxidoreductase
NCgl2048	-0.4	Methionine synthase II
NCgl1641	-0.4	Hypothetical protein
NCgl1389	-0.4	Hypothetical protein
NCgl2083	-0.4	UDP-N-acetylmuramoylalanyl-D-glutamate--2, 6-diaminopimelate ligase
NCgl0047	-0.4	Hypothetical protein
NCgl0108	-0.4	Mannitol-1-phosphate/altronate dehydrogenase
NCgl1060	-0.4	Hypothetical protein
NCgl0600	-0.4	Geranylgeranyl pyrophosphate synthase
NCgl1749	-0.4	Hypothetical protein
NCgl1998	-0.4	ABC transporter ATPase and permease
NCgl1983	-0.4	Ammonia permease
NCgl1021	-0.4	Transposase
NCgl2467	-0.4	Dehydrogenase
NCgl1902	-0.4	Inosine-uridine nucleoside N-ribohydrolase
NCgl1827	-0.4	1-Deoxy-D-xylulose-5-phosphate synthase
NCgl0216	-0.4	Hypothetical protein
NCgl2218	-0.4	ABC transporter ATPase and permease
NCgl0348	-0.4	Transposase
NCgl1260	-0.4	Guanosine polyphosphate pyrophosphohydrolase/synthetase
NCgl2022	-0.4	Hypothetical protein
NCgl1348	-0.4	Hypothetical protein
NCgl2680	-0.3	Multidrug resistance protein
NCgl2491	-0.3	4-amino-4-deoxychorismate lyase
NCgl0692	-0.3	Hypothetical protein
NCgl1073	-0.3	Glucose-1-phosphate adenylyltransferase
NCgl0024	-0.3	Transcriptional regulator
NCgl1200	-0.3	Siderophore-interacting protein
NCgl2219	-0.3	Zn-dependent oligopeptidase
NCgl0518	-0.3	30S ribosomal protein S5
NCgl2658	-0.3	Ferredoxin/ferredoxin-NADP reductase
NCgl1751	-0.3	Hypothetical protein
NCgl0881	-0.3	Hypothetical protein
NCgl1570	-0.3	Alanyl-tRNA synthetase
NCgl1687	-0.3	Hypothetical protein
NCgl2150	-0.3	Hypothetical protein
NCgl1631	-0.3	Hypothetical protein
NCgl2386	-0.3	Oligoribonuclease
NCgl2253	-0.3	Hypothetical protein
NCgl2474	-0.3	Serine acetyltransferase

Table A 5 continued

Gene-identifier	log2fold Change	Feature
NCgl1367	-0.3	Hypothetical protein
NCgl2959	-0.3	Hypothetical protein
NCgl2041	-0.3	Coenzyme F420-dependent N5,N10-methylene tetrahydromethanopterin reductase
NCgl0352	-0.3	Hypothetical protein
NCgl1740	-0.3	Hypothetical protein
NCgl2242	-0.3	2'-5' RNA ligase
NCgl2703	-0.3	Permease
NCgl0120	-0.3	Transcriptional regulator
NCgl2779	-0.3	Esterase
NCgl2896	-0.3	Hypothetical protein
NCgl1741	-0.3	Hypothetical protein
NCgl0701	-0.3	Hypothetical protein
NCgl0916	-0.3	Gamma-glutamyltranspeptidase
NCgl2363	-0.3	Chromate transport protein ChrA
NCgl1134	-0.3	Hypothetical protein
NCgl0179	-0.3	Transposase
NCgl0700	-0.3	Helicase
NCgl0593	-0.3	Hypothetical protein
NCgl2040	-0.3	Hypothetical protein
NCgl2195	-0.3	Chromosome segregation ATPase
NCgl2191	-0.3	Glucosamine-fructose-6-phosphate aminotransferase
NCgl2667	-0.3	Two-component system, sensory transduction histidine kinase
NCgl0301	-0.3	Hypothetical protein
NCgl2438	-0.3	Ribonucleotide-diphosphate reductase subunit beta
NCgl0805	-0.3	Hypothetical protein
NCgl2914	-0.3	Hypothetical protein
NCgl0591	-0.3	Hypothetical protein
NCgl2640	-0.3	Carboxylate-amine ligase
NCgl0194	-0.3	Hypothetical protein
NCgl0212	-0.3	Hypothetical protein
NCgl0106	-0.3	Lactoylglutathione lyase or related lyase
NCgl0135	-0.3	Ammonia monooxygenase
NCgl0891	-0.3	Hypothetical protein
NCgl1548	-0.3	Carbamoyl phosphate synthase small subunit
NCgl2091	-0.3	5,10-methylenetetrahydrofolate reductase
NCgl2229	-0.3	Coenzyme F420-dependent N5,N10-methylene tetrahydromethanopterin reductase
NCgl0107	-0.2	Phosphohistidine phosphatase SixA
NCgl2181	-0.2	Hypothetical protein
NCgl2334	-0.2	Hypothetical protein
NCgl0195	-0.2	Glycosyltransferase
NCgl0625	-0.2	O-acetylhomoserine aminocarboxypropyltransferase
NCgl2458	-0.2	Hypothetical protein
NCgl0691	-0.2	Hypothetical protein
NCgl0146	-0.2	Methylated DNA-protein cysteine methyltransferase
NCgl1185	-0.2	Hypothetical protein
NCgl1354a	-0.2	Hypothetical protein
NCgl2290	-0.2	Hypothetical protein
NCgl1831	-0.2	Hypothetical protein
NCgl1965	-0.2	Thiamine biosynthesis protein ThiF
NCgl2813	-0.2	Flavoprotein
NCgl1340	-0.2	N-acetyl-gamma-glutamyl-phosphate reductase
NCgl0699	-0.2	Hypothetical protein

Table A 5 continued

Gene-identifier	log2fold Change	Feature
NCgl2583	-0.2	Hypothetical protein
NCgl1837	-0.2	Hypothetical protein
NCgl1240	-0.2	DNA polymerase III epsilon subunit
NCgl0131	-0.2	Hypothetical protein
NCgl0480	-0.2	Elongation factor Tu
NCgl1755	-0.2	Hypothetical protein
NCgl0603	-0.2	Nucleoside-diphosphate-sugar epimerase
NCgl0357	-0.2	Hypothetical protein
NCgl2946	-0.2	Hypothetical protein
NCgl2052	-0.2	Co/Zn/Cd cation transporter
NCgl2111	-0.2	Cytochrome C
NCgl1945	-0.2	Hypothetical protein
NCgl2152	-0.2	Galactokinase
NCgl2777	-0.2	Esterase
NCgl0596	-0.2	C50 carotenoid epsilon cyclase
NCgl0655	-0.2	Transcriptional regulator
NCgl1116	-0.2	Na+/proline, Na+/panthothenate symporter
NCgl0890	-0.2	Hypothetical protein
NCgl0737	-0.2	Helicase
NCgl2581	-0.2	Hypothetical protein
NCgl2833	-0.2	Transcriptional regulator
NCgl1867	-0.2	Hypothetical protein
NCgl1074	-0.2	Hypothetical protein
NCgl0834	-0.2	50S ribosomal protein L28
NCgl2880	-0.2	Single-stranded DNA-binding protein
NCgl0656	-0.2	Phosphomannomutase
NCgl2456	-0.2	Hypothetical protein
NCgl0672	-0.2	Hypothetical protein
NCgl0791	-0.2	rRNA methylase
NCgl0033	-0.2	Peptidyl-prolyl cis-trans isomerase (rotamase)
NCgl1929	-0.2	Hypothetical protein
NCgl2702	-0.2	Molecular chaperone DnaK
NCgl1646	-0.2	Hypothetical protein
NCgl0405	-0.2	Transcriptional regulator
NCgl0502	-0.2	Hypothetical protein
NCgl2276	-0.2	Xanthine/uracil permease
NCgl0717	-0.2	Hypothetical protein
NCgl0605	-0.2	Cell wall biogenesis glycosyltransferase
NCgl0375	-0.2	Cation transport ATPase
NCgl2387	-0.2	Hypothetical protein
NCgl2881	-0.2	30S ribosomal protein S6
NCgl2495	-0.2	Amidophosphoribosyltransferase
NCgl2077	-0.1	UDP-N-acetylmuramate--L-alanine ligase
NCgl2124	-0.1	Leucyl aminopeptidase
NCgl1085	-0.1	ABC transporter duplicated ATPase
NCgl1924	-0.1	Hypothetical protein
NCgl1216	-0.1	Glutathione S-transferase
NCgl0959	-0.1	Sortase or related acyltransferase
NCgl0727a	-0.1	Hypothetical protein
NCgl1163	-0.1	ATP synthase F0F1 subunit alpha
NCgl0920	-0.1	Hypothetical protein
NCgl2360	-0.1	Cystathionine gamma-synthase
NCgl2289	-0.1	Acetyltransferase
NCgl1322	-0.1	Excinuclease ABC subunit A
NCgl1574	-0.1	Metalloprotease
NCgl1070	-0.1	SAM-dependent methyltransferase

Table A 5 continued

Gene-identifier	log2fold Change	Feature
NCgl0213	-0.1	ABC transporter atpase
NCgl1026	-0.1	Hypothetical protein
NCgl0797	-0.1	Acetyl-CoA carboxylase beta subunit
NCgl2740	-0.1	Hemoglobin-like flavoprotein
NCgl2409	-0.1	3-oxoacyl-ACP synthase
NCgl1626	-0.1	Phosphopantothenoylcysteine synthetase/decarboxylase
NCgl2405	-0.1	4'-Phosphopantetheinyl transferase
NCgl0801	-0.1	Hypothetical protein
NCgl2241	-0.1	ABC transporter duplicated ATPase
NCgl0130	-0.1	Permease
NCgl0779	-0.1	ABC-type cobalamin/Fe3+-siderophore transport system, ATPase
NCgl0032	-0.1	Hypothetical protein
NCgl1169	-0.1	Hypothetical protein
NCgl2305	-0.1	Hypothetical protein
NCgl2576	-0.1	DNA integrity scanning protein DisA
NCgl2262	-0.1	Threonine efflux protein
NCgl2720	-0.1	Hypothetical protein
NCgl2433	-0.1	Rad3-related DNA helicase
NCgl2154	-0.1	Hypothetical protein
NCgl2060	-0.1	ABC transporter ATPase
NCgl2940	-0.1	Hypothetical protein
NCgl2589	-0.1	Hypothetical protein
NCgl0620	-0.1	Bifunctional 5,10-methylene-tetrahydrofolate dehydrogenase/ 5,10-methylene-tetrahydrofolate cyclohydrolase
NCgl1628	-0.1	Hypothetical protein
NCgl0747	-0.1	Hypothetical protein
NCgl0815	-0.1	Hypothetical protein
NCgl2100	-0.1	Hypothetical protein
NCgl2693	-0.1	Hypothetical protein
NCgl2986	-0.1	N-acetylmuramoyl-L-alanine amidase
NCgl0602	-0.1	Lipocalin
NCgl1838	-0.1	Hypothetical protein
NCgl2750	-0.1	UDP-glucose 6-dehydrogenase
NCgl0750	-0.1	Hypothetical protein
NCgl0802	-0.1	Fatty-acid synthase
NCgl2298	-0.1	Transcriptional regulator
NCgl1754	-0.1	Hypothetical protein
NCgl0355	-0.1	Dihydrolipoamide dehydrogenase
NCgl2447	-0.1	Hypothetical protein
NCgl1365	-0.1	ABC transporter duplicated ATPase
NCgl0978	-0.1	Hypothetical protein
NCgl2050	-0.1	Permease
NCgl0340	-0.1	Nucleoside-diphosphate sugar epimerase
NCgl2789	-0.1	Hypothetical protein
NCgl2401	-0.1	Amidase
NCgl1826	-0.1	Ribonuclease D
NCgl1255	-0.1	Glucan phosphorylase
NCgl1417	-0.1	Sulfate permease

7. References

Abdel-Aziz H, Wadie W, Scherner O, Efferth T, Khayyal MT. 2015. Bacteria-derived compatible solutes ectoine and 5α-hydroxyectoine act as intestinal barrier stabilizers to ameliorate experimental inflammatory bowel disease. Journal of natural products 78(6):1309-1315.

Abe S, Takayama K, Kinoshita S. 1967. Taxonomical studies on glutamic acid-producing bacteria. J. Gen. Appl. Microbiol 13:279-301.

Albersmeier A, Pfeifer-Sancar K, Rückert C, Kalinowski J. 2017. Genome-wide determination of transcription start sites reveals new insights into promoter structures in the actinomycete *Corynebacterium glutamicum*. Journal of biotechnology 257:99-109.

Arakawa T, Timasheff SN. 1985. The stabilization of proteins by osmolytes. Biophysical Journal 47(3):411-414.

Araki M, Sugimoto M, Yoshihara Y, Nakamatsu T. 1999. Method for producing L-lysine. Patent No. 6,004,773.

Aranda PS, LaJoie DM, Jorcyk CL. 2012. Bleach gel: a simple agarose gel for analyzing RNA quality. Electrophoresis 33(2):366-369.

Becker J, Gießelmann G, Hoffmann SL, Wittmann C. 2016. *Corynebacterium glutamicum* for sustainable bioproduction: from metabolic physiology to systems metabolic engineering. Synthetic biology–metabolic engineering: Springer. p 217-263.

Becker J, Klopprogge C, Herold A, Zelder O, Bolten CJ, Wittmann C. 2007. Metabolic flux engineering of L-lysine production in *Corynebacterium glutamicum*--over expression and modification of G6P dehydrogenase. Journal of Biotechnology 132(2):99-109.

Becker J, Klopprogge C, Schröder H, Wittmann C. 2009. Metabolic engineering of the tricarboxylic acid cycle for improved lysine production by *Corynebacterium glutamicum*. Applied and Environmental Microbiology 75(24):7866-9.

Becker J, Klopprogge C, Wittmann C. 2008. Metabolic responses to pyruvate kinase deletion in lysine producing *Corynebacterium glutamicum*. Microbial Cell Factories 7:8.

Becker J, Klopprogge C, Zelder O, Heinzle E, Wittmann C. 2005. Amplified expression of fructose 1,6-bisphosphatase in *Corynebacterium glutamicum* increases *in*

vivo flux through the pentose phosphate pathway and lysine production on different carbon sources. Applied and Environmental Microbiology 71(12):8587-96.

Becker J, Kuhl M, Kohlstedt M, Starck S, Wittmann C. 2018a. Metabolic engineering of *Corynebacterium glutamicum* for the production of cis, cis-muconic acid from lignin. Microbial cell factories 17(1):115.

Becker J, Rohles CM, Wittmann C. 2018b. Metabolically engineered *Corynebacterium glutamicum* for bio-based production of chemicals, fuels, materials, and healthcare products. Metabolic engineering.

Becker J, Schäfer R, Kohlstedt M, Harder BJ, Borchert NS, Stöveken N, Bremer E, Wittmann C. 2013. Systems metabolic engineering of *Corynebacterium glutamicum* for production of the chemical chaperone ectoine. Microbial Cell Factories 12:110.

Becker J, Wittmann C. 2012. Systems and synthetic metabolic engineering for amino acid production - the heartbeat of industrial strain development. Current Opinion in Biotechnology 23(5):718-26.

Becker J, Wittmann C. 2015. Advanced Biotechnology: Metabolically Engineered Cells for the Bio-Based Production of Chemicals and Fuels, Materials, and Health-Care Products. Angewandte Chemie 54:3328-3350.

Becker J, Zelder O, Haefner S, Schröder H, Wittmann C. 2011. From zero to hero--design-based systems metabolic engineering of *Corynebacterium glutamicum* for L-lysine production. Metabolic Engineering 13(2):159-68.

Bellmann A, Vrljic M, Patek M, Sahm H, Krämer R, Eggeling L. 2001. Expression control and specificity of the basic amino acid exporter LysE of *Corynebacterium glutamicum*. Microbiology 147(Pt 7):1765-74.

Binder S, Schendzielorz G, Stäbler N, Krumbach K, Hoffmann K, Bott M, Eggeling L. 2012. A high-throughput approach to identify genomic variants of bacterial metabolite producers at the single-cell level. Genome biology 13(5):R40.

Booth IR. 2014. Bacterial mechanosensitive channels: progress towards an understanding of their roles in cell physiology. Current opinion in microbiology 18:16-22.

Börngen K, Battle AR, Möker N, Morbach S, Marin K, Martinac B, Krämer R. 2010. The properties and contribution of the *Corynebacterium glutamicum* MscS variant to

fine-tuning of osmotic adaptation. Biochimica et Biophysica Acta (BBA)-Biomembranes 1798(11):2141-2149.

Braga A, Oliveira J, Silva R, Ferreira P, Rocha I, Kallscheuer N, Marienhagen J, Faria N. 2018. Impact of the cultivation strategy on resveratrol production from glucose in engineered *Corynebacterium glutamicum*. Journal of biotechnology 265:70-75.

Brown MH, Skurray RA. 2001. Staphylococcal multidrug efflux protein QacA. Journal of molecular microbiology and biotechnology 3(2):163-170.

Brunef R, Kumar KS, Guillen-Gosalbez G, Jimenez L. 2011. Integrating process simulation, multi-objective optimization and LCA for the development of sustainable processes: application to biotechnological plants. Computer Aided Chemical Engineering: Elsevier. p 1271-1275.

Buenger J, Driller H. 2004. Ectoin: an effective natural substance to prevent UVA-induced premature photoaging. Skin Pharmacology and Physiology 17(5):232-237.

Bursy J, Kuhlmann AU, Pittelkow M, Hartmann H, Jebbar M, Pierik AJ, Bremer E. 2008. Synthesis and uptake of the compatible solutes ectoine and 5-hydroxyectoine by *Streptomyces coelicolor* A3(2) in response to salt and heat stresses. Applied and environmental microbiology 74(23):7286-7296.

Buschke N, Becker J, Schäfer R, Kiefer P, Biedendieck R, Wittmann C. 2013. Systems metabolic engineering of xylose-utilizing *Corynebacterium glutamicum* for production of 1,5-diaminopentane. Biotechnology Journal 8(5):557-70.

Buschke N, Schröder H, Wittmann C. 2011. Metabolic engineering of *Corynebacterium glutamicum* for production of 1,5-diaminopentane from hemicellulose. Biotechnology Journal 6(3):306-17.

Cánovas D, Vargas C, Iglesias-Guerra F, Csonka LN, Rhodes D, Ventosa A, Nieto JnJ. 1997. Isolation and characterization of salt-sensitive mutants of the moderate halophile *Halomonas elongata* and cloning of the ectoine synthesis genes. Journal of Biological Chemistry 272(41):25794-25801.

Cantera S, Muñoz R, Lebrero R, López JC, Rodríguez Y, García-Encina PA. 2018. Technologies for the bioconversion of methane into more valuable products. Current opinion in biotechnology 50:128-135.

Chen W, Zhang S, Jiang P, Yao J, He Y, Chen L, Gui X, Dong Z, Tang S-Y. 2015. Design of an ectoine-responsive AraC mutant and its application in metabolic engineering of ectoine biosynthesis. Metabolic engineering 30:149-155.

Chen Y, Vu J, Thompson MG, Sharpless WA, Chan LJG, Gin JW, Keasling JD, Adams PD, Petzold CJ. 2019. A rapid methods development workflow for high-throughput quantitative proteomic applications. PloS one 14(2):e0211582.

Cheng F, Luozhong S, Guo Z, Yu H, Stephanopoulos G. 2017. Enhanced biosynthesis of hyaluronic acid using engineered *Corynebacterium glutamicum* via metabolic pathway regulation. Biotechnology journal 12(10):1700191.

Cheng J, Chen P, Song A, Wang D, Wang Q. 2018. Expanding lysine industry: industrial biomanufacturing of lysine and its derivatives. Journal of industrial microbiology & biotechnology:1-16.

Cho JS, Choi KR, Prabowo CPS, Shin JH, Yang D, Jang J, Lee SY. 2017. CRISPR/Cas9-coupled recombineering for metabolic engineering of *Corynebacterium glutamicum*. Metabolic Engineering 42 157-167.

Chung S-C, Park J-S, Yun J, Park JH. 2017. Improvement of succinate production by release of end-product inhibition in *Corynebacterium glutamicum*. Metabolic engineering 40:157-164.

Corbin-Lickfett KA, Souki SK, Cocco MJ, Sandri-Goldin RM. 2010. Three arginine residues within the RGG box are crucial for ICP27 binding to herpes simplex virus 1 GC-rich sequences and for efficient viral RNA export. Journal of virology 84(13):6367-6376.

Cox CD, Bavi N, Martinac B. 2018. Bacterial mechanosensors. Annual review of physiology 80:71-93.

Cremer J, Treptow C, Eggeling L, Sahm H. 1988. Regulation of enzymes of lysine biosynthesis in *Corynebacterium glutamicum*. Journal of General Microbiology 134(12):3221-9.

Csonka LN. 1989. Physiological and genetic responses of bacteria to osmotic stress. Microbiological reviews 53(1):121-147.

Czech L, Hermann L, Stöveken N, Richter AA, Höppner A, Smits SH, Heider J, Bremer E. 2018. Role of the Extremolytes Ectoine and Hydroxyectoine as Stress Protectants and Nutrients: Genetics, Phylogenomics, Biochemistry, and Structural Analysis. Genes 9(4):177.

Davies S, Morris P, Baker R. 1997. Partial substitution of fish meal and full-fat soya bean meal with wheat gluten and influence of lysine supplementation in diets for rainbow trout, *Oncorhynchus mykiss* (Walbaum). Aquaculture Research 28(5):317-328.

Diesveld R, Tietze N, Fürst O, Reth A, Bathe B, Sahm H, Eggeling L. 2009. Activity of exporters of *Escherichia coli* in *Corynebacterium glutamicum*, and their use to increase L-threonine production. Journal of molecular microbiology and biotechnology 16(3-4):198-207.

Dobson CM. 2003. Protein folding and disease: a view from the first Horizon Symposium. Nature Reviews Drug Discovery 2(2):154.

Eggeling L, Bott M. 2015. A giant market and a powerful metabolism: L-lysine provided by *Corynebacterium glutamicum*. Applied Microbiology and Biotechnology 99(8):3387-3394.

Eggeling L, Oberle S, Sahm H. 1998. Improved L-lysine yield with *Corynebacterium glutamicum*: use of dapA resulting in increased flux combined with growth limitation. Applied microbiology and biotechnology 49(1):24-30.

Eggeling L, Sahm H. 1999. L-Glutamate and L-lysine: traditional products with impetuous developments. Applied microbiology and biotechnology 52(2):146-153.

Eggeling L, Sahm H. 2003. New ubiquitous translocators: amino acid export by *Corynebacterium glutamicum* and *Escherichia coli*. Archives of microbiology 180(3):155-160.

Ehira S, Teramoto H, Inui M, Yukawa H. 2009. Regulation of *Corynebacterium glutamicum* heat shock response by the extracytoplasmic-function sigma factor SigH and transcriptional regulators HspR and HrcA. Journal of Bacteriology 191(9):2964-72.

Fallet C, Rohe P, Franco-Lara E. 2010. Process optimization of the integrated synthesis and secretion of ectoine and hydroxyectoine under hyper/hypo-osmotic stress. Biotechnology and bioengineering 107(1):124-133.

Feng L-Y, Xu J-Z, Zhang W-G. 2018. Improved L-Leucine Production in *Corynebacterium glutamicum* by Optimizing the Aminotransferases. Molecules 23(9):2102.

Flodin NW. 1997. The metabolic roles, pharmacology, and toxicology of lysine. Journal of the American College of Nutrition 16(1):7-21.

Fondi M, Liò P. 2015. Multi-omics and metabolic modelling pipelines: challenges and tools for systems microbiology. Microbiological research 171:52-64.

Fränzel B, Trötschel C, Rückert C, Kalinowski J, Poetsch A, Wolters DA. 2010. Adaptation of *Corynebacterium glutamicum* to salt-stress conditions. Proteomics 10(3):445-457.

García-Estepa R, Argandoña M, Reina-Bueno M, Capote N, Iglesias-Guerra F, Nieto JJ, Vargas C. 2006. The *ectD* gene, which is involved in the synthesis of the compatible solute hydroxyectoine, is essential for thermoprotection of the halophilic bacterium *Chromohalobacter salexigens*. Journal of bacteriology 188(11):3774-3784.

Gatto GJ, Boyne MT, Kelleher NL, Walsh CT. 2006. Biosynthesis of pipecolic acid by RapL, a lysine cyclodeaminase encoded in the rapamycin gene cluster. Journal of the American Chemical Society 128(11):3838-3847.

Georgi T, Rittmann D, Wendisch VF. 2005. Lysine and glutamate production by *Corynebacterium glutamicum* on glucose, fructose and sucrose: roles of malic enzyme and fructose-1,6-bisphosphatase. Metabolic Engineering 7(4):291-301.

Glanemann C, Loos A, Gorret N, Willis L, O'brien X, Lessard P, Sinskey A. 2003. Disparity between changes in mRNA abundance and enzyme activity in *Corynebacterium glutamicum*: implications for DNA microarray analysis. Applied microbiology and biotechnology 61(1):61-68.

Gourdon P, Baucher MF, Lindley ND, Guyonvarch A. 2000. Cloning of the malic enzyme gene from *Corynebacterium glutamicum* and role of the enzyme in lactate metabolism. Applied and Environmental Microbiology 66(7):2981-7.

Graf R, Anzali S, Buenger J, Pfluecker F, Driller H. 2008. The multifunctional role of ectoine as a natural cell protectant. Clinics in dermatology 26(4):326-333.

Guillouet S, Engasser J. 1995. Growth of *Corynebacterium glutamicum* in glucose-limited continuous cultures under high osmotic pressure. Influence of growth rate on the intracellular accumulation of proline, glutamate and trehalose. Applied microbiology and biotechnology 44(3-4):496-500.

Hagerty SB, Van Groenigen KJ, Allison SD, Hungate BA, Schwartz E, Koch GW, Kolka RK, Dijkstra P. 2014. Accelerated microbial turnover but constant growth efficiency with warming in soil. Nature Climate Change 4(10):903.

He M. 2006. Pipecolic acid in microbes: biosynthetic routes and enzymes. Journal of Industrial Microbiology and Biotechnology 33(6):401-407.

He S, Wurtzel O, Singh K, Froula JL, Yilmaz S, Tringe SG, Wang Z, Chen F, Lindquist EA, Sorek R. 2010. Validation of two ribosomal RNA removal methods for microbial metatranscriptomics. Nature methods 7(10):807.

He Y-Z, Gong J, Yu H-Y, Tao Y, Zhang S, Dong Z-Y. 2015. High production of ectoine from aspartate and glycerol by use of whole-cell biocatalysis in recombinant *Escherichia coli*. Microbial cell factories 14:55.

Held C, Neuhaus T, Sadowski G. 2010. Compatible solutes: Thermodynamic properties and biological impact of ectoines and prolines. Biophysical Chemistry 152(1):28-39.

Henke N, Heider S, Peters-Wendisch P, Wendisch V. 2016. Production of the marine carotenoid astaxanthin by metabolically engineered *Corynebacterium glutamicum*. Marine drugs 14(7):124.

Hilker R, Stadermann KB, Schwengers O, Anisiforov E, Jaenicke S, Weisshaar B, Zimmermann T, Goesmann A. 2016. ReadXplorer 2—detailed read mapping analysis and visualization from one single source. Bioinformatics 32(24):3702-3708.

Hirao T, Nakano T, Azuma T, Sugimoto M, Nakanishi T. 1989. L-Lysine production in continuous culture of an L-lysine hyperproducing mutant of *Corynebacterium glutamicum*. Applied microbiology and biotechnology 32(3):269-273.

Hoffmann SL, Jungmann L, Schiefelbein S, Peyriga L, Cahoreau E, Portais J-C, Becker J, Wittmann C. 2018. Lysine production from the sugar alcohol mannitol: Design of the cell factory *Corynebacterium glutamicum* SEA-3 through integrated analysis and engineering of metabolic pathway fluxes. Metabolic engineering 47:475-487.

Ikeda M. 2012. Sugar transport systems in *Corynebacterium glutamicum*: features and applications to strain development. Applied Microbiology and Biotechnology 96(5):1191-200.

Ikeda M, Mizuno Y, Awane S, Hayashi M, Mitsuhashi S, Takeno S. 2011. Identification and application of a different glucose uptake system that functions as an alternative to the phosphotransferase system in *Corynebacterium glutamicum*. Applied Microbiology and Biotechnology 90(4):1443-51.

Ikeda M, Nakagawa S. 2003. The *Corynebacterium glutamicum* genome: features and impacts on biotechnological processes. Applied microbiology and biotechnology 62(2-3):99-109.

Ikeda M, Takeno S. 2013. Amino acid production by *Corynebacterium glutamicum*. *Corynebacterium glutamicum*: Springer. p 107-147.

Itou H, Okada U, Suzuki H, Yao M, Wachi M, Watanabe N, Tanaka I. 2005. The CGL2612 Protein from *Corynebacterium glutamicum* Is a Drug Resistance-related Transcriptional Repressor. Journal of Biological Chemistry 280(46):38711-38719.

Jäger W, Schäfer A, Pühler A, Labes G, Wohlleben W. 1992. Expression of the *Bacillus subtilis sacB* gene leads to sucrose sensitivity in the gram-positive bacterium *Corynebacterium glutamicum* but not in *Streptomyces lividans*. Journal of Bacteriology 174(16):5462-5.

Jeschek M, Gerngross D, Panke S. 2016. Rationally reduced libraries for combinatorial pathway optimization minimizing experimental effort. Nature communications 7:11163.

Jessop-Fabre MM, Dahlin J, Biron MB, Stovicek V, Ebert BE, Blank LM, Budin I, Keasling JD, Borodina I. 2019. The transcriptome and flux profiling of Crabtree-negative hydroxy acid producing strains of *Saccharomyces cerevisiae* reveals changes in the central carbon metabolism. Biotechnology Journal 0(ja):1900013.

Jetten M, Follettie M, Sinskey A. 1995. Effect of different levels of aspartokinase of the lysine production by *Corynebacterium lactofermentum*. Applied microbiology and biotechnology 43(1):76-82.

Jiang Y, Qian F, Yang J, Liu Y, Dong F, Xu C, Sun B, Chen B, Xu X, Li Y. 2017. CRISPR-Cpf1 assisted genome editing of *Corynebacterium glutamicum*. Nature communications 8:15179.

Jojima T, Noburyu R, Sasaki M, Tajima T, Suda M, Yukawa H, Inui M. 2015. Metabolic engineering for improved production of ethanol by *Corynebacterium glutamicum*. Applied microbiology and biotechnology 99(3):1165-1172.

Jones J, Koffas M. 2016. Optimizing metabolic pathways for the improved production of natural products. Methods in enzymology: Elsevier. p 179-193.

Jones JA, Vernacchio VR, Lachance DM, Lebovich M, Fu L, Shirke AN, Schultz VL, Cress B, Linhardt RJ, Koffas MA. 2015. ePathOptimize: a combinatorial approach for transcriptional balancing of metabolic pathways. Scientific reports 5:11301.

Junker B, Lester M, Leporati J, Schmitt J, Kovatch M, Borysewicz S, Maciejak W, Seeley A, Hesse M, Connors N. 2006. Sustainable reduction of bioreactor contamination in an industrial fermentation pilot plant. Journal of bioscience and bioengineering 102(4):251-268.

Kalinowski J, Bathe B, Bartels D, Bischoff N, Bott M, Burkovski A, Dusch N, Eggeling L, Eikmanns BJ, Gaigalat L, Goesmann A, Hartmann M, Huthmacher K, Krämer R, Linke B, McHardy AC, Meyer F, Möckel B, Pfefferle W, Pühler A, Rey DA, Rückert C, Rupp O, Sahm H, Wendisch VF, Wiegrabe I, Tauch A. 2003. The complete *Corynebacterium glutamicum* ATCC 13032 genome sequence and its impact on the production of L-aspartate-derived amino acids and vitamins. Journal of Biotechnology 104(1-3):5-25.

Kallscheuer N, Marienhagen J. 2018. *Corynebacterium glutamicum* as platform for the production of hydroxybenzoic acids. Microbial cell factories 17(1):70.

Kanapathipillai M, Ku SH, Girigoswami K, Park CB. 2008. Small stress molecules inhibit aggregation and neurotoxicity of prion peptide 106–126. Biochemical and biophysical research communications 365(4):808-813.

Kanapathipillai M, Lentzen G, Sierks M, Park CB. 2005. Ectoine and hydroxyectoine inhibit aggregation and neurotoxicity of Alzheimer's β-amyloid. FEBS letters 579(21):4775-4780.

Kang Z, Zhang C, Zhang J, Jin P, Zhang J, Du G, Chen J. 2014. Small RNA regulators in bacteria: powerful tools for metabolic engineering and synthetic biology. Applied Microbiology and Biotechnology 98(8):3413-3424.

Kar M, Malvi B, Das A, Panneri S, Gupta SS. 2011. Synthesis and characterization of poly-L-lysine grafted SBA-15 using NCA polymerization and click chemistry. Journal of Materials Chemistry 21(18):6690-6697.

Kats L, Nelssen J, Tokach M, Goodband R, Weeden T, Dritz S, Hansen J, Friesen K. 1994. The effects of spray-dried blood meal on growth performance of the early-weaned pig. Journal of animal science 72(11):2860-2869.

Kelle R, Hermann T, Bathe B. 2005. L-Lysine production. In: Eggeling L, Bott M, editors. Handbook of *Corynebacterium glutamicum*. Boca Raton: CRC Press. p 465-488.

Kempf B, Bremer E. 1998. Uptake and synthesis of compatible solutes as microbial stress responses to high-osmolality environments. Archives of Microbiology 170(5):319-30.

Kim H-M, Heinzle E, Wittmann C. 2006. Deregulation of aspartokinase by single nucleotide exchange leads to global flux rearrangement in the central metabolism of *Corynebacterium glutamicum*. Journal of microbiology and biotechnology 16(8):1174-1179.

Kim HT, Baritugo K-A, Oh YH, Hyun SM, Khang TU, Kang KH, Jung SH, Song BK, Park K, Kim I-K. 2018. Metabolic Engineering of *Corynebacterium glutamicum* for the High-Level Production of Cadaverine That Can Be Used for the Synthesis of Biopolyamide 510. ACS Sustainable Chemistry & Engineering 6(4):5296-5305.

Kind S, Becker J, Wittmann C. 2013. Increased lysine production by flux coupling of the tricarboxylic acid cycle and the lysine biosynthetic pathway-metabolic engineering of the availability of succinyl-CoA in *Corynebacterium glutamicum*. Metabolic Engineering 15:184-95.

Kind S, Jeong WK, Schröder H, Wittmann C. 2010. Systems-wide metabolic pathway engineering in *Corynebacterium glutamicum* for bio-based production of diaminopentane. Metabolic Engineering 12(4):341-51.

Kind S, Kreye S, Wittmann C. 2011. Metabolic engineering of cellular transport for overproduction of the platform chemical 1,5-diaminopentane in *Corynebacterium glutamicum*. Metabolic Engineering 13(5):617-27.

Kind S, Neubauer S, Becker J, Yamamoto M, Völkert M, Abendroth GV, Zelder O, Wittmann C. 2014. From zero to hero - Production of bio-based nylon from renewable resources using engineered *Corynebacterium glutamicum*. Metabolic Engineering 25:113-23.

Kind S, Wittmann C. 2011. Bio-based production of the platform chemical 1,5-diaminopentane. Applied Microbiology and Biotechnology 91(5):1287-96.

Kinoshita S, Udaka S, Shimono M. 1957. Studies on the amino acid fermentation. Part 1. Production of L-glutamic acid by various microorganisms. The Journal of General and Applied Microbiology 3(3):193-205.

Kiss RD, Stephanopoulos G. 1992. Metabolic characterization of a l-lysine-producing strain by continuous culture. Biotechnology and bioengineering 39(5):565-574.

Kjeldsen KR, Nielsen J. 2009. *In silico* genome-scale reconstruction and validation of the *Corynebacterium glutamicum* metabolic network. Biotechnology and Bioengineering 102(2):583-97.

Knoll A, Buechs J. 2006. L-Lysine–Coupling of Bioreaction and Process Model. Development of Sustainable Bioprocesses: Modeling and Assessment:155-167.

Kohlstedt M, Becker J, Wittmann C. 2010. Metabolic fluxes and beyond-systems biology understanding and engineering of microbial metabolism. Applied Microbiology and Biotechnology 88(5):1065-75.

Kohlstedt M, Sappa PK, Meyer H, Maass S, Zaprasis A, Hoffmann T, Becker J, Steil L, Hecker M, van Dijl JM, Lalk M, Mader U, Stülke J, Bremer E, Völker U, Wittmann C. 2014. Adaptation of *Bacillus subtilis* carbon core metabolism to simultaneous nutrient limitation and osmotic challenge: a multi-omics perspective. Environmental Microbiology 16(6):1898-917.

Krömer JO, Fritz M, Heinzle E, Wittmann C. 2005. *In vivo* quantification of intracellular amino acids and intermediates of the methionine pathway in *Corynebacterium glutamicum*. Analytical Biochemistry 340(1):171-3.

Krömer JO, Sorgenfrei O, Klopprogge K, Heinzle E, Wittmann C. 2004. In-depth profiling of lysine-producing *Corynebacterium glutamicum* by combined analysis of the transcriptome, metabolome, and fluxome. Journal of bacteriology 186(6):1769-1784.

Kruger NJ. 2009. The Bradford method for protein quantitation. The protein protocols handbook: Springer. p 17-24.

Kuhlmann AU, Bremer E. 2002. Osmotically regulated synthesis of the compatible solute ectoine in *Bacillus pasteurii* and related *Bacillus spp*. Applied and environmental microbiology 68(2):772-783.

Kunte HJ, Lentzen G, Galinski EA. 2014. Industrial production of the cell protectant ectoine: protection mechanisms, processes, and products. Current Biotechnology 3:10-25.

Lai J-Y, Wang P-R, Luo L-J, Chen S-T. 2014. Stabilization of collagen nanofibers with l-lysine improves the ability of carbodiimide cross-linked amniotic membranes to preserve limbal epithelial progenitor cells. International journal of nanomedicine 9:5117.

Lanéelle M-A, Tropis M, Daffé M. 2013. Current knowledge on mycolic acids in *Corynebacterium glutamicum* and their relevance for biotechnological processes. Applied microbiology and biotechnology 97(23):9923-9930.

Lange J, Müller F, Takors R, Blombach B. 2018. Harnessing novel chromosomal integration loci to utilize an organosolv-derived hemicellulose fraction for isobutanol production with engineered *Corynebacterium glutamicum*. Microbial biotechnology 11(1):257-263.

Langmead B, Salzberg SL. 2012. Fast gapped-read alignment with Bowtie 2. Nature methods 9(4):357.

Lee GH, Hur W, Bremmon CE, Flickinger MC. 1996. Lysine production from methanol at 50°C using *Bacillus methanolicus*: Modeling volume control, lysine concentration, and productivity using a three-phase continuous simulation. Biotechnology and bioengineering 49(6):639-653.

Lemme A, Strobel E, Hoehler D, Matzke W, Pack M, Jeroch H. 2002. Impact of graded levels of dietary lysine on performance in turkey toms 5 to 8 and 13 to16 weeks of age. Arch. Geflügelk 66:102-107.

Leuchtenberger W, Huthmacher K, Drauz K. 2005. Biotechnological production of amino acids and derivatives: current status and prospects. Applied Microbiology and Biotechnology 69(1):1-8.

Li M, Li D, Huang Y, Liu M, Wang H, Tang Q, Lu F. 2014. Improving the secretion of cadaverine in *Corynebacterium glutamicum* by cadaverine-lysine antiporter. Journal of Industrial Microbiology & Biotechnology 41(4):701-9.

Liu J, Barry CE, Besra GS, Nikaido H. 1996. Mycolic acid structure determines the fluidity of the mycobacterial cell wall. Journal of Biological Chemistry 271(47):29545-29551.

Liu X, Zhao Z, Zhang W, Sun Y, Yang Y, Bai Z. 2017. Bicistronic expression strategy for high-level expression of recombinant proteins in *Corynebacterium glutamicum*. Engineering in Life Sciences 17(10):1118-1125.

Louis P, Galinski EA. 1997. Characterization of genes for the biosynthesis of the compatible solute ectoine from *Marinococcus halophilus* and osmoregulated expression in *Escherichia coli*. Microbiology 143(4):1141-1149.

Lu JH, Liao CC. 1997. Site-directed mutagenesis of the aspartokinase gene *lysC* and its characterization in *Brevibacterium flavum*. Letters in applied microbiology 24(3):211-3.

Ma Y, Ma Q, Cui Y, Du L, Xie X, Chen N. 2019. Transcriptomic and metabolomics analyses reveal metabolic characteristics of L-leucine-and L-valine-producing *Corynebacterium glutamicum* mutants. Annals of Microbiology:1-12.

Mainzer SE, Hempfling WP. 1976. Effects of growth temperature on yield and maintenance during glucose-limited continuous culture of *Escherichia coli*. Journal of bacteriology 126(1):251-256.

Malin G, Lapidot A. 1996. Induction of synthesis of tetrahydropyrimidine derivatives in *Streptomyces* strains and their effect on *Escherichia coli* in response to osmotic and heat stress. Journal of bacteriology 178(2):385-395.

Mansour FH, Pestov DG. 2013. Separation of long RNA by agarose–formaldehyde gel electrophoresis. Analytical biochemistry 441(1):18-20.

Marker S, Le Mouel A, Meyer E, Simon M. 2010. Distinct RNA-dependent RNA polymerases are required for RNAi triggered by double-stranded RNA versus truncated transgenes in *Paramecium tetraurelia*. Nucleic acids research 38(12):4092-4107.

Marx A, Hans S, Möckel B, Bathe B, de Graaf AA, McCormack AC, Stapleton C, Burke K, O'Donohue M, Dunican LK. 2003. Metabolic phenotype of phosphoglucose isomerase mutants of *Corynebacterium glutamicum*. Journal of Biotechnology 104(1-3):185-97.

Matano C, Uhde A, Youn JW, Maeda T, Clermont L, Marin K, Krämer R, Wendisch VF, Seibold GM. 2014. Engineering of *Corynebacterium glutamicum* for growth and L-lysine and lycopene production from N-acetyl-glucosamine. Applied microbiology and biotechnology:98(12), 5633-5643.

Melmer G, Schwarz T. 2009. Ectoines: A new type of compatible solutes with great commercial potential. EXTREMOPHILES-Volume II 3:298.

Melzer G, Esfandabadi ME, Franco-Lara E, Wittmann C. 2009. Flux Design: *In silico* design of cell factories based on correlation of pathway fluxes to desired properties. BMC Systems Biology 3:120.

Metz AH, Hollis T, Eichman BF. 2007. DNA damage recognition and repair by 3-methyladenine DNA glycosylase I (TAG). The EMBO journal 26(9):2411-2420.

Moghaieb RE, Nakamura A, Saneoka H, Fujita K. 2011. Evaluation of salt tolerance in ectoine-transgenic tomato plants (*Lycopersicon esculentum*) in terms of photosynthesis, osmotic adjustment, and carbon partitioning. GM crops 2(1):58-65.

Moon MW, Park SY, Choi SK, Lee JK. 2007. The Phosphotransferase System of *Corynebacterium glutamicum*: Features of Sugar Transport and Carbon Regulation. Journal of molecular microbiology and biotechnology 12(1-2):43-50.

Morbach S, Krämer R. 2005. 18 Osmoregulation. Handbook of *Corynebacterium glutamicum*:417.

Mustakhimov I, Reshetnikov A, Khmelenina V, Trotsenko YA. 2010. Regulatory aspects of ectoine biosynthesis in halophilic bacteria. Microbiology 79(5):583-592.

Mutalik VK, Guimaraes JC, Cambray G, Lam C, Christoffersen MJ, Mai Q-A, Tran AB, Paull M, Keasling JD, Arkin AP. 2013. Precise and reliable gene expression via standard transcription and translation initiation elements. Nature methods 10(4):354.

Nakano T, Azuma T, Kuratsu Y. 1994. Process for producing L-lysine by iodothyronine resistant strains of *Mucorynebacterium glutamicum*. Google Patents.

Nakayama H, Yoshida K, Ono H, Murooka Y, Shinmyo A. 2000. Ectoine, the compatible solute of *Halomonas elongata*, confers hyperosmotic tolerance in cultured tobacco cells. Plant physiology 122(4):1239-1248.

Ng CY, Khodayari A, Chowdhury A, Maranas CD. 2015. Advances in *de novo* strain design using integrated systems and synthetic biology tools. Current Opinion in Chemical Biology 28:105-114.

Nguyen AQ, Schneider J, Wendisch VF. 2015. Elimination of polyamine N-acetylation and regulatory engineering improved putrescine production by *Corynebacterium glutamicum*. Journal of Biotechnology 201:75-85.

Nie L, Wu G, Culley DE, Scholten JC, Zhang W. 2007. Integrative analysis of transcriptomic and proteomic data: challenges, solutions and applications. Critical reviews in biotechnology 27(2):63-75.

Nikaido H. 1994. Prevention of drug access to bacterial targets: permeability barriers and active efflux. Science 264(5157):382-388.

Ning Y, Wu X, Zhang C, Xu Q, Chen N, Xie X. 2016. Pathway construction and metabolic engineering for fermentative production of ectoine in *Escherichia coli*. Metabolic Engineering 36:10-18.

Oguiza JA, Malumbres M, Eriani G, Pisabarro A, Mateos L, Martin F, Martin J. 1993. A gene encoding arginyl-tRNA synthetase is located in the upstream region of the *lysA* gene in *Brevibacterium lactofermentum*: regulation of *argS-lysA* cluster expression by arginine. Journal of bacteriology 175(22):7356-7362.

Oh YH, Choi JW, Kim EY, Song BK, Jeong KJ, Park K, Kim IK, Woo HM, Lee SH, Park SJ. 2015. Construction of Synthetic Promoter-Based Expression Cassettes for

the Production of Cadaverine in Recombinant *Corynebacterium glutamicum*. Applied Biochemistry and Biotechnology:176(7), 2065-2075.

Ohnishi J, Hayashi M, Mitsuhashi S, Ikeda M. 2003. Efficient 40 C fermentation of L-lysine by a new *Corynebacterium glutamicum* mutant developed by genome breeding. Applied Microbiology and Biotechnology 62(1):69-75.

Ohnishi J, Katahira R, Mitsuhashi S, Kakita S, Ikeda M. 2005. A novel *gnd* mutation leading to increased L-lysine production in *Corynebacterium glutamicum*. FEMS Microbiology Letters 242(2):265-74.

Okibe N, Suzuki N, Inui M, Yukawa H. 2010. Isolation, evaluation and use of two strong, carbon source-inducible promoters from *Corynebacterium glutamicum*. Letters in Applied Microbiology 50(2):173-80.

Ono H, Sawada K, Khunajakr N, Tao T, Yamamoto M, Hiramoto M, Shinmyo A, Takano M, Murooka Y. 1999. Characterization of biosynthetic enzymes for ectoine as a compatible solute in a moderately halophilic eubacterium, *Halomonas elongata*. Journal of bacteriology 181(1):91-99.

Otten A, Brocker M, Bott M. 2015. Metabolic engineering of *Corynebacterium glutamicum* for the production of itaconate. Metabolic Engineering:156-165.

Özcan N, Krämer R, Morbach S. 2005. Chill activation of compatible solute transporters in Corynebacterium glutamicum at the level of transport activity. Journal of bacteriology 187(14):4752-4759.

Pacella E, Collini S, Pacella F, Piraino D, Santamaria V, De Blasi R. 2010. Levobupivacaine vs. racemic bupivacaine in peribulbar anaesthesia: a randomized double blind study in ophthalmic surgery. Eur Rev Med Pharmacol Sci 14(6):539-544.

Pacheco LG, Castro TL, Carvalho RD, Moraes PM, Dorella FA, Carvalho NB, Slade SE, Scrivens JH, Feelisch M, Meyer R. 2012. A role for sigma factor σ^E in *Corynebacterium pseudotuberculosis* resistance to nitric oxide/peroxide stress. Frontiers in Microbiology 3:126.

Park J-S, Lee J-Y, Kim H-J, Kim E-S, Kim P, Kim Y, Lee H-S. 2012. The role of *Corynebacterium glutamicum spiA* gene in whcA-mediated oxidative stress gene regulation. FEMS Microbiology Letters 331(1):63-69.

Park S-D, Youn J-W, Kim Y-J, Lee S-M, Kim Y, Lee H-S. 2008. *Corynebacterium glutamicum* σ^E is involved in responses to cell surface stresses and its activity is controlled by the anti-σ factor CseE. Microbiology 154(3):915-923.

Park SJ, Oh YH, Noh W, Kim HY, Shin JH, Lee EG, Lee S, David Y, Baylon MG, Song BK, Jegal J, Lee SY, Lee SH. 2014. High-level conversion of L-lysine into 5-aminovalerate that can be used for nylon 6,5 synthesis. Biotechnology Journal 9(10):1322-8.

Pastor JM, Salvador M, Argandona M, Bernal V, Reina-Bueno M, Csonka LN, Iborra JL, Vargas C, Nieto JJ, Canovas M. 2010. Ectoines in cell stress protection: uses and biotechnological production. Biotechnology Advances 28(6):782-801.

Pérez-García F, Peters-Wendisch P, Wendisch VF. 2016. Engineering *Corynebacterium glutamicum* for fast production of L-lysine and L-pipecolic acid. Applied microbiology and biotechnology 100(18):8075-8090.

Pérez-García F, Ziert C, Risse JM, Wendisch VF. 2017. Improved fermentative production of the compatible solute ectoine by *Corynebacterium glutamicum* from glucose and alternative carbon sources. Journal of biotechnology 258 (2017) 59-68.

Peter H, Weil B, Burkovski A, Krämer R, Morbach S. 1998. Corynebacterium glutamicum is equipped with four secondary carriers for compatible solutes: identification, sequencing, and characterization of the proline/ectoine uptake system, ProP, and the ectoine/proline/glycine betaine carrier, EctP. Journal of bacteriology 180(22):6005-6012.

Peters-Wendisch PG, Schiel B, Wendisch VF, Katsoulidis E, Möckel B, Sahm H, Eikmanns BJ. 2001. Pyruvate carboxylase is a major bottleneck for glutamate and lysine production by *Corynebacterium glutamicum*. Journal of molecular Microbiology and Biotechnology 3(2):295-300.

Pfeifer-Sancar K, Mentz A, Rückert C, Kalinowski J. 2013. Comprehensive analysis of the *Corynebacterium glutamicum* transcriptome using an improved RNAseq technique. BMC Genomics 14:888.

Pistikopoulos EN, Georgiadis MC, Kokossis A. 2011. 21st European Symposium on Computer Aided Process Engineering: Elsevier.

Qu Y, Bolen CL, Bolen DW. 1998. Osmolyte-driven contraction of a random coil protein. Proceedings of the National Academy of Sciences 95(16):9268-9273.

Radoš D, Carvalho AL, Wieschalka S, Neves AR, Blombach B, Eikmanns BJ, Santos H. 2015. Engineering *Corynebacterium glutamicum* for the production of 2, 3-butanediol. Microbial cell factories 14(1):171.

Robertson JL. 2019. Interrogating the conformational dynamics of BetP transport. The Journal of general physiology:jgp. 201812315.

Rohles CM, Gießelmann G, Kohlstedt M, Wittmann C, Becker J. 2016. Systems metabolic engineering of *Corynebacterium glutamicum* for the production of the carbon-5 platform chemicals 5-aminovalerate and glutarate. Microbial Cell Factories 15(1):154.

Rohles CM, Gläser L, Kohlstedt M, Gießelmann G, Pearson S, del Campo A, Becker J, Wittmann C. 2018. A bio-based route to the carbon-5 chemical glutaric acid and to bionylon-6, 5 using metabolically engineered *Corynebacterium glutamicum*. Green Chemistry 20(20):4662-4674.

Rosen R, Ron EZ. 2002. Proteome analysis in the study of the bacterial heat-shock response. Mass Spectrometry Reviews 21(4):244-265.

Rosner A. 1975. Control of lysine biosynthesis in *Bacillus subtilis*: inhibition of diaminopimelate decarboxylase by lysine. Journal of bacteriology 121(1):20-28.

Rouch D, Cram D, Di Berardino D, Littlejohn T, Skurray R. 1990. Efflux-mediated antiseptic resistance gene qacA from *Staphylococcus aureus:* common ancestry with tetracycline-and sugar-transport proteins. Molecular microbiology 4(12):2051-2062.

Ruffert S, Lambert C, Peter H, Wendisch VF, Krämer R. 1997. Efflux of compatible solutes in *Corynebacterium glutamicum* mediated by osmoregulated channel activity. European Journal of Biochemistry 247(2):572-580.

Rytter JV, Helmark S, Chen J, Lezyk MJ, Solem C, Jensen PR. 2014. Synthetic promoter libraries for *Corynebacterium glutamicum*. Applied Microbiology and Biotechnology 98(6):2617-23.

Saier Jr MH. 2000. Families of transmembrane transporters selective for amino acids and their derivatives. Microbiology 146(8):1775-1795.

Sallam A, Steinbüchel A. 2010. Dipeptides in nutrition and therapy: cyanophycin-derived dipeptides as natural alternatives and their biotechnological production. Applied microbiology and biotechnology 87(3):815-828.

Sano K, Shiio I. 1970. Microbial production of L-lysine III: Production by mutants resistant to *S*-(2-aminoethyl)-L-cysteine. The Journal of General and Applied Microbiology 16:373-391.

Sassi AH, Deschamps A, Lebeault J. 1996. Process analysis of L-lysine fermentation with *Corynebacterium glutamicum* under different oxygen and carbon dioxide supplies and redox potentials. Process biochemistry 31(5):493-497.

Sauer T, Galinski EA. 1998. Bacterial milking: A novel bioprocess for production of compatible solutes. Biotechnology and Bioengineering 57(3):306-13.

Schäfer A, Tauch A, Jäger W, Kalinowski J, Thierbach G, Pühler A. 1994. Small mobilizable multi-purpose cloning vectors derived from the *Escherichia coli* plasmids pK18 and pK19: selection of defined deletions in the chromosome of *Corynebacterium glutamicum*. Gene 145(1):69-73.

Schäfer RA. 2016. Improvement of *Corynebacterium glutamicum* for production of lysine and ectoine from industrial raw materials.

Schendzielorz G, Dippong M, Grünberger A, Kohlheyer D, Yoshida A, Binder S, Nishiyama C, Nishiyama M, Bott M, Eggeling L. 2013. Taking control over control: use of product sensing in single cells to remove flux control at key enzymes in biosynthesis pathways. ACS synthetic biology 3(1):21-29.

Schluesener D, Fischer F, Kruip J, Rögner M, Poetsch A. 2005. Mapping the membrane proteome of *Corynebacterium glutamicum*. Proteomics 5(5):1317-1330.

Schrumpf B, Eggeling L, Sahm H. 1992. Isolation and prominent characteristics of an L-lysine hyperproducing strain of *Corynebacterium glutamicum*. Applied microbiology and biotechnology 37(5):566-571.

Schulz A, Hermann L, Freibert SA, Bonig T, Hoffmann T, Riclea R, Dickschat JS, Heider J, Bremer E. 2017. Transcriptional regulation of ectoine catabolism in response to multiple metabolic and environmental cues. Environ Microbiol 19(11):4599-4619.

Seok J, Ko YJ, Lee M-E, Hyeon JE, Han SO. 2019. Systems metabolic engineering of *Corynebacterium glutamicum* for the bioproduction of biliverdin via protoporphyrin independent pathway. Journal of Biological Engineering 13(1):28.

Siebert D, Wendisch VF. 2015. Metabolic pathway engineering for production of 1,2-propanediol and 1-propanol by *Corynebacterium glutamicum*. Biotechnology for Biofuels 8:91.

Silberbach M, Schäfer M, Hüser AT, Kalinowski J, Pühler A, Krämer R, Burkovski A. 2005. Adaptation of *Corynebacterium glutamicum* to ammonium limitation: a

global analysis using transcriptome and proteome techniques. Applied and Environmental Microbiology 71(5):2391-402.

Stöveken N, Pittelkow M, Sinner T, Jensen RA, Heider J, Bremer E. 2011. A specialized aspartokinase enhances the biosynthesis of the osmoprotectants ectoine and hydroxyectoine in *Pseudomonas stutzeri* A1501. Journal of Bacteriology 193(17):4456-68.

Strong P, Kalyuzhnaya M, Silverman J, Clarke W. 2016. A methanotroph-based biorefinery: potential scenarios for generating multiple products from a single fermentation. Bioresource technology 215:314-323.

Sun H, Zhao D, Xiong B, Zhang C, Bi C. 2016. Engineering *Corynebacterium glutamicum* for violacein hyper production. Microbial cell factories 15(1):148.

Sun Y, Guo W, Wang F, Zhan C, Yang Y, Liu X, Bai Z. 2017. Transcriptome analysis of *Corynebacterium glutamicum* in the process of recombinant protein expression in bioreactors. PloS One 12(4):e0174824.

Sydlik U, Gallitz I, Albrecht C, Abel J, Krutmann J, Unfried K. 2009. The compatible solute ectoine protects against nanoparticle-induced neutrophilic lung inflammation. American journal of respiratory and critical care medicine 180(1):29-35.

Takeno S, Hori K, Ohtani S, Mimura A, Mitsuhashi S, Ikeda M. 2016. l-Lysine production independent of the oxidative pentose phosphate pathway by *Corynebacterium glutamicum* with the *Streptococcus mutans gapN* gene. Metabolic Engineering 37:1-10.

Takeno S, Murata N, Kura M, Takasaki M, Hayashi M, Ikeda M. 2018. The *accD3* gene for mycolic acid biosynthesis as a target for improving fatty acid production by fatty acid-producing *Corynebacterium glutamicum* strains. Applied microbiology and biotechnology 102(24):10603-10612.

Takeno S, Murata R, Kobayashi R, Mitsuhashi S, Ikeda M. 2010. Engineering of *Corynebacterium glutamicum* with an NADPH-Generating Glycolytic Pathway for l-Lysine Production. Applied and environmental microbiology 76(21):7154-7160.

Takeno S, Takasaki M, Urabayashi A, Mimura A, Muramatsu T, Mitsuhashi S, Ikeda M. 2013. Development of fatty acid-producing *Corynebacterium glutamicum* strains. Applied and Environmental Microbiology 79(21):6776-83.

Taniguchi H, Henke NA, Heider SA, Wendisch VF. 2017. Overexpression of the primary sigma factor gene *sigA* improved carotenoid production by *Corynebacterium glutamicum*: Application to production of β-carotene and the non-native linear C50 carotenoid bisanhydrobacterioruberin. Metabolic engineering communications 4:1-11.

Tsuge Y, Hasunuma T, Kondo A. 2015. Recent advances in the metabolic engineering of *Corynebacterium glutamicum* for the production of lactate and succinate from renewable resources. Journal of Industrial Microbiology & Biotechnology 42(3):375-89.

Tsuge Y, Kawaguchi H, Yamamoto S, Nishigami Y, Sota M, Ogino C, Kondo A. 2018. Metabolic engineering of *Corynebacterium glutamicum* for production of sunscreen shinorine. Bioscience, biotechnology, and biochemistry:1-8.

Tsuge Y, Tateno T, Sasaki K, Hasunuma T, Tanaka T, Kondo A. 2013. Direct production of organic acids from starch by cell surface-engineered *Corynebacterium glutamicum* in anaerobic conditions. AMB Express 3(1):72.

Unthan S, Baumgart M, Radek A, Herbst M, Siebert D, Bruhl N, Bartsch A, Bott M, Wiechert W, Marin K, Hans S, Krämer R, Seibold G, Frunzke J, Kalinowski J, Rückert C, Wendisch VF, Noack S. 2015. Chassis organism from *Corynebacterium glutamicum*-a top-down approach to identify and delete irrelevant gene clusters. Biotechnology Journal 10(2):290-301.

Vargas C, Jebbar M, Carrasco R, Blanco C, Calderón M, Iglesias-Guerra F, Nieto J. 2006. Ectoines as compatible solutes and carbon and energy sources for the halophilic bacterium *Chromohalobacter salexigens*. Journal of applied microbiology 100(1):98-107.

Vassilev I, Gießelmann G, Schwechheimer SK, Wittmann C, Virdis B, Krömer JO. 2018. Anodic Electro-Fermentation: Anaerobic production of L-Lysine by recombinant *Corynebacterium glutamicum*. Biotechnology and bioengineering 115.6 (2018):1499-1508.

Vogt M, Krumbach K, Bang WG, van Ooyen J, Noack S, Klein B, Bott M, Eggeling L. 2015. The contest for precursors: channelling L-isoleucine synthesis in *Corynebacterium glutamicum* without byproduct formation. Applied Microbiology and Biotechnology 99(2):791-800.

Vrljic M, Garg J, Bellmann A, Wachi S, Freudi R, Malecki M, Sahm H, Kozina V, Eggeling L, Saier Jr M. 1999. The LysE superfamily: topology of the lysine

exporter LysE of *Corynebacterium glutamicum*, a paradyme for a novel superfamily of transmembrane solute translocators. Journal of molecular microbiology and biotechnology 1(2):327-336.

Vrljic M, Sahm H, Eggeling L. 1996. A new type of transporter with a new type of cellular function: L-lysine export from *Corynebacterium glutamicum*. Molecular Microbiology 22(5):815-26.

Walz O. 1985. Studies on the effect of a frequent administration of a daily lysine supplement on the utilization of nutrients with pigs from 20-100 kg liveweight, Balances of calcium and phosphorus, blood constituents, pig carcass evaluation. Zeitschrift fuer Tierphysiologie, Tierernaehrung und Futtermittelkunde (Germany, FR).

Wang X, Su R, Feng J, Chen K, Xu S, Ouyang P. 2019. Engineering a microbial consortium based whole-cell system for efficient production of glutarate from L-lysine. Frontiers in Microbiology 10:341.

Wang Y, Cao G, Xu D, Fan L, Wu X, Ni X, Zhao S, Zheng P, Sun J, Ma Y. 2018. A Novel *Corynebacterium glutamicum* l-Glutamate Exporter. Applied and Environmental Microbiology 84(6):e02691-17.

Wang Y, Zhang L. 2010. Ectoine improves yield of biodiesel catalyzed by immobilized lipase. Journal of Molecular Catalysis B: Enzymatic 62(1):90-95.

Wehrmann A, Phillipp B, Sahm H, Eggeling L. 1998. Different Modes of Diaminopimelate Synthesis and Their Role in Cell Wall Integrity: a Study with *Corynebacterium glutamicum*. Journal of bacteriology 180(12):3159-3165.

Wei L, Xu N, Wang Y, Zhou W, Han G, Ma Y, Liu J. 2018. Promoter library-based module combination (PLMC) technology for optimization of threonine biosynthesis in *Corynebacterium glutamicum*. Applied Microbiology and Biotechnology:1-14.

Weigelt S, Huber T, Hofmann F, Jost M, Ritzefeld M, Luy B, Freudenberger C, Majer Z, Vass E, Greie JC. 2012. Synthesis and conformational analysis of efrapeptins. Chemistry–A European Journal 18(2):478-487.

Wellerdiek M, Winterhoff D, Reule W, Brandner J, Oldiges M. 2009. Metabolic quenching of *Corynebacterium glutamicum*: efficiency of methods and impact of cold shock. Bioprocess and biosystems engineering 32(5):581-592.

Wendisch VF, Bott M, Eikmanns BJ. 2006a. Metabolic engineering of *Escherichia coli* and *Corynebacterium glutamicum* for biotechnological production of organic acids and amino acids. Current Opinion in Microbiology 9(3):268-74.

Wendisch VF, Bott M, Kalinowski J, Oldiges M, Wiechert W. 2006b. Emerging *Corynebacterium glutamicum* systems biology. Journal of Biotechnology 124(1):74-92.

Wittmann C, Becker J. 2007. The L-lysine story. From metabolic pathways to industrial production. In: Wendisch VF, editor. Amino Acid Biosynthesis - Pathways, Regulation and Metabolic Engineering. Berlin Heidelberg: Springer. p 40 - 68.

Wittmann C, Kiefer P, Zelder O. 2004. Metabolic fluxes in *Corynebacterium glutamicum* during lysine production with sucrose as carbon source. Applied and Environmental Microbiology 70(12):7277-87.

Wolf A, Krämer R, Morbach S. 2003. Three pathways for trehalose metabolism in *Corynebacterium glutamicum* ATCC13032 and their significance in response to osmotic stress. Molecular Microbiology 49(4):1119-34.

Wood JM. 1999. Osmosensing by bacteria: signals and membrane-based sensors. Microbiology and molecular biology reviews 63(1):230-262.

Wood JM, Bremer E, Csonka LN, Kraemer R, Poolman B, van der Heide T, Smith LT. 2001. Osmosensing and osmoregulatory compatible solute accumulation by bacteria. Comparative Biochemistry and Physiology Part A: Molecular & Integrative Physiology 130(3):437-460.

Wu G, Yan Q, Jones JA, Tang YJ, Fong SS, Koffas MAG. 2016. Metabolic Burden: Cornerstones in Synthetic Biology and Metabolic Engineering Applications. Trends in Biotechnology no. 8 (2016): 652-664.

Wu W, Zhang Y, Liu D, Chen Z. 2019. Efficient mining of natural NADH-utilizing dehydrogenases enables systematic cofactor engineering of lysine synthesis pathway of *Corynebacterium glutamicum*. Metabolic engineering 52:77-86.

Wyatt MD, Allan JM, Lau AY, Ellenberger TE, Samson LD. 1999. 3-methyladenine DNA glycosylases: structure, function, and biological importance. Bioessays 21(8):668-676.

Xafenias N, Kmezik C, Mapelli V. 2017. Enhancement of anaerobic lysine production in *Corynebacterium glutamicum* electrofermentations. Bioelectrochemistry 117:40-47.

Xu J-Z, Wu Z-H, Gao S-J, Zhang W. 2018a. Rational modification of tricarboxylic acid cycle for improving L-lysine production in *Corynebacterium glutamicum*. Microbial cell factories 17(1):105.

Xu J, Han M, Zhang J, Guo Y, Zhang W. 2014. Metabolic engineering *Corynebacterium glutamicum* for the l-lysine production by increasing the flux into l-lysine biosynthetic pathway. Amino Acids 46(9):2165-2175.

Xu JZ, Yang HK, Liu LM, Wang YY, Zhang WG. 2018b. Rational modification of *Corynebacterium glutamicum* dihydrodipicolinate reductase to switch the nucleotide-cofactor specificity for increasing l-lysine production. Biotechnology and bioengineering 115(7):1764-1777.

Yang DS, Yip CM, Huang TH, Chakrabartty A, Fraser PE. 1999. Manipulating the amyloid-beta aggregation pathway with chemical chaperones. J Biol Chem 274(46):32970-4.

Yim SS, An SJ, Kang M, Lee J, Jeong KJ. 2013. Isolation of fully synthetic promoters for high-level gene expression in *Corynebacterium glutamicum*. Biotechnology and Bioengineering 110(11):2959-69.

Yim SS, Choi JW, Lee SH, Jeong KJ. 2016. Modular Optimization of Hemicellulose-utilizing Pathway in *Corynebacterium glutamicum* for Consolidated Bioprocessing of Hemicellulosic Biomass. ACS Synthetic Biology 5(4):334-343.

Zhang B, Zhou N, Liu Y-M, Liu C, Lou C-B, Jiang C-Y, Liu S-J. 2015. Ribosome binding site libraries and pathway modules for shikimic acid synthesis with *Corynebacterium glutamicum*. Microbial cell factories 14(1):71.

Zhang L, Wang Y, Zhang C, Wang Y, Zhu D, Wang C, Nagata S. 2006. Supplementation effect of ectoine on thermostability of phytase. Journal of bioscience and bioengineering 102(6):560-563.

Zhang Q, Zheng X, Wang Y, Yu J, Zhang Z, Dele-Osibanjo T, Zheng P, Sun J, Jia S, Ma Y. 2018. Comprehensive optimization of the metabolomic methodology for metabolite profiling of *Corynebacterium glutamicum*. Applied microbiology and biotechnology 102(16):7113-7121.

Zhang X, Yao L, Xu G, Zhu J, Zhang X, Shi J, Xu Z. 2017. Enhancement of fructose utilization from sucrose in the cell for improved l-serine production in engineered *Corynebacterium glutamicum*. Biochemical engineering journal 118:113-122.

Zhao Z, Liu X, Zhang W, Yang Y, Dai X, Bai Z. 2016. Construction of genetic parts from the *Corynebacterium glutamicum* genome with high expression activities. Biotechnology letters 38(12):2119-2126.

Zhou Z, Wang C, Chen Y, Zhang K, Xu H, Cai H, Chen Z. 2015. Increasing available NADH supply during succinic acid production by *Corynebacterium glutamicum*. Biotechnology Progress 31(1):12-9.